

Activation and pathogenic potential of MOG-specific B cells in spontaneous experimental autoimmune encephalomyelitis

Dissertation der Fakultät für Biologie

Der Ludwigs-Maximilians-Universität München



Dipl.-Biol. Bettina Martin

München 2018

*"It is not the strongest of the species that survives, nor the most intelligent.
It is the one that is most adaptable to change." - Charles Darwin*

Erstgutachter: PD Dr. Oliver Griesbeck
Max-Planck-Institut für Neurobiologie, München
Fachbereich Biologie

Zweitgutachter: Prof. Dr. Laura Busse
Ludwig-Maximilians-Universität, München
Fachbereich Systemische Neurobiologie

Abgabetermin: 01.10.2018

Mündliche Prüfung: 26.03.2019

EIDESSTATTLICHE ERKLÄRUNG

Ich versichere hiermit an Eides statt, dass meine Dissertation selbständig und ohne unerlaubte Hilfsmittel angefertigt worden ist. Die vorliegende Dissertation wurde weder ganz, noch teilweise bei einer anderen Prüfungskommission vorgelegt. Ich habe noch zu keinem früheren Zeitpunkt versucht, eine Dissertation einzureichen oder an einer Doktorprüfung teilzunehmen.

Bettina Martin

Tuttlingen, den 01.10.2018

Datum, Unterschrift

ABSTRACT

Multiple Sclerosis (MS) is an autoimmune inflammatory disease of the central nervous system (CNS) predominantly mediated by self-reactive T and B cells. T cells have been long considered as major players in disease development. However, the success of B cell depletion therapies in MS patients highlights a complex role of B cells in disease initiation and progression. B cells can have both proinflammatory and regulatory effects. They can produce potentially pathogenic autoantibodies, act as antigen-presenting cells (APCs), and/or secrete cytokines shaping the local milieu. Actively induced Experimental Autoimmune Encephalomyelitis (EAE), the most common animal model of MS, is not optimally suited to study the role of B cells in autoimmune responses, as immunization with myelin peptide bypasses antigen processing and presentation by B cells. However, spontaneous EAE (sEAE) mouse models featuring transgenic T cell receptors (TCRs) specific for myelin oligodendrocyte glycoprotein (MOG) develop B cell-dependent disease, and can thus provide insights into the role of B cells in initiation of pathogenesis. To evaluate when and where B cells become activated in sEAE possible activation sites were investigated with different methodological approaches. First, we tried to determine whether myelin proteins from the CNS are transported to cervical lymph nodes (CLNs) in soluble form or via exosomes in spontaneous relapsing-remitting EAE (TCR¹⁶⁴⁰ mice) to investigate if autoreactive B cells are activated directly in CLNs. Alternatively, B cells might be activated in a different place and recruited to CLNs. Therefore, we explored the intestine as a potential site for priming of autoreactive B cells via B cell transfer and activation studies. However, as B cell analysis *ex vivo* and functional studies were not feasible due to low B cell frequencies in the intestine after transfer, in this study we focused on establishing a new B cell culture system, allowing expansion, differentiation, and manipulation of primary B cells and testing the use of this system for studying pathogenic properties of B cells upon transfer *in vivo*. After successful establishment of *in vitro* induced germinal center B cell (iGB) culture, we adoptively transferred MOG-specific iGB cells (from a mouse model expressing a MOG-specific BCR, called TH mouse), into 2D2 mice, which carry a transgenic MOG-specific TCR, to test their pathogenic potential. Results demonstrated that MOG-specific iGB cells can trigger development of EAE. These data support a role of B cells in the initiation of EAE probably acting as APCs. In summary, the new B cell culture system is a unique tool to expand and manipulate B cells and thereby characterize their role in the development of EAE and MS.

ZUSAMMENFASSUNG

Multiple Sklerose (MS) ist eine entzündliche Autoimmunerkrankung des zentralen Nervensystems (ZNS), die überwiegend durch selbstreaktive T- und B-Zellen vermittelt wird. T-Zellen wurden lange als Hauptakteure bei der Krankheitsentwicklung betrachtet. Jedoch weist der Erfolg von B-Zell-Depletionstherapien bei MS-Patienten auf eine komplexe Rolle der B-Zellen im Krankheitsverlauf hin. B-Zellen können sowohl proinflammatorische, als auch regulatorische Effekte haben. Sie produzieren potentiell pathogene Autoantikörper, wirken als Antigen-präsentierende Zellen und/oder sezernieren Zytokine, die das lokale entzündliche Milieu prägen. Die aktiv induzierte experimentelle Autoimmunenzephalomyelitis (EAE), ein MS Tiermodell, ist nicht gut geeignet, um die Rolle der B-Zellen während der Autoimmunantwort optimal zu studieren, da die Antigen-Prozessierung und Präsentation durch B-Zellen bei der Immunisierung mit Myelin-Peptiden umgangen wird. Allerdings können spontane EAE (sEAE) Mausmodelle, wo es unter anderem zu Rekrutierung endogener autoreaktiver B-Zellen kommt, Einblicke in die Rolle der B-Zellen in der Pathogenese gewähren. Um zu verstehen, wann und wo autoreaktive B-Zellen in sEAE aktiviert werden, wurden mögliche Aktivierungsorte mit verschiedenen methodologischen Ansätzen untersucht. Zuerst wurde getestet, ob in spontaner schubförmiger EAE (TCR¹⁶⁴⁰ Mäuse) Myelinproteine in löslicher Form oder über Exosome aus dem ZNS zu den zervikalen Lymphknoten (ZLK) transportiert werden, um B-Zellen direkt in den ZLK zu aktivieren. Alternativ könnten B-Zellen an einem anderen Ort aktiviert und dann in ZLK rekrutiert werden. Daher wurde das Priming von autoreaktiven B Zellen im Darm mit B Zell-Transfer und Aktivierungsstudien untersucht. Da jedoch eine aussagekräftige Analyse durch niedrige B Zell-Frequenzen im Darm nach dem Transfer nicht realisierbar erschien, wurde der Fokus dieser Arbeit auf die Etablierung eines neuen B-Zellkultursystems gelegt, welches die Expansion, Differenzierung und Manipulation von primären B-Zellen ermöglicht, sowie auf die Nutzung des Kultursystems für die Untersuchung pathogener Eigenschaften von B-Zellen nach Transfer *in vivo*. Nach erfolgreicher Etablierung von *in vitro* induzierten Keimzentrums B-Zellen (iGB) wurden MOG-spezifische iGB-Zellen (aus der TH Maus, welche einen MOG-spezifischen B Zellrezeptor besitzt) in 2D2 Mäuse, die einen transgenen MOG-spezifischen T-Zellrezeptor tragen, adoptiv transferiert, um ihr pathogenes Potential zu untersuchen. Die Ergebnisse zeigten, dass MOG-spezifische iGB Zellen eine EAE auslösen können. Diese Daten unterstützen eine Rolle der B-Zellen bei der Initiierung von EAE, wobei sie wahrscheinlich als Antigen-Präsentierer agieren. Zusammenfassend ist das neue B-Zellkultursystem ein einzigartiges Werkzeug, um B-Zellen zu expandieren und zu manipulieren, und so ihre Rolle bei der Entwicklung von EAE und MS zu charakterisieren.

TABLE OF CONTENTS

ABSTRACT.....	IV
ZUSAMMENFASSUNG	V
TABLE OF CONTENTS.....	VI
ABBREVIATIONS	VIII
1 INTRODUCTION	1
1.1 Multiple Sclerosis	1
1.1.1 Etiology	2
1.1.2 Pathogenesis.....	2
1.2 Experimental Autoimmune Encephalomyelitis.....	3
1.2.1 Actively induced EAE mouse model	3
1.2.2 Spontaneous EAE mouse models	4
1.3 Insights in MS disease triggers	5
1.3.1 T cells in MS and EAE	5
1.3.2 B cells in MS and EAE	6
1.3.3 Antigen transport and priming of autoreactive lymphocytes in MS and EAE	9
OBJECTIVE	13
2 MATERIAL AND METHODS	14
2.1 Material.....	14
2.1.1 Animals	14
2.1.2 Antibodies.....	15
2.1.3 Buffers and solutions.....	19
2.1.4 Cell culture.....	21
2.1.5 Media.....	22
2.1.6 Primers.....	23
2.2 Methods	24
2.2.1 Animal Routine	24
2.2.2 Cell culture routine	26
2.2.3 Electron microscopy for exosomes.....	28
2.2.4 DNA techniques	28
2.2.5 Enzyme linked immunosorbent assay (ELISA)	29
2.2.6 Exosome analysis.....	29
2.2.7 Fluorescence-activated cell sorting (FACS).....	30
2.2.8 Immunohistochemistry.....	30

2.2.9	Production of MOG tetramer	31
2.2.10	RNA techniques	31
2.2.11	Western Blot.....	31
3	RESULTS.....	33
3.1	Antigen transport and priming of autoreactive lymphocytes in spontaneous EAE.....	33
3.1.1	Detection of CNS draining pathways with fluorescent tracers	33
3.1.2	Detection of CNS autoantigens in CLNs with immunohistochemistry	36
3.1.3	Detection of MOG in exosomes from different cell types.....	40
3.2	B cell activation studies in the intestine.....	43
3.3	<i>In-vitro</i> induced GC B cells are a new tool for B cells studies in EAE	47
3.3.1	The iGB cell culture system.....	47
3.3.2	Adjustment of the iGB culture system for low B cell numbers	52
3.3.3	Tracking tools for iGB cells <i>in vitro</i> and <i>in vivo</i>	54
3.3.4	Expansion of MOG-specific B cells in the iGB culture.....	56
3.3.5	Selective expansion of MOG-specific B cells with the FAIS system.....	57
3.3.6	Adoptive transfer of TH or WT iGB cells as a tool for B cell studies	60
3.3.7	TH iGB cells trigger development of EAE in 2D2 recipient mice.....	63
4	DISCUSSION	64
4.1	Antigen transport.....	64
4.2	B cell activation studies in the intestine.....	67
4.3	New tool for B cell studies in EAE	68
5	CONCLUSION	76
6	REFERENCES	78
7	RESOURCES AND CONTRIBUTIONS	89
8	CURRICULUM VITAE	90
9	ACKNOWLEDGEMENTS	92

ABBREVIATIONS

2-ME	2-Mercaptoethanol
ACK	Ammonium-Chloride-Potassium
Ag	Antigen
AID	Activation-induced cytidine deaminase
aLN	Axillary lymph node
APC	Antigen presenting cell
B	Bone marrow-derived
BAFF	B cell-activating factor
BBB	Blood brain barrier
BCR	B cell receptor
BL6	C57BL/6
BrdU	Bromdesoxyuridin
BSA	Bovine serum albumin
CCR	Chemokine receptor
CFA	Complete Freund's adjuvant
CLN	Cervical lymph nodes
dCLN	Deep cervical lymph node
sCLN	Superficial cervical lymph node
CMV	Cytomegalovirus
CNS	Central nervous system
CSF	Cerebrospinal fluid
CSR	Class-switch recombination
CR2	Complement receptor 2
DAMPs	Damage-associated molecular patterns
DC	Dendritic cells
ddH ₂ O	Purified water
DNA	Deoxyribonucleic acid
DTR	Diphtheria toxin receptor
EAE	Experimental Autoimmune Encephalomyelitis
EBV	Epstein-Barr virus
EDTA	Ethylenediaminetetraacetic acid
EGFP	Enhanced green fluorescent protein
ELISA	Enzyme linked immunosorbent assay
FACS	Fluorescence-activated cell sorting

FDCs	Follicular dendritic cells
FCS	Fetal calf serum
GALT	Gut-associated lymphoid tissue
GC	Germinal centers
GFP	Green fluorescent protein
GM-CSF	Granulocyte macrophage - colony stimulating factor
H	Hour
H2M	MOG over expressing
HEL	Hen egg lysozyme
HLA	Human leukocyte antigen
IFN	Interferon
IL	Interleukin
iLN	Inguinal lymph nodes
Ig	Immunoglobulin
IgH	Immunoglobulin heavy
IgL	Immunoglobulin light
IHC	Immunohistochemistry
LT	Lymphotoxin
MAP-2	Microtubule-associated protein 2
MBP	Myelin basic protein
MHCII	Major histocompatibility complex class II
MLN	Mesenteric lymph nodes
Mm	Millimolar
MOG	Myelin oligodendrocyte glycoprotein
MS	Multiple Sclerosis
MVB	Multivesicular body
NTA	Nanoparticle Tracking Analysis
NF- κ B	Nuclear-factor κ B
NSE	Neuron specific enolase
NTLs	Non-transgenic littermates
NMO	Neuromyelitis optica
NOD	Non-obese diabetic
OCB	Oligoclonal bands
ON	Overnight
OSE	Opticospinal EAE

PAMPs	Pathogen-associated molecular patterns
PBS	Phosphate buffered saline
PCR	Polymerase chain reaction
PLP	Proteolipid protein
qPCR	Quantitative PCR
RAG	Recombination-activating gene
RFP	Red Fluorescent Protein
RNA	Ribonucleic acid
RR	Relapsing-remitting
RT	Room temperature
SDS	Sodium dodecyl sulfate
SHM	Somatic hyper mutation
SIP	Stock isotonic percoll
T	Thymus derived
TCR	T cell receptor
T _{FH}	Follicular helper T cells
TGF- β	Transforming growth factor- β
TH	IgH ^{MOG}
TLOs	Tertiary lymphoid organs
TLR	Toll-like receptor
TMB	3,3',5,5'-Tetramethylbenzidin
TNF	Tumor necrosis factor
Tris	Tris(hydroxymethyl)aminomethane

1 INTRODUCTION

1.1 Multiple Sclerosis

Multiple sclerosis (MS) is a chronic inflammatory disease of the spinal cord and brain affecting approximately 2.5 million people worldwide with increasing numbers [1]. Clinical manifestations of this autoimmune disease are sensory and visual disturbances, motor impairments, fatigue, pain and cognitive deficits [2]. The clinical manifestations correlate with active lesions in the CNS. These lesions are caused by immune cell infiltration across the blood-brain barrier (BBB) promoting inflammation, demyelination, gliosis and neuroaxonal degeneration [3]. The current concept is that autoreactive T and B cells are the main drivers of disease progress, and thus, common therapies are immunomodulatory drugs. Unfortunately, they are often associated with several strong side effects from development of other autoimmune disorders and malignancies to fatal infections [4]. This indicates the important need to identify more specific therapeutic targets. However, deeper knowledge about molecular mechanisms in immunopathology of MS is required.

The most common form affecting approximately 85% of patients is relapsing-remitting MS [5]. This form is characterized by an initial episode where the patient shows neurological dysfunction, followed by a remission period of clinical recovery. Most patients (80%) develop after several relapses a secondary progressive MS, where lesions are no longer characteristic, and instead neurological dysfunction is accompanied by decreased brain volume and increased axonal loss, also called CNS atrophy [6]. Only 10% of patients develop primary progressive MS featuring progressive decline from the outset and the absence of relapses [4]. MS usually appears in adults in their late twenties or early thirties but it can rarely start in childhood and after 50 years of age [2, 7]. The primary progressive subtype is more common in people in their fifties [8]. Similar to many other autoimmune disorders, the disease is more common in women, and the trend to disease development may be increasing [9].

Another form of demyelinating disease is Neuromyelitis optica (NMO), also known as Devic's disease. This disease actually comprises a spectrum of disorders characterized by simultaneous inflammation and demyelination of the optic nerve (optic neuritis) and the spinal cord (myelitis), whereas the brain is largely spared. Inflammatory lesions are different from those observed in MS. Most patients with NMO have been found to have no or very few nonspecific white matter lesions on brain MRI. Spinal cord MRI also shows

distinctive findings: a majority of patients have extensive longitudinal lesions covering three or more vertebral segments. Furthermore, NMO patients frequently have CSF pleocytosis of more than 50 leukocytes per μl , with or without the presence of neutrophils [10]. Aquaporin 4 (AQP4) antibody, an autoantibody that binds to the water channel AQP4, in combination with diagnostic criteria support the distinction of NMO from other autoimmune disorders of the CNS [11]. However, not all NMO patients have AQP4 antibodies. There is a subgroup of patients, which are negative for AQP4 but positive for myelin oligodendrocyte protein (MOG) antibodies, but this seems to be rare [12].

1.1.1 Etiology

The exact cause of MS remains elusive. Genetic variation accounts for approximately 30% of the overall disease risk, however, environmental factors and/or immunological heterogeneity in general also greatly contribute to the risk [13, 14]. The majority of MS related genes are immunological, thus, the human leukocyte antigen (HLA), located within the major histocompatibility complex (MHC) region, has been consistently associated with MS in all populations tested [15]. Other genes are tumor necrosis factor receptor 1 (TNFR1), interferons (IFNs), interleukin-2 (IL-2) and NF κ B [16, 17]. The data implicate central and peripheral tolerance mechanisms, as well as peripheral differences in effector T cell function [4]. Considering that the numerous genetic risk factors for MS probably affect a multitude of immunological pathways, environmental factors that influence any of these different pathways may also contribute to disease development. Several environmental risk factors have been reported including vitamin D, human cytomegalovirus infection, circadian disruption, smoking, and Epstein-Barr virus (EBV) infection [18, 19]. Moreover, a relatively new link between MS and diet/gut microbiota has been proposed which will be discussed in 1.3.3.

1.1.2 Pathogenesis

An open question is whether MS is triggered in the periphery or in the CNS. In the peripheral model, autoreactive T cells and B cells are activated in secondary lymphoid organs potentially through release of previously sequestered CNS antigen, molecular mimicry, bystander activation or co-expression of TCRs with different specificities [4, 20]. Molecular mimicry is defined as a theory where sequence similarities between foreign and self-peptides or proteins are sufficient to result in the cross-activation of autoreactive T or B cells by a foreign antigen [21, 22]. In bystander activation, T cells are activated in absence of specific TCR stimulation or stimulation, which allows T cells to bypass

checkpoints of central and peripheral tolerance. After activation, these autoreactive T cells traffic to the CNS as a primary phenomenon, become re-activated through contact with autoantigen, and initiate an inflammatory cascade attracting other cells including more T cells, B cells and monocytes.

Alternatively, in CNS-triggered disease development, the infiltration of autoreactive B and T cells occurs as a secondary phenomenon while inflammation and demyelination are already established in the CNS by other immune cells for example monocytes and neutrophils. Studies in the EAE model indicate that these cell types are enriched among CNS infiltrating cells during the preclinical phase and could play a role in nascent lesion development by mediating BBB and blood-cerebrospinal fluid (CSF) barrier breakdown, and/or by stimulating the maturation of local APCs [23-25].

All together, MS is a heterogeneous autoimmune disease which involves genetic as well as environmental factors leading to dysfunction of checkpoint mechanisms and escape of autoreactive or defect immune cells which can initiate attack on self proteins.

1.2 Experimental Autoimmune Encephalomyelitis

1.2.1 Actively induced EAE mouse model

To identify new therapeutic approaches for MS treatment, animal models offer the opportunity for in-depth analysis of disease processes. Experimental autoimmune encephalomyelitis (EAE) is the most commonly studied mouse model of MS [26]. Here, EAE can be actively induced by immunization with myelin peptides, such as MOG₃₅₋₅₅, in complete Freund's adjuvant (CFA) and two additional injections of pertussis toxin [27]. However, active EAE has certain limitations and is often insufficient to investigate the highly dynamic nature of pathogenic immune cells during trafficking, recruitment and infiltration of the CNS. Several key aspects of the model have to be considered when translating EAE results to MS: first of all, the harsh and strong activation stimulus using myelin peptides together with potent adjuvant represents a highly artificial situation for activation of autoreactive T cells and thus is not suitable for studying the very early activation events in the natural development of disease. Second, most mouse strains including C57BL/6 mice (BL6) show a monophasic disease course, but no relapses and therefore poorly reflect human disease. Third, most EAE models show focused inflammation in the spinal cord, whereas MS is usually dominated by brain inflammation. Also, due to the immunization regimen, T cell responses are heavily biased towards CD4⁺

T cells in EAE, whereas CD8⁺ T cell responses play a significant role in MS. The earlier viewpoint that B cells are not required for EAE was supported by work in mice lacking B cells. Disease induced in B cell-deficient C57BL/6 mice immunized with rodent MOG₃₅₋₅₅ is indistinguishable from disease in WT mice, indicating that T cell responses to this Ag are sufficient to induce CNS inflammation and demyelination in this model [28, 29]. However, immunization with MOG peptide and CFA bypasses antigen processing and presentation by B cells and thus, the active EAE model cannot properly reflect the importance of B cells in pathogenic processes.

1.2.2 Spontaneous EAE mouse models

To overcome some of these limitations, mouse models with spontaneous EAE development can be studied exhibiting an etiopathology that is more comparable to human disease. During the past years, two spontaneous EAE mouse models were developed. One model on BL6 background combines 2D2 mice, expressing a transgenic MOG₃₅₋₅₅ peptide-specific TCR, with IgH^{MOG} (TH) mice, expressing a BCR derived from a rearranged heavy chain of a MOG-specific antibody [30, 31]. About 60% of 2D2xTH double transgenic mice develop spontaneous EAE around 6 weeks of age. The observed pathology is similar to NMO, characterized by the presence of inflammatory foci restricted to the spinal cord and optic nerve [32, 33]. Therefore, the model was also named opticospinal EAE (OSE) mice. The other mouse model is on the SJL/J background: TCR¹⁶⁴⁰ mice or relapsing-remitting (RR) mice, feature T cells with a transgenic TCR recognizing the MOG₉₂₋₁₀₆ peptide. These T cells recruit MOG-specific B cells from the endogenous immune repertoire. Spontaneous EAE develops within two to three months of age, with an incidence of over 80 % and the majority of mice show a relapsing-remitting (RR) disease course. Thus, TCR¹⁶⁴⁰ mice represent the first spontaneous RR animal model for the most common form of MS in the Western Society [34]. Both spontaneous EAE models develop B cell-dependent disease and offer special advantages over actively induced EAE models due to the less artificial disease induction and the closer resemblance of the human disease. These models allow us to characterize the role of B cells in initiating events in spontaneous EAE, which will provide insight into the pathogenesis of MS.

1.3 Insights in MS disease triggers

1.3.1 T cells in MS and EAE

Both in MS and EAE, T cells play the most important role in the disease development. Demyelination is a key feature in the pathology of MS and therefore myelin protein-derived antigens have been hypothesized to be the main autoreactive targets. The myelin sheath is a greatly extended and modified plasma membrane wrapped around the nerve axon in a spiral fashion and functions as an electrical insulator. It consists of lipids and contains many different proteins. In patients with MS, but also in healthy individuals, myelin proteins like MOG, proteolipid protein (PLP) and myelin basic protein (MBP) have been demonstrated to be recognized by circulating CD4⁺ T cells [35]. Some EAE studies implicate the reactivation of infiltrating CD4⁺ T cells in the CNS by CD11c⁺ dendritic cells (DCs) with the resulting inflammatory response leading to monocyte recruitment, as well as naive CD4⁺ T cell activation that further fuels inflammation [36]. Pestic et al. showed that infiltrating T cells interact with macrophage-like cells rather than DCs, as reported previously [37, 38].

The main CD4⁺ T cell subsets implicated in disease are Th1 and Th17 cells, and in the mouse both subsets can induce disease independently of each other [39]. However, in MS conflicting studies report the predominance of one cell type over the other at initial diagnosis and during subsequent relapses [40, 41]. Compared with controls, in MS patients myelin-reactive peripheral CD4⁺ T cells expressing the CC-chemokine receptor 6 (CCR6) show increased expression of Th1 and Th17 cell signature cytokines IFN- γ and IL-17A [42], indicating that both subsets may contribute to the inflammatory processes. Additionally, lesional CD4⁺ T cells have an intermediate phenotype expressing IFN- γ and IL-17A simultaneously [43], a phenomenon that has also been observed in the mouse and may stem from the substantial plasticity of Th17 cells. Despite these evidences, ustekinumab, an antibody which targets both IL-12 and IL-23 which are crucial for Th1 and Th17 cell differentiation, failed in a Phase II clinical trial in patients with relapsing-remitting MS [44]. There are several hypotheses for the lack of therapeutic efficacy of this antibody. The therapeutic efficacy of ustekinumab might depend on the disease stages. In the EAE model, this antibody was shown to be more effective in the prevention regimen than the therapeutic treatment for established disease [45]. Thus, IL-12/IL-23 might be most important for differentiation and expansion of pathogenic T cells before clinical onset of disease. Additionally, the blood–brain barrier (BBB) might be insufficiently

disrupted in MS compared to EAE and thus, with an approximate molecular weight of 150 kDa, ustekinumab might not have crossed the BBB.

In contrast to EAE, in MS CD8⁺ T cells are found in higher frequencies in white matter and in grey matter cortical lesions than CD4⁺ T cells [3]. CD8⁺ T cells predominate in active MS lesions, and analyses of their TCR repertoire indicate local expansion of the infiltrated cells [46, 47]. These data suggest an active role of CD8⁺ T cells in the formation of MS lesions. Unfortunately, in the vast majority of EAE models the disease is mediated by CD4⁺ T cells, while CD8⁺ T cells are found only in very low frequency in the CNS infiltrates. Thus, their role is difficult to study and poorly understood.

1.3.2 B cells in MS and EAE

In comparison to T cells, infiltrating B cells in the CNS vary in numbers, localisation and pathology throughout disease progression depending on stage and type of MS [48-50]. Clonally expanded B cells can be found in the meninges, and in the perivascular space, but also in parenchyma and CSF. Intrathecal B cells produce antibodies detectable in CSF as oligoclonal bands (OCBs) and to date OCBs are a prominent immunodiagnostic criterion [50]. Plasma cells, which are the main antibody producers, are increased with age in patients with primary and secondary progressive MS [3]. Some patients with secondary progressive MS have aggregates of plasma cells, B cells, T cells and FDCs in the meninges, also called tertiary lymphoid structures which may be a product of long term inflammation [51]. In contrast, meningeal infiltration is diffuse and without structures in primary progressive MS [52].

B cells have several functions through which they could contribute to the pathology of MS. One important function of B cells is their ability to present antigens to T cells in context of major histocompatibility complex class II (MHC II) [53]. If they are specific for the same antigen as the interacting T cell, B cells are 10.000 fold more potent in antigen presentation than DCs, and they are especially effective in presenting low concentrations of antigen [34, 54]. Moreover, B cells can differentiate into antibody-secreting plasma cells that cause tissue damage either via complement activation or antibody-dependent cell-mediated toxicity. Long lived plasma cells produce IgG antibodies which lead to Fc receptor activation on macrophages and DCs, inducing production of cytokines, which attract and activate other immune cells and cause further tissue injury [53].

In most MS patients, the autoantigen is unknown which makes treatment more difficult. The most prominent autoantigens in MS are MOG, neurofascin, contactin and the ATP-dependent inwardly rectifying potassium channel KIR4.1 [55-58]. However, only a fraction of patients shows detectable reactivity against one or several of these antigens. A promising approach for the identification of antigens recognized by antibodies that form oligoclonal bands is to produce recombinant immunoglobulin from B cells or plasma cells that are clonally expanded in CSF [59, 60]. Brändle and colleagues produced six recombinant antibodies from four MS patients and identified three different autoantigens. All of them are conformational epitopes of ubiquitous intracellular proteins not specific to brain tissue. These findings indicate that the B cell response in MS is heterogeneous and partly directed against intracellular autoantigens released during tissue destruction [61]. Another group tried to produce recombinant antibodies from B cell clones from MS CSF in human tissue culture but failed to find immunoreactivity to myelin antigens [59, 60]. These studies demonstrate, that it is still difficult to find target antigens or even potential markers to identify onset of disease development.

Activated B cells can produce pro- and anti-inflammatory cytokines to activate and differentiate T cells and macrophages or block their activation. Pro-inflammatory B cell cytokines include IL-6, IL-12, Granulocyte macrophage - colony stimulating factor (GM-CSF), TNF and lymphotoxin (LT), which modulate T cell differentiation, migration of DCs, activation of macrophages and provide feedback stimulatory signals for further B cell activation. Several studies show an increase of B cells in MS patients producing proinflammatory cytokines [62-64]. Anti-inflammatory B cell cytokines like IL-10 can inhibit T cell or macrophage activation. Recently, a B cell subset that can produce IL-10 and resembles mouse regulatory B cells has been identified in humans [65].

The importance and differential roles of B cells for the development of EAE was shown by depletion experiments. B cells can be efficiently depleted by antibodies targeting the surface marker CD20. While anti-CD20-mediated B cell depletion before the induction of active EAE exacerbated disease symptoms, depletion of B cells during disease progression profoundly suppressed symptoms. The increased severity of EAE with early B cell depletion resulted from an increased influx of encephalitogenic T cells into the CNS, due to the depletion of the rare IL-10-secreting CD1d^{hi}/CD5⁺ regulatory B cell subset. During late depletion, B cells that promoted continuous generation of autoantigen-specific CD4⁺ T cells and sustained entry of encephalitogenic T cells into the CNS were removed from the system [66]. Thus, B cells can have dual functions: either in driving autoimmunity as

APCs, by producing autoantibodies, or by secreting inflammatory cytokines, such as IFN- γ and IL-6; or in suppressing autoimmunity as IL-10 producing regulatory B cells, dampening the inflammatory potential of effector T cells or modulating the activity of other surrounding APCs [67].

Antigen presentation by B cells is of particular importance for the T – B cell crosstalk observed in the spontaneous EAE models mentioned before. IgH^{MOG} B cells in the OSE mouse model can concentrate MOG with their antigen-specific BCR, and efficiently present it to MOG-reactive T cells. This results in mutual activation, proliferation, and differentiation, and B cells of those mice switch their isotype and produce high titers of MOG-specific IgG1 autoantibodies, while T cells in the CNS secrete more IFN- γ and IL-17 than single-transgenic controls [32]. In the TCR¹⁶⁴⁰ (RR) mouse model, MOG-specific B cells from the endogenous repertoire are recruited by MOG-reactive transgenic T cells and are driven into germinal center reactions, leading to the appearance of spontaneous anti-MOG autoantibodies in the serum of these mice [34, 68]. In addition to T cells, in the RR model B cells infiltrate into the CNS parenchyma, too. Deposits of antibodies along with some activated complement can be found in demyelinated lesions of diseased RR mice. The recruitment of MOG-specific B cells is strictly dependent on the presence of the target antigen, since TCR¹⁶⁴⁰ mice deficient for MOG do not develop RR-EAE nor show any corresponding autoantibodies [34]. In addition, early infiltration of T and B cells into the CNS of RR mice could already be found at pre-clinical stages at an age of four weeks, and anti-MOG autoantibodies were present in the serum at around five weeks after birth. Active germinal centers were found in cervical lymph nodes of RR mice, and MOG-specific B cells (IgH^{MOG}) preferentially migrated to GCs in cervical lymph nodes but not to other lymphoid organs [68]. This could be due to myelin debris draining from the subclinically inflamed CNS or being transported by phagocytes to cervical lymph nodes. This would induce further activation of MOG-specific T cells, which then in turn drive MOG-specific B cells into germinal center reactions, resulting in a full attack on the target organ by autoreactive T cells along with the emergence of isotype class switched autoantibodies [69].

In summary, B cells have multifunctional immunomodulatory effects in pathogenesis of MS suggesting that modulation of specific B cell functions may be an interesting therapeutic target. Currently, several therapies affect B cell immunology. Phase II clinical trials with the CD20-specific monoclonal antibodies rituximab or ocrelizumab have shown great efficacy of B cell depletion therapy to reduce relapse rates in patients with relapsing-

remitting MS [70, 71]. These drugs deplete the majority of B cell subsets but not plasma cells indicating that the role of B cells as antigen presenting cells and cytokine producers may be more important in disease development and progression than their role as antibody producers.

1.3.3 Antigen transport and priming of autoreactive lymphocytes in MS and EAE

Auto-antigen presentation followed by activation of autoreactive B and T cells is a crucial event in the development of EAE and MS. There are several potential locations where autoreactive B and T cells could find their antigen. One option is that autoreactive B and T cells find antigens directly in the CNS, meaning there is initially no antigen transport to regional lymph nodes or only after inflammation has started, causing the BBB to become leaky. Another option is that antigens are transported to regional lymph nodes - either in soluble form, via APCs or exosomes - and activate B and T cells there, which then migrate to the CNS in search of antigen. In another scenario, activation of autoreactive immune cells could take place in the intestine *via* molecular mimicry or bystander activation (Figure 1) followed by migration to the target organ.

A current theory is that APCs or soluble auto-antigens can migrate from the CNS to regional lymph nodes and initiate an autoimmune response [72]. Lymph nodes close to the CNS include superficial CLNs (sCLN), and deep CLNs (dCLN). Cells and antigens from the brain could reach CLNs either by entering the nasal lymphatics via the drainage channels leading from the subarachnoid space inferior to the olfactory bulbs to the cribriform plate. Alternatively, they can enter blood vessels through the arachnoid villi of the venous sinuses [73]. Previous studies with rats showed that radioiodinated serum albumin injected into brain and cerebrospinal fluid (CSF) drains to CLNs [74]. Furthermore, monocytes and dendritic cells (DCs) are able to migrate from CSF to CLNs when injected [73, 75]. In addition to these drainage pathways, Louveau et al. recently discovered lymphatic vessels lining dural sinuses, which express all molecular hallmarks of lymphatic endothelial cells, are able to drain immune cells from CSF, and are connected to dCLNs [76]. However, if cells and auto-antigens also migrate from the CNS to CLNs in EAE and MS, and whether that could be an important mechanism for the induction of disease is still not fully understood.

Immune reactions in CLNs have been suggested to play a significant role in EAE development. Phillips and colleagues demonstrated that the removal of CLNs decreases

the lesion number in the brain in a cryolesion-induced cerebral EAE model in rats by 40 % [77]. In addition, surgical removal of CLNs and lumbar lymph nodes in acute, chronic, and chronic-relapsing EAE reduced disease in all models, most strikingly in chronic-relapsing EAE [78]. Furthermore, in human brain-derived antigens can be found in CLNs after stroke [79] indicating a specific drainage pathway. The auto-antigen MBP, neural lipids and PLP are present in the CLNs of marmoset monkeys with MOG-induced EAE and patients with MS [80, 81]. Moreover, neuronal antigens like microtubule-associated protein 2 (MAP-2), neuron specific enolase (NSE) and neurofilament (NF-H) were found in CLNs of MS patients [80]. Collectively, these studies support the hypothesis that antigen-specific immune responses in CLNs are important for initiating disease. However, when, how and along which pathway myelin proteins are transported from the brain into the CLNs has not been clearly demonstrated yet.

One mechanism how CNS auto-antigens could be transported in EAE and MS is by exosome formation. Exosomes are small membrane vesicles of about 150 nm in size, generated by the endosomal system and released directly from the plasma membrane or upon fusion of multivesicular bodies (MVBs) with the plasma membrane [82]. Immune cells like dendritic cells and B cells, but also non-immune cells, including astrocytes and oligodendrocytes, are able to secrete exosomes. Consequently, body fluids like serum, urine and CSF contain high amounts of microvesicles [83]. Exosomes can carry cell-type specific components such as integrins, tetraspanins (CD9, CD63), proteins involved in MVB biogenesis (Alix, Tsg101), but also mRNAs and miRNAs which can alter protein expression [84, 85]. Importantly, exosomes are able to migrate between cells, and could thus act as a transportation system for different antigens like MBP, PLP, and MOG [86, 87]. Possibly, exosomes could indirectly trigger an autoimmune T cell response after being taken up and thus delivering the autoantigen to APCs such as DCs or macrophages, which in turn present the autoantigens on their surface to activate T cells [87]. In addition, several studies have shown that exosomes can also directly present antigen in complex with MHC class II to T cells and modulate immune functions [82, 88, 89]. For example, insulinoma-released exosomes in the non-obese diabetic (NOD) mouse model can activate autoreactive T cells and may cause insulinitis [86]. Taken together, studies for the possible involvement of exosomes in transport of autoantigens are highly relevant.

APCs and exosomes may present autoantigens to activate autoreactive B and T cells. However, also peptides/epitopes from microbes could potentially cross-activate autoreactive T or B cells due to sequence similarities between “self” and pathogen-

derived peptides/epitopes, a phenomenon which is called molecular mimicry [90]. Furthermore, it has been shown that autoreactive T cells are activated *de novo* by self epitopes released secondary to pathogen-specific T cell-mediated bystander damage [91]. Humans carry $3.8 \cdot 10^{13}$ microorganisms, a value of about 1:1 to the total number of human cells in the body [92]. These microorganisms live in symbiosis with their hosts contributing to the digestion and fermentation of carbohydrates, and production of vitamins. In addition, they also protect the host from colonization with pathogenic microbes and shape the hosts immune system [93-95]. Thus, the microbiota is important for the development of gut-associated lymphoid tissues (GALTs) and responsible for Peyer's Patch size and organization in germ-free mice compared to colonized controls [96]. On the other hand, the host's innate immune system also shapes the intestinal ecosystem. As a consequence, complex interactions between the microbiota and the host immune system are essential for gut homeostasis [93]. Environmental factors like diet and lifestyle can disturb the balance of the microbiota [97], and an imbalance can affect the host immune system and disease [98]. For instance, it has recently been shown that rheumatoid arthritis and type I diabetes are linked to an altered composition of gut microbiota [99, 100]. First studies also hint towards an important role of the microbiota in EAE development. The early events that lead to the development of MS as well as EAE are not well understood. Accumulating evidence indicates that composition of commensal microbiota could be relevant for the induction of autoimmunity [101]. Thus, it has been shown that oral treatment with antibiotics reduces the symptoms of EAE and induces a protective population of CD5⁺ B cells [102, 103]. Furthermore, relapsing-remitting (RR) mice are fully protected from spontaneous EAE, when housed under germ-free conditions, suggesting that the microbiota contribute somehow to the generation of a pathogenic autoimmune response in this model [68]. Additionally, microbiota derived from MS patients in a twin study (one twin healthy, the other has MS) gavaged to RR mice triggered a higher spontaneous EAE incidence than the microbiota derived from the healthy twin [104]. The colonized mice had different microbial profiles and recipients of MS-twin samples produced less IL-10 indicating an immunomodulatory effect of microbiota in MS disease. These findings prompted us to hypothesize that auto-reactive B and T cells may initially be activated in the gut either by bystander activation or *via* molecular mimicry by microbial antigens and consequently migrate to the CLNs and/or the CNS to promote the development of EAE.

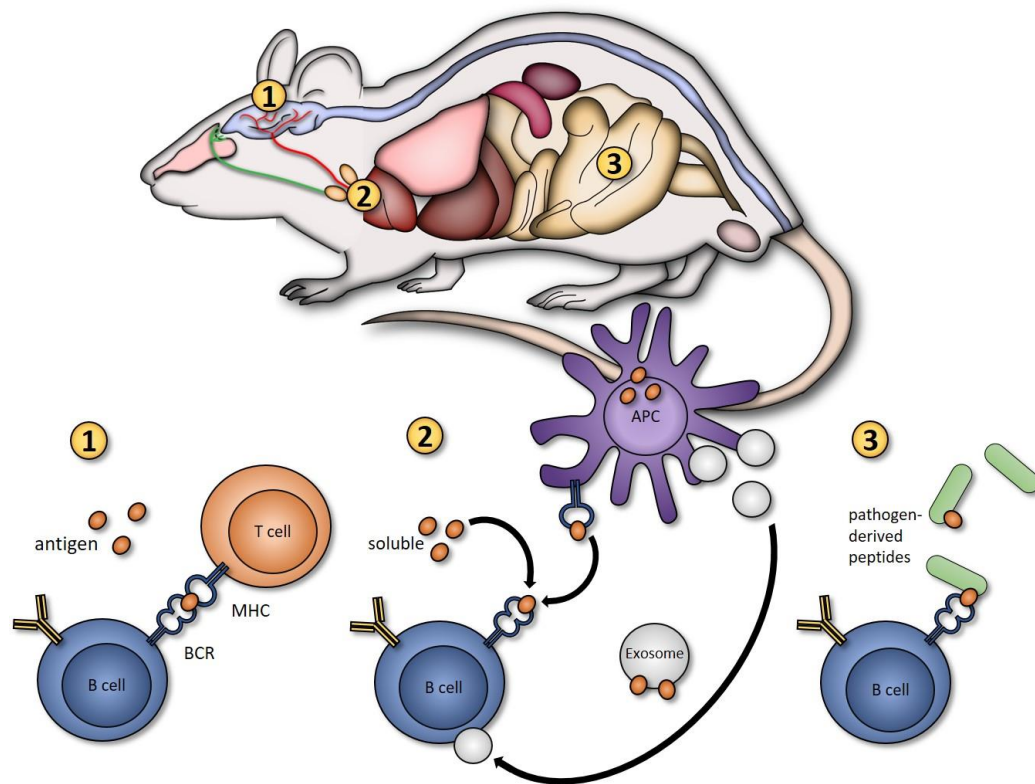


Figure 1: Potential locations for activation of autoreactive B cells in the RR mouse model

In RR mice MOG-specific B cells are recruited from the endogenous immune repertoire. When and where B cells become activated is still unknown. Possible autoreactive B cell activation sites could be CNS (1), CLNs (2) or the gut (3). (1) In CNS, B cells could be activated through antigen presentation. (2) Antigens could be alternatively transported to CLN *via* APCs, exosomes, or in soluble form. (3) Furthermore, B cells could be activated in the gut by molecular mimicry or bystander activation (created by Bettina Martin).

OBJECTIVE

In the RR mouse model, T cells recruit MOG-specific B cells from the endogenous immune repertoire and EAE develops spontaneously in a B cell-dependent manner within two to three months of age with a relapsing-remitting (RR) disease course. Thus, the RR mouse represents an excellent animal model for the most common form of MS. This model raises general questions regarding when and where autoreactive B cells become activated during EAE and MS, and which effector functions and molecular mechanisms contribute to B cell pathogenicity.

Regarding the site of activation there are several options in the RR mouse model, which may also be relevant in other EAE models as well as in MS: first, B cells could be activated directly in the CNS, migrate to regional lymph nodes and undergo proliferation and differentiation. Second, antigens from the CNS may be transported to regional lymph nodes where they activate B cells, which then undergo proliferation and differentiation. Or third, B cells are activated in the periphery, possibly the intestine, and then recruited to CNS related lymph nodes. Therefore, one objective of the present study was to examine antigen transport and priming of autoreactive lymphocytes in spontaneous EAE. Firstly, transport and presence of myelin antigens in peripheral CLNs in RR mice was investigated with several methods, as well as exosomes as a potential transportation system for myelin antigens and their involvement in initiating MOG-specific T and B cell responses in EAE. Secondly, activation of autoreactive B cells in the gut as the site of initial priming *via* molecular mimicry or bystander activation was studied with secondary recruitment to CLNs during development of spontaneous EAE.

Regarding pathogenic B cell effector functions and properties in EAE and MS, several aspects have to be considered including production of pathogenic antibodies, presentation of autoantigen to autoreactive T cells and production of cytokines. However, functional studies have so far been hampered by limited possibilities to expand, differentiate and manipulate B cells *in vitro*. Thus, the second objective of this study was to establish a new cell culture system for B cell expansion, differentiation and specific selection to overcome current limitations to study autoreactive B cells. With this new tool it is now possible to study origin, migration and repertoire of auto-reactive B cells from RR mice and to study/manipulate pathogenic properties of auto-reactive B cells in EAE.

2 MATERIAL AND METHODS

2.1 Material

2.1.1 Animals

All animals used in this study were bred in the animal facilities of the Max-Planck-Institutes of Biochemistry and Neurobiology. The animal procedures were in accordance with guidelines of the committee on animals of the Max-Planck-Institute of Neurobiology, and with the licenses of the Regierung von Oberbayern.

2D2 mice

MOG-specific TCR transgenic mouse on the C57Bl/6 background: CD4⁺ T cells express a transgenic TCR recognizing MOG₃₅₋₅₅ peptide in the context of I-A_b [30].

Actin GFP mice

Transgenic strain carrying the Green Fluorescent Protein (GFP) under the control of the chicken beta-actin promoter and human cytomegalovirus (CMV) intermediate early enhancer. The transgene was found on the X chromosome [105].

H2M mice

For the generation of transgenic MOG over expressing mice (H2M), the entire coding region of murine MOG from mouse brain cDNA was amplified by RT-PCR using the primers SaMOG: 5'-ACGCGTCGACCTCAGCTTGGCCTGACCC-3' and BgMOG: 5'-CGAAGATCTGCTGGGCTCTCCTT-CCGC-3' which bear the restriction sites Sal I and Bgl II, respectively. The amplified cDNA was inserted into the sites Sal I and Bgl II of the vector pHSE3' containing H2-Kb promoter and immunoglobulin heavy chain enhancer for transgenic expression. The transgenic mouse was obtained by pronuclear microinjection of a purified Xho I DNA fragment into C57BL/6 oocytes and a founder mouse that expressed the transgene was bred with C57BL/6 mice [106].

HEL mice

SW_{HEL} mice carry B cells with a hen egg lysozyme (HEL)-specific heavy chain and light chain genes in knock-in and transgenic configurations [107] resulting in HEL-specific B cells that are still able to switch isotype.

PLP-eGFP mice

EGFP was fused to 3'UTR of the PLP promoter. Three founder lines were selected (EGFP3, EGFP5 and EGFP10) and bred homozygously. It was shown previously that transgene expression of EGFP together with PLP is consistent in all stages of oligodendrocyte differentiation. Mice were provided by Prof. Dr. Martin Kerschensteiner [108].

R&D mice

R&D mice were created by Marsilius Mues. The R&D mouse is a valuable tool to study B cell functions in EAE since B cells express red fluorescent protein (RFP) for in vivo tracking, and the human Diphtheria toxin receptor (DTR), which allows for depletion of B cells at any given timepoint via administration of diphtheria toxin [109]. A tandem dimer RFP (tdRFP) was chosen that is suitable for sustained and high expression in murine lymphocytes. TdRFP consists of two monomeric RFPs interlinked by a flexible linker. For simultaneous expression of tdRFP and DTR (termed R&D), both genes were placed in succession, separated by an internal ribosomal entry site (IRES), and subcloned into the cytomegalovirus (CMV) promoter-driven expression vector pCMV to obtain pCMV-R&D.

RR mice

TCR¹⁶⁴⁰ mice feature T cells with a transgenic TCR recognizing the MOG92-106 peptide in the context of I-A_g on the SJL/J background [34].

TH mice

This mouse model expresses a BCR, derived from a rearranged heavy chain of a MOG-specific antibody [31, 32]. The mouse was generated as a knock-in mutant, in which the VDJ region of the MOG-specific H chain from the hybridoma 8.18-C5 was inserted into the natural location of rearranged V genes in the H gene locus. MAb 8.18-C5 mediates demyelination both *in vitro* and *in vivo* [110, 111] and exacerbates clinical disease in EAE [112]. In mature mutant mice the transgenic Ig H chain is expressed in almost all B cells, resulting in a high frequency of MOG-specific B cells (80-90 %) and high levels of MOG-specific Ig in the serum. Importantly, TH B cells can undergo normal isotype switching and – due to the endogenous pool of light chains – a certain degree of affinity maturation.

2.1.2 Antibodies

ELISA antibodies were purified or biotinylated and used in conjunction with streptavidin coupled with HRP.

Table 1: Capture antibodies and proteins for Ig-ELISA

Specificity	Label	Clone	Host/Isotype	Dilution	Company (Catalog Number)
Rat α -m IgM	Purified	II/41	Rat IgG2a, κ	1:500	BD Biosciences (553435)
Rat α -m IgG1	Purified	A85-3	Rat IgG1, κ	1:500	BD Biosciences (553445)
rMOG	Purified	-	Produced in bacteria	10 μ g/ml	In house

Table 2: Standard antibodies for Ig-ELISA

Specificity	Label	Clone	Host/Isotype	Dilution	Company (Catalog Number)
Mouse IgM i.c.	Purified	G155-228	BALB/c IgM, κ	1:500	BD Biosciences (553472)
Mouse IgG1 i.c.	Purified	107.3	BALB/c IgG1, κ	1:500	BD Biosciences (553447)
MOG (8.18c5)	Purified	8.18c5	Mouse mIgG1a	1 μ g/ml	In house produced [113]

Table 3: Detection antibodies for Ig-ELISA

Specificity	Label	Clone	Host/Isotype	Dilution	Company (Catalog Number)
Rat α -m IgM	Biotin	R6-60.2	LOU/M IgG2a, κ	1:1000	BD Biosciences (553406)
Rat α -m IgG1	Biotin	A-85	LOU/M IgG1, κ	1:1000	BD Biosciences (553406)
Mouse IgG1 [a]	Biotin	10.9	SJL IgG2a, κ	1:1000	BD Biosciences (553500)
Mouse IgM [a]	Biotin	DS-1	C57BL/6 IgG1, κ	1:1000	BD Biosciences (553515)
Streptavidin	HRP	-	-	1:2000	BD Biosciences (18-4100-51)

Flow cytometry antibodies were labeled with eFluor450, FITC, PE, PerCP, PE-Cy7, APC, APC-Cy7, BV 605, Alexa Fluor 647, or were biotinylated and used in conjunction with streptavidin coupled fluorophores.

Table 4: Primary antibodies and reagents for FACS

Specificity	Label	Clone	Host/Isotype	Dilution	Company (Catalog Number)
7AAD	PerCP	-	Viability dye	3 μ l/well	BioLegend (420404)
B220 (CD45R)	PerCP	RA3-6B2	Rat IgG1, κ	1:200	Pharmigen (01125B)
BAFF	FITC	Buffy-2	Rat IgM	1:100	Abcam (ab16082)
CD4	PerCP BV605	RM4-5	Rat IgG2a, κ	1:200	BD Biosciences (45-0042-82) BioLegend (100547)
CD9	APC	M-L13	Rat IgG2a, κ	1:200	Becton Dickinson (341648)
CD11b	PE-Cy7	M1/70	Rat IgG2b, κ	1:200	BioLegend (101215)
CD11c	BV 605	N418	Ar Ham IgG	1:200	BioLegend (117334)

CD19	FITC PerCP eFluor450	1D3	Rat IgG2a, κ	1:200	Pharmigen (553785) BD Biosciences (45-0193-82) BD Biosciences (48-0193-82)
CD38	eFluor 450	-	Rat IgG2a, κ	1:200	BD Biosciences (48-0381-82)
CD40L (CD154)	PE	MR1	Ar Ham IgG3, κ	1:200	Pharmigen (553658)
CD45	eFluor 450	30-F11	Rat IgG2b, κ	1:200	BD Biosciences (48-0451-80)
CD45.1	FITC	A20	Mouse IgG2a, κ	1:200	BD Biosciences (11-0453-82)
CD45.2	APC	104	Mouse IgG2a, κ	1:200	BD Biosciences (17-0454-81)
CD63	PE	NVG-2	Rat IgG2a, κ	1:200	BioLegend (143903)
CD80	PE	16-10A1	Ar Ham IgG	1:200	BioLegend (104707)
CD86	Biotin	GL1	Rat IgG2a, κ	1:200	BD Biosciences (13-0862-82)
CD90.2	Biotin	30-H12	Rat IgG2a, κ	1:200	BD Biosciences (13-0903-82)
CD95 (Fas)	PE-Cy7	Jo2	Ar Ham IgG2	1:200	Pharmigen (557653)
CD95L (FasL)	PE	MR1	Mouse IgG	1:200	BD Biosciences (12-1541-82)
CD138	PE APC	281-2	Rat IgG2a, κ	1:200	Pharmigen (553713) Pharmigen (558626)
GL7	Alexa Fluor 647	GL7	Rat IgM	1:200	BD Biosciences (50-5902-82)
H-2kb (MHCI)	FITC	AF6- 88.5.5.3	Mouse IgG2a, κ	1:200	BD Biosciences (11-5958-80)
H-2kd (MHCI)	PerCP	SF1-1.1	Mouse IgG2a, κ	1:200	BioLegend (116618)
HEL	Biotin	-	-	1:100	Sigma (L6876)
IgA	PE	11-44-2	Rat IgG1, κ	1:200	BD Biosciences (12-5994-82)
IgD	FITC	11-26c.2a	Rat IgG2a, κ	1:200	Pharmigen (553439)
IgE	PE	RME-1	Rat IgG1, κ	1:200	BioLegend (406907)
IgG1	BV 605	A85-1	Rat IgG2a, κ	1:200	BD Horizon (563285)
IgG2a/b	FITC	R2-40	Rat IgG1, κ	1:200	Pharmigen (553399)
IgM	PE-Cy7	II/41	Rat IgG2a, κ	1:200	BD Biosciences (25-5790-82)
IgMa	PE	DS-1	C57BL/6 IgG1, κ	1:200	BD Bioscience (553517)
mMOG	FITC	-	Produced in HEK cells	1:100	In house produced [114]
MOG (8.18c5)	Purified	8.18c5	Mouse mIgG1a	1:200	In house produced [113]
MOG (Z2)	FITC	Z2	Mouse mIgG1a	1:100	In house produced [115]
MOGtet	FITC, PE	-	-	1:100	In house produced [114]

PNA	Biotin	-	-	1:200	Vector (B-1075)
V α 3.2	APC	RR3-16	Rat IgG2b, κ	1:200	BD Biosciences (553218)
V α 8.3	PE	B21.14	Rat IgG2b, κ	1:200	BD Biosciences (12-5803-82)
V β 4	FITC	KT4	Rat IgG2b, κ	1:200	BD Biosciences (553365)
V β 11	PE	RR3-15	Rat IgG2b, κ	1:200	BD Biosciences (553198)

Table 5: Secondary antibodies and reagents for FACS

Specificity/Anion	Label	Clone	Host/Isotype	Dilution	Company (Catalog Number)
Azide	Alexa Fluor 647	-	-		Thermo Fisher (A10277)
Streptavidin	PE APC-Cy7	-	-	1:1000	Pharmigen (554061) BD Biosciences (47-4317-82)

IHC antibodies were labeled with Alexa Fluor 488, 568 or 647, or were biotinylated and used in conjunction with streptavidin coupled fluorophores.

Table 6: Primary antibodies for IHC

Specificity	Label	Clone	Host/Isotype	Dilution	Company (Catalog Number)
B220	Purified Biotin	RA3-6B2	Rat IgG2a, κ	1:200	Pharmingen (550286) Pharmingen (553085)
CD4	Alexa Fluor 647	RM4-5	Rat IgG2a, κ	1:200	BioLegend (100530)
CD11b	AlexaFluor 647	M1/70	Rat IgG2a, κ	1:200	BioLegend (101220)
CD68	Alexa Fluor 647	ED1	Mouse IgG1	1:20	Biorad (MCA341A647)
MBP	Purified	Polyclonal	Rabbit IgG	1:200	Abcam (ab40390)
MOG (8.18-C5)	Biotin	8.18-C5	Mouse IgG1	1:200	In house hybridoma
MOG (Z2)	Biotin	Z2	Mouse IgG2a	1:500	In house hybridoma
MOG Fab ₂	Biotin	Z2	Mouse IgG2a	1:200	In house hybridoma
Mouse IgG1	Biotin	A85-1	Mouse IgG1	1:200	Pharmigen (553441)
PLP	Purified	Polyclonal	Rabbit IgG	1:200	Abcam (ab28486)
Rabbit IgG	Purified	-	Rabbit IgG	1:200	Dako (Z025902-2)
Rat IgG2a	Purified	DD13	Rat IgG2a, κ	1:200	Millipore (CBL605)

Table 7: Secondary antibodies and reagents for IHC

Specificity	Label	Clone	Host/Isotype	Dilution	Company (Catalog Number)
Rat IgG	Alexa Fluor 488	Polyclonal	Goat IgG	1:1000	Invitrogen (A-11006)

Rat IgG	Alexa Fluor 568	Polyclonal	Goat IgG	1:1000	Invitrogen (A-11077)
Rabbit IgG	Alexa Fluor 488	Polyclonal	Goat IgG	1:1000	Abcam (ab150077)
Streptavidin	Alexa Fluor 488	-	-	1:1000	Invitrogen (ab150077)
Streptavidin	Alexa Fluor 568	-	-	1:1000	Invitrogen (S-11226)

Western Blot antibodies were purified and used in conjunction with anti-species IgG secondary antibody coupled with HRP.

Table 8: Primary antibodies for Western Blot

Specificity	Label	Clone	Host/Isotype	Dilution	Company (Catalog Number)
Alix	Purified	49/AIP1	Mouse IgG1	1:300	BD Biosciences (611620)
Calnexin	Purified	3H4A7	Mouse IgG2b	1:1000	Santa Cruz (sc-130059)
MOG (8.18-C5)	Purified	8.18-C5	Mouse IgG1	1:500	In house hybridoma
Tsg101	Purified	C-2	Mouse IgG2a	1:500	Santa Cruz (sc-7964)

Table 9: Secondary antibodies for Western Blot

Specificity	Label	Clone	Host/Isotype	Dilution	Company (Catalog Number)
Goat IgG	HRP	-	Donkey	1:2000	Santa Cruz (sc-2020)
Mouse IgG	HRP	-	-	1:2000	Cell signaling (7076S)
Rabbit IgG	HRP	-	-	1:2000	Santa Cruz (sc-32906)

2.1.3 Buffers and solutions

Buffers for ELISA

Phosphate Buffered Saline (PBS)

137 mM NaCl

10 mM Na₂HPO₄

1.8 mM KH₂PO₄

2.7 mM KCl

Add ddH₂O, pH to 7.2 with HCl

Washing solution

0.05% (v/v) of Tween-20 in PBS

Blocking solution

10% (v/v) fetal bovine serum in PBS

TMB Substrate and Stop solution

TMB Substrate Set (A and B) – BioLegend (421101), store at 4°C

TMB Stop solution – BioLegend (423001), store at RT

Buffers for FACSFACS staining buffer

1% (w/v) BSA, 0.1% (w/v) sodium azide in PBS

Intracellular cytokine staining buffer

FACS buffer + 0.1% Saponin or Fixation and Permeabilization Buffer KIT (eBioscience, 00-5523-00)

Buffers for ImmunohistochemistryBlocking solution

4% (w/v) BSA+ 4% (v/v) goat serum in PBS

Staining and washing solution

1% (w/v) BSA + 1% (v/v) goat serum in PBS

Buffers for Western BlotCell lysis buffer (native)

150 mM NaCl, 20 mM Tris-HCl, 1% (v/v) Triton-X 100

RIPA buffer

50 mM Tris-HCl, pH 7.5, 150 mM NaCl, 1 mM EDTA, 1% Triton-X 100, 0.5% (w/v) sodium deoxycholate, 0.1% (w/v) SDS

Lämmli running buffer 10x

250 mM Tris-base, pH 8.8, 1% (w/v) SDS, 1.92 M glycine

Lämmli loading buffer 2x

200 mM Tris-HCl, pH 6.8, 10% SDS, 10% (v/v) glycerol, 10%-ME, bromophenol blue as needed

Anode buffer I

300 mM Tris, pH 10.4, 20% (v/v) methanol

Anode buffer II

25 mM Tris, pH 10.4, 20% (v/v) methanol

Cathode buffer

25 mM Tris, pH 9.4, 40 mM 6-aminohexanoic acid, 20% (v/v) methanol

Erythrocytes lysis and lymphocyte extraction from CNS and intestineACK buffer

150 mM NH₄Cl, 10 mM KHCO₃, 0.1 mM EDTA

Percoll (GE Healthcare)

Stock Isotonic Percoll (SIP): 9 parts (v/v) Percoll + 1 part (v/v) of NaCl 1.5 M (d=1.123)

Percoll d=1.080: 10 ml SIP + 5.7 ml PBS

Genotyping analysis buffersHeparin solution

200 units heparin (Sigma) in PBS

Mouse tail digestion buffer

100 mM Tris-HCl, pH 8.5, 200 mM NaCl, 5 mM EDTA, 1% Tween-20, 1 mg/ml Proteinase K

TAE running buffer

40 mM Tris-HCl, 40 mM acetic acid, pH 8.0, 1 mM EDTA

DNA loading dye 10x

50 mM Tris-HCl, pH 7.6, 60% (v/v) glycerol, 0.05% (w/v) bromophenol blue, 0.05% (w/v) xylene cyanol FF

2.1.4 Cell culture40LB cells

40LB cells were created in the Kitamura lab [116]. BALB/c 3T3 fibroblast were transfected with mouse CD40L cDNA cloned into the expression vector pAuro2. Stable clones were selected by puromycin (40L cells). 40L cells were transfected with BAFF cDNA cloned into pCA-neo vector and selected with G418 (40LB cells).

Bone marrow derived dendritic cells (BMDCs)

BMDCs were isolated from either C57BL/6 or from H2M mice (2.1.4 and 2.2.1).

EL4 and EL4 MOG cells

EL4 cells were originally isolated from a T cell lymphoma induced in a C57BL/6 mouse by 9,10-dimethyl-1,2-benzanthracene treatment (suspension cells) and are commercially available. For EL4-MOG cells, the mouse MOG cDNA was cloned into the retroviral vector pLXSN (Clontech Laboratories, Inc.) and transformed into a GP+E-86 packaging cell line. Virus-containing supernatant was used to stably transduce the mouse EL4 lymphoma cell line [34].

FasL cells

FasL cells were created in the Kitamura lab [29]. 40LB cells were first transduced with pSIREN-RetroQ-shFas vector and consequently Fas negative cells were further transduced with pMX-FasLIRE5-hCD8 vector. A single clone expressing FasL and hCD8 was obtained by limiting dilution assay.

HEL-40LB cells

HEL-40LB cells were created in the Kitamura lab [117]. 40LB cells were transduced with the pMX-mHEL-IRES-GFP vector, and a single clone expressing mHEL and eGFP, termed 40LB-mHEL, was selected by limiting dilution.

MOG-40LB cells and MOG-FasL cells

Cell lines were created via viral transduction by Anneli Peters. Phoenix cells were transfected with pLXSN-MOG and pCLEco and cultured for virus production. Afterwards feeder cells were infected with virus-containing supernatant from phoenix cells. Expression of MOG was determined by FACS and high expressors were cloned in a limiting dilution assay.

2.1.5 Media

Medium for exosome collection

FCS was either centrifuged at 100,000 rcf 4 °C ON and filtered, or RPMI complemented medium was prepared without FCS to remove exosomes from medium, which influences exosome analysis and production from other cells.

Medium for iGB cell culture

RPMI 1640 (Sigma-Aldrich, Taufkirchen) were complemented with 100 µM MEM non-essential amino acids, 1 mM sodium pyruvate, 50,000 units penicillin, 50 mg streptomycin, 2 mM L-glutamine (all Gibco, Karlsruhe), 10mM HEPES (Sigma) and 10% fetal calf serum (FCS)

(Lot 094M3277 Sigma). RPMI 1640 medium was further complemented with 550 μ M 2-ME. Prior to use FCS was inactivated for 1 h at 56°C. Media were sterilized by filtration (pore size 0.2 μ m). All quantities refer to 500 ml of medium.

Medium for intestine preparation

CMF/Hepes Buffer (500ml)

10% (v/v) 10 x HBSS

10 mM Hepes

Add ddH₂O up to 500 ml (For CMF/Hepes/EDTA Buffer add additionally 5 ml EDTA 0.5 M)

RPMI-10

10 mM Hepes

5% (v/v) FCS

Add ddH₂O up to 500 ml

RPMI and DMEM medium (complemented)

Media RPMI 1640 and DMEM (both Sigma-Aldrich, Taufkirchen) were complemented with 100 μ M MEM non-essential amino acids, 1 mM sodium pyruvate, 50,000 units penicillin, 50 mg streptomycin, 2 mM L-glutamine (all Gibco, Karlsruhe), and 10% FCS (Biochrome, Berlin). RPMI 1640 medium was further complemented with 200 μ M 2-ME. Prior to use FCS was inactivated for 1 h at 56°C. Media were sterilized by filtration (pore size 0.2 μ m).

2.1.6 Primers

Table 10: Primers for qPCR mMOG Exon1-3

Primer name	Gene	Oligo sequence (5' → 3')	Label	References
mMOG sense #8	MOG	GTGCTGACTCTCATCGCACTTG	FAM/TAMRA	-
mMOG AS #9	MOG	GCACCCTCAGGAAGTGAGGAT	FAM/TAMRA	-
mMOG Probe #10	MOG	CGTGCAAGAAGTAGAGAATCTCCATCGGAC	FAM/TAMRA	-
mMog-Exon 1-sense #17	MOG	CTTGGAGGAAGGGACATGCA	FAM/TAMRA	Taqman-Mog Exon1
mMog-Exon 1-AS #18	MOG	CTC CAC AAA CAG GCC ATC TTT AT	FAM/TAMRA	Taqman-Mog Exon1
mMog-Exon 1-Probe #19	MOG	AGGACCTCAGCTTGGCCTGACCCT	FAM/TAMRA	Taqman-Mog Exon1
mMog-Exon 2-sense #14	MOG	CCCATCCGGGCTTTAGTTG	FAM/TAMRA	Taqman-Mog Exon2

mMog-Exon 2-sense #15	MOG	GCC CGT GGC ATT TTT CC	FAM/TAMRA	Taqman-Mog Exon2
mMog-Exon 2-sense #13	MOG	CAGAGCTGCCGTGCCGCATC	FAM/TAMRA	Taqman-Mog Exon2

2.2 Methods

2.2.1 Animal Routine

Alum immunization

Mice were injected with 100 µg of rMOG i.p. in 200 µl per mouse. Protein is in 10% alum $KAl(SO_4)_2$ (Sigma) with 5 N NaOH (Merck). The precipitated protein solution and the alum 1:1 were calibrated to a pH of 6.5-7.5 with NaOH (Merck). Then, the precipitated protein was incubated on ice for 30 min, washed 2 times with PBS and resuspended in PBS for i.p. injection.

EAE induction

EAE was induced by injecting the mice subcutaneously into the tail base with 200 µl of emulsion containing 200 µg MOG₃₅₋₅₅ peptide (MEVGWYRSPFSRVVHLYRNGK) and 500 µg M. tuberculosis H37 Ra (Difco) in incomplete Freund Adjuvant oil (Difco). In addition, the mice received 400 ng pertussis toxin (List Biological Laboratories) intraperitoneally (i.p.) on days 0 and 2 after immunization. Clinical signs of EAE were assessed daily according to the following criteria: score 0 – no disease; score 0.5 – reduced tail tonus; score 1 – limp tail; score 1.5 – limp tail and ataxia; score 2 – limp tail, ataxia and hind limb weakness; score 2.5 – at least one hind limb paralyzed/weakness; score 3 – both hind limbs paralyzed/weakness; score 3.5 – complete paralysis of hind limbs; score 4 – paralysis until hip; score 5 – moribund or dead.

Genotyping

Transgenic mice were genotyped either by tail biopsy digested ON in tail digestion buffer followed by phenol-chloroform extraction of DNA (Roth, Karlsruhe) and PCR with transgene-specific primers; by FACS analysis of PBMCs for expression of fluorophores or presence of certain surface markers; or by whole mount illumination to test for ubiquitous fluorophore expression in the skin in a custom-built illumination chamber.

Intrathecal injection

Dextran-FITC, Dextran AlexaFluor 488, 657 or mMOG FITC were intrathecally injected (Cisterna magna) into anesthetized mice. 8h later organs were taken for further analysis.

Leukocyte isolation from peripheral blood

3 to 6 drops of blood were collected from anesthetized mice by retro-orbital bleeding into 100 µl of 200 U/ml heparin (Sigma-Aldrich) in PBS. Erythrocytes were lysed by incubation in 1 ml ACK buffer (5 min, RT) and leukocytes were spun down (500 rcf, 5 min, 4 °C). After repeating the ACK incubation and centrifugation, leukocytes were finally resuspended in 150 µl FACS buffer.

Mononuclear leukocyte isolation from organs

Mice were anesthetized and perfused transcardially through the left ventricle with 20 ml cold PBS. Lymphoid organs (spleen, inguinal, axillary, mesenteric, CLNs, Peyer's Patches and intestine), brain and spinal cord were dissected.

For lymphoid organs, single cell suspensions were prepared in RPMI by using 40 µm cell strainers (BD). Cells were centrifuged 10 min at 500 rcf 4 °C and cell pellet was resuspended in complemented RPMI for further analysis. For spleen preparation, erythrocyte lysis was performed by resuspending and incubating the cells in 0.83 % NH₄Cl for 3 min at RT. Cells were washed with RPMI, centrifuged and resuspended in complemented RPMI.

CNS was cut in pieces and digested with 1.25 mg/ml DnaseI and 3.75 mg/ml Collagenase D (Roche) for 30 min at 37 °C and single cell suspension was prepared in RPMI by using 100 µm cell strainers (BD). After centrifugation for 10 min at 500 rcf 4 °C, cell pellet was resuspended in 5 ml RPMI plus 2.16 ml Stock Isotonic Percoll (SIP) and was overlaid on 5 ml Percoll d=1.080. The gradient was centrifuged at 1200 rcf 30 min, RT and the interface, containing the mononuclear cells, was collected, washed with complemented RPMI and resuspended in complemented RPMI for further analysis.

For intestine, duodenum, jejunum, and ileum were cut into small pieces and put in ice-cold CMF/Hepes. Intestinal pieces were washed by swirling a 10 cm cell culture dish onto 100 µm Nylonmesh. Intestinal pieces were transferred back to dish and 13 ml of ice-cold CMF/Hepes was added. Washing steps were repeated 3 times. After washing, intestinal pieces were transferred to Erlenmeyer flask and 25 ml of CMF/Hepes/EDTA were added. Tissue pieces were stirred for 15 min at RT on a magnetic stirrer (10 rcf). After incubation, content of flask was poured on Nylonmesh, new medium was added and washings were repeated for 3 times. Residual EDTA was removed by rinsing flask with RPMI-10, followed by washing pieces for 5 min in RPMI-10, stirring for 5 min at RT. Then, intestinal pieces were incubated with 12 ml RPMI-10 with 100U/ml Collagenase D (Sigma) and stirred for 1h at 37 °C (30 rcf). Digested tissue was forced through a 100 µm Nylonmesh and washed twice with CMF/Hepes/EDTA. Pellet was resuspended in 5 ml 40% Percoll and put on 2.5 ml 80% Percoll in a 15 ml Falcon

tube. Cells were centrifuged for 20 min at 1200 rcf at RT. Cells were collected from interface and washed with RPMI, centrifuged and resuspended in complemented RPMI.

Adoptive transfer EAE

For induction of adoptive transfer (passive) EAE, iGB cells from in vitro cultures were centrifuged at 150 rcf for 10 min RT, washed once with iGB cell medium, and filtered through a 100 µm cell strainer. Cells were centrifuged and washed 2 times with PBS and filtered through a 40 µm cell strainer. 2D2 recipient mice were anesthetized and 200 µl of cells ($15\text{--}25 \times 10^6$) were injected intraperitoneally. Clinical symptoms were evaluated by classical EAE scores: score 0 – no disease; score 0.5 – reduced tail tonus; score 1: limp tail; score 1.5 – limp tail and ataxia; score 2 – limp tail and hind limb weakness; score 2.5 – at least one hind limb paralyzed/weakness; score 3 – both hind limbs paralyzed/weakness; score 3.5 – complete paralysis of hind limbs; score 4 – paralysis until hip; score 5 – moribund or dead.

2.2.2 Cell culture routine

Cell lysate preparation (native)

Lysates were prepared by resuspending cells in 500 µl cell lysis buffer, followed by incubation for 30 min at 4°C. Lysates were spun down by centrifugation at 20,000 rcf for 1 hour (h), before supernatant was recovered and analyzed.

Cultivation of cell lines

Cell lines or primary cells were cultured in fully complemented RPMI or DMEM medium in standard cell culture-treated plastic dishes (BD; Nunc, Denmark; Corning) in a humidified incubator (Heraeus) at 37°C and 5% or 10% CO₂, respectively. Cells growing in suspension were harvested by resuspending the culture; semi-adherent cells were flushed off the culture dish surface; and adherent cells were first briefly rinsed with PBS and then detached with Trypsin-EDTA (Sigma) for 3 to 5 min at 37°C. Cell numbers were regularly determined using a Neubauer hemocytometer (Neubauer). Cultures were kept subconfluent by regular dilution with fresh medium at ratios of 1:2, 1:10 or 1:20. Cells were pelleted by centrifugation at 150 rcf for 10 min at 4°C and resuspended in complemented RPMI or DMEM for culturing or further downstream analyses.

Cultivation of BMDCs

BMDCs were prepared from femur of both legs. Femurs were rinsed in 70% EtOH to ensure sterility and epiphysis were removed with a scissor. Bone marrow was flushed out with cold incomplete RPMI and collected in a centrifuge tube. Cells were washed with 50 ml

incomplete medium and erythrocytes were removed using 0.84% ammonium chloride solution. After centrifugation cells were resuspended in complete RPMI and plated with density of 2.5×10^6 cells in bacteriological Petri dishes with 9 ml complete RPMI and 1ml medium collected from a GM-CSF producing hybridoma. On day 3 and 6 medium was exchanged with 8 ml complete RPMI and 2 ml medium collected from GM-CSF producing hybridoma cells. On day 8 cells were stimulated with $1 \mu\text{g/ml}$ LPS ON and fresh exosome free medium was applied.

Cultivation of iGB cells

iGB cell culture conditions were based on Kitamura's instructions [116]. 40LB feeder cells were split the day before culture and fresh DMEM complete medium was added. Feeder cells were cultured in different densities and medium volume according to plate size (Table 11). On day 0, feeder cells were either irradiated ($120 \text{ Gy } \gamma\text{-ray}$) or treated with Mitomycin C for 1h ($25 \mu\text{g/ml}$) to stop further growth. Naïve B cells were either isolated from spleens of mice with a B cell isolation kit (Stemcell, 19854) or whole splenocytes were cultured on 40LB cells. B cells were cultured first for 4 days in the presence of 1 ng/ml IL-4 (BioLegend, 574304) in iGB medium and afterwards for 4 days in presence of 10 ng/ml IL-21 (BioLegend, 574506) with fresh (irradiated or Mitomycin-treated) 40LB cells. B cells were detached with warm PBS/BSA/EDTA (0.5 % BSA, 2 mM EDTA) for 5 min at RT. After day 4 and 8, B cells were counted and analyzed by FACS. For adoptive transfer, splenocytes were cultured for 4 days and then iGB cells were purified by washing (see 2.2.1).

Table 11: Culture conditions of iGB cells for different plate types

Dish size	Surface	40LB cells	B cells plated on day 1	iGB cells plated on day 4	iGB medium
10 cm	55 cm ²	1.2×10^6	800 000 or 2.0×10^6 (Adoptive transfer)	50 000	20 ml (day 0) 10 ml (day 4)
6 well	9 cm ²	196 000	180 000	9900	9 ml
12 well	4 cm ²	87 000	80 000	4400	4 ml
24 well	2 cm ²	43 500	40 000	2200	2 ml
48 well	1 cm ²	21 800	20 000	1100	1 ml
96 well	0.32 cm ²	7000	4000	220	200 μl

Freezing and thawing of stocks

For preparation of long-term stocks, full dishes were harvested and resuspended in 500 μl 10% DMSO in FCS. Stocks were frozen in a Cryo Freezing Container (Thermo Fisher Scientific,

Schwerte) at -80°C . For thawing, stocks were transferred to 37°C and washed once with 10 ml fresh medium to remove DMSO, before resuspension in 10 ml warm medium.

Proliferation assay

2×10^5 B cells or iGB cells and T cells (1:5 ratio) per well were seeded in 96-well round-bottom plates in a total volume of 200 μl growth medium and stimulated with rMOG (20 $\mu\text{g}/\text{ml}$, 1:10 dilution factor) or MOG Peptide₃₅₋₅₅ (20 $\mu\text{g}/\text{ml}$). After a culture period of 48 hours 2 μM of EdU (Thermo Fisher, A10044) was added per well. Samples were harvested 16 hours later and EdU incorporation was measured by FACS.

2.2.3 Electron microscopy for exosomes

For electron microscopy (EM) a drop of approximately 10 μg of exosomes in PBS was placed on a Parafilm. Then, with forceps, gently a formvar carbon coated nickel grid was positioned on top of each drop for 30-60 min. Three drops were placed, each 30 μl PBS on the Parafilm and grid was washed by sequentially positioning the grid on top of the droplets of PBS, and using an absorbing paper in between. Sample was fixed by deposit a drop of 2% paraformaldehyde on the Parafilm and grid was placed on top of the drop for 10 min. Washing step was repeated. Sample was fixed by adding a drop of 2.5% glutaraldehyde to the Parafilm and grid was incubated on top of the drop for 10 min. Sample was contrasted by adding a drop of 2% uranyl acetate to the Parafilm and grid on top of the drop for 15 min. Afterwards, sample was embedded by adding a drop of 0.13% methyl cellulose and 0.4% uranyl acetate to the Parafilm and grid on top of the drop for 10 min. Excess liquid was removed by gently using an absorbing paper, before positioning the grid on a paper with the coated side up and was air dried for 5 min.

2.2.4 DNA techniques

Agarose gel electrophoresis

DNA fragments were separated in agarose gels (1.5% agarose in TAE buffer, 1 $\mu\text{g}/\text{ml}$ ethidiumbromide) using approx. 1 V/cm^2 . DNA bands in analytical gels were visualized in the Geldoc XR system (Bio-Rad, München). For excision of DNA bands from preparative gels, long wavelength UV light (312 nm) on an IL 200 M transilluminator (Bachofer, Reutlingen) was used.

DNA amplification by PCR

DNA was amplified by polymerase chain reaction using DreamTaq (Invitrogen, Karlsruhe), according to the instructions of the manufacturers, run on a PTC-200 DNAEngine (MJ Research, Bio-Rad, München) cycler.

2.2.5 Enzyme linked immunosorbent assay (ELISA)

ELISA plates (Nunc) were coated with rMOG (10 µg/ml in PBS), overnight at 4°C. Plates were washed and blocked for 1-2h. Afterwards plates were washed and incubated with 100 µl per well of samples at RT for 2 hours or ON at 4°C. Plates were then washed, and 100 µl per well of the respective biotinylated secondary antibodies (1:1000) in blocking buffer was added and incubated for 1 h. After extensive washing, streptavidin-HRP (1:2000) was added and incubated at RT for 30 min. After washing, 100 µl of TMB Substrate was added per well. After TMB stop solution was added, absorbance was measured at 450 nm in an ELISA reader (Victor2™ 1420 Multilabel counter; Perkin Elmer life sciences).

2.2.6 Exosome analysis

Exosome producing cells were cultured in exosome-free media ON and supernatant was collected. Supernatant was first centrifuged for 30 min at 4000 rcf to deplete cell debris and then another 45 min at 10000 rcf to remove large membrane-derived vesicles. Finally, supernatant was centrifuged for 75 min at 100000 rcf to pellet small microvesicles. Afterwards, exosomes were characterized by either electron microscopy (2.2.3), western blot (2.2.11), nanosight or flow cytometry (FACS, 2.2.7).

Nanosight based analysis

With the Nanosight (Malvern Panalytical), exosomes can be analyzed by the nanoparticle tracking analysis. This is a method for visualizing and analyzing particles in liquids that relates the rate of Brownian motion to particle size. The rate of movement is related to the viscosity and temperature of the liquid. With this method, the determination of a size distribution profile of small particles with a diameter of approximately 10-1000 nm in liquid suspension is shown. Exosomes are resuspended in PBS and directly analyzed.

2.2.7 Fluorescence-activated cell sorting (FACS)

For cells

Cells to be analyzed were transferred into 96-well V-bottom plates and centrifuged at 250 rcf for 10 min at 4°C. Cells were washed in 150 µl FACS buffer twice, resuspended in 50 µl FACS buffer containing directly labeled surface marker-binding antibodies at appropriate dilutions and Fc block (1:2000, BD Bioscience), and incubated for 20 min at 4°C. After washing and resuspension in 150 µl FACS buffer, samples were acquired on a FACS VERSE (BD, Heidelberg), and analyzed using FlowJo 7.6 software (TreeStar, Ashland, OR, USA).

For exosomes

To analyze exosomes 30 µg purified exosomes as measured by Bradford assay were incubated with 10 µl latex beads (surfactant-free aldehydesulfate, 4 % solids; Interfacial Dynamics 12-4000) for 15 min at RT, in a 1.5-ml tube. PBS was added to a final volume of 1 ml and mixture was incubated on a tube rotator wheel ON at 4°C. To block free binding sites on beads, 110µl of 1 M glycine (i.e., 100 mM final) were added, mixed gently and incubated on the bench at RT for 30 min. Exosomes were centrifuged for 5 min at 2000 rcf, RT. Supernatant was removed and discarded. Bead pellet was resuspended in 1 ml FACS-Buffer and centrifuged for 5 min at 4000 rpm, RT. Supernatant was discarded and bead pellet was resuspended and centrifuged in 1 ml FACS-Buffer. Then, pellet was resuspended in 200 µl FACS Buffer and transferred to V-bottom plate with 10 µl coated beads per well. 50 µl anti-exosomal protein antibody diluted in FACS Buffer (1:200) was added and incubated 30 min at 4°C in the dark. After washing and resuspension in 150 µl FACS buffer, samples were acquired on a FACS VERSE, and analyzed using FlowJo 7.6 software.

2.2.8 Immunohistochemistry

Organs from PFA perfused mice were fixed in 4% PFA in PBS for 1 hour, and then immersed in 30% sucrose, overnight. Tissues were embedded in tissue-tek O.C.T. compound (Sakura), and 7 µm sections were cut on a CM3050 S Cryocutter (Leica). Tissue sections were thawed, fixed in cold acetone for 10 min, and blocked with 5% BSA in PBS for 2h at RT. Incubation with primary antibody was done in 5% BSA in PBS ON at 4°C. Incubation with secondary antibody was done in 5% BSA in PBS for 2 h at RT. Cell nuclei were stained with DAPI (Invitrogen, Karlsruhe) in PBS for 5 min at RT, before sections were rinsed with H₂O and embedded in anti-fading mounting medium (Sigma-Aldrich, Taufkirchen). Images were acquired on an inverted SP2 confocal microscope (Leica, Wetzlar) or an inverted AxioVert

200M microscope (Carl Zeiss, München). Individual images were assembled for overviews of whole organs using ImageJ (Wayne Rasband).

2.2.9 Production of MOG tetramer

Mouse MOG₁₋₁₂₅ was transiently expressed in human embryonic kidney cells (HEK) transformed with EBNA-1 gene cell line. Purified MOG₁₋₁₂₅ protein from HEK cells was biotinylated with BirA ligase in order to multimerize them to form tetramers. Tetramerization was achieved based on the ability of streptavidin (SA) to spontaneously assemble stable tetramer-structures composed of four biotinylated MOG₁₋₁₂₅ protein monomers (MOGtet). Since the SA used was directly conjugated to fluorophores like AF488 or PE, MOGtet could be used as detection tool for MOG specific B cells via flow cytometry.

2.2.10 RNA techniques

RNA extraction

Total RNA was isolated from purified cells by TRI Reagent (Sigma-Aldrich, Taufkirchen) following the instructions provided by the manufacturer.

Reverse transcription

cDNA was generated from RNA using SuperScript II Reverse Transcriptase (Invitrogen, Karlsruhe) or the Verso cDNA Kit (Thermo Fisher Scientific, Schwerte), according to the manufacturer's instructions.

Quantitative PCR

Real-time qPCR was performed using the ABsolute QPCR Mixes (Thermo Fisher Scientific, Schwerte) according to the instructions of the manufacturer, and samples were run on a 7900HT Fast Real-Time PCR System and analyzed by SDS 2.3 software (both Applied Biosystems, Darmstadt).

2.2.11 Western Blot

BCA assay

Protein concentration was estimated using the BCA protein assay following the manufacturer's instructions (Thermo Scientific Pierce, Rockford, IL, USA).

SDS-PAGE

Separation of proteins was achieved by denaturing, discontinuous, one-dimensional SDS polyacrylamide gel electrophoresis (Lämmli, 1970), using pre-cast Novex 4-12% tris-glycine gels (Invitrogen, Karlsruhe). 2x Lämmli buffer was added to 10 µl cell lysate, boiled for 5 min at 100°C, and loaded to each lane. Electrophoresis was performed in Lämmli running buffer at 100 V for stacking, and at 130 V for resolving of proteins in a Mighty Small gel chamber (Hoefer, San Francisco, CA, USA). To verify appropriate sample loading, gels were stained with Coomassie Brilliant Blue G-250 (Bio-Rad, München).

Western transfer

Proteins were electrophoretically transferred from polyacrylamide gels to Immobilon-FL PVDF membranes (Millipore, Schwalbach) using the semi-dry blot technique. Configuration of the Western blot was: 6 layers Whatman paper wetted in anode buffer I, 3 layers Whatman paper pre-wetted in anode buffer II, PVDF membrane (pre-equilibrated in methanol), polyacrylamide gel, 6 layers Whatman paper wetted in cathode buffer. The transfer was carried out at a current of 0.8 mA/cm² for one hour at RT.

Immunodetection of proteins

All incubations were done on a rocking table. After transfer of proteins, the membrane was blocked by incubation in PBS with 5% milk powder ON at 4°C. The primary antibody was diluted in PBS 0.1% Tween-20 1% milk powder. Primary antibody incubation was done for 1 hour at RT. After four washes with PBS 0.2% Tween-20 for 5 min, the membrane was incubated with HRP-coupled secondary antibody in PBS 0.1% Tween-20 1% milk powder for 1 hour at RT in the dark. The membrane was washed four times for 5 min; final washing was done in PBS without Tween-20. Bands were detected using ECL Western Blotting Substrate (Thermo Scientific Pierce, Rockford, IL, USA) on Amersham Hyperfilm ECL (GE Healthcare, München).

3 RESULTS

3.1 Antigen transport and priming of autoreactive lymphocytes in spontaneous EAE

Presentation of auto-antigen to B and T cells is a crucial event in the development of EAE. However, when and where autoreactive lymphocytes encounter antigen is not well understood, especially in spontaneous EAE models. One hypothesis is that APCs and/or soluble auto-antigens may migrate from the CNS to regional lymph nodes to initiate an autoimmune response [72]. In this chapter, the possible drainage pathways of myelin antigens to CLN in soluble form or exosomes were investigated, as well as B cell activation in the gut as a potential activation site.

3.1.1 Detection of CNS draining pathways with fluorescent tracers

In order to visualize the drainage pathway from the CNS to regional lymph nodes and determine, which cell types may be involved in the transport, different fluorescent tracers were employed. SJL/J WT mice were intrathecally injected with either 20 µg of dextran FITC, Alexa Fluor 488, Alexa Fluor 647 or PBS. Different fluorophores were tested to optimize the signal. After 24h, mice were killed and different organs were analyzed for the presence of those fluorescent tracers by FACS (Figure 2 A-E). Higher frequencies of dextran⁺ cells were detected in the CNS (A-B), deep (d) and superficial (s) CLN (B) compared to low frequencies in spleen, axillary (aLN) and inguinal lymph nodes (iLN). In the CNS, B220⁺ B cells, CD11c⁺ dendritic cells and CD11b⁺ macrophages equally carried dextran-FITC (data not shown), whereas in d CLNs and s CLNs dextran was mostly carried by CD11b⁺ cells (C-E). As expected, dextran was not detectable on non-APC populations like CD4⁺ T cells.

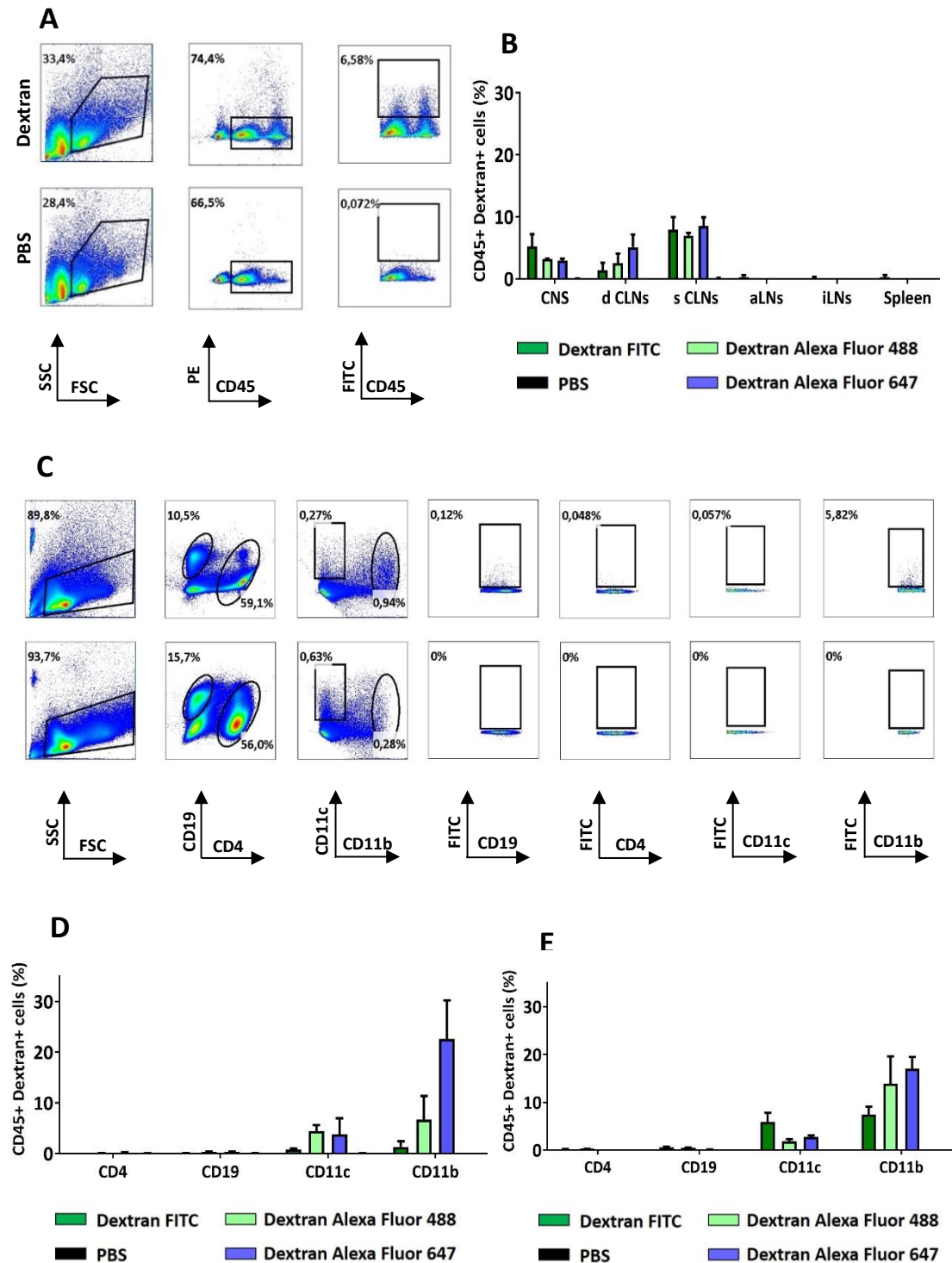


Figure 2: Cervical lymph nodes are drainage sites for intrathecally injected dextran.

SJL/J WT mice were intrathecally injected with 20 μ g of dextran FITC (green bars), dextran Alexa 488 (dark green), dextran Alexa 647 (purple) or PBS (black bars), organs were taken after 24 hours and analyzed by flow cytometry. A) Plots show gating strategy and frequency of dextran-FITC⁺ cells in CNS. B) Summary of dextran⁺ cells in CNS, deep and superficial cervical, axillary, inguinal lymph nodes and spleen. C) Dextran-FITC⁺ cells in different cell types in d CLNs. Left three plots show gating strategy for B cells (CD45⁺CD19⁺), T cells (CD45⁺CD4⁺), dendritic cells (CD45⁺CD11c⁺) and macrophages (CD45⁺CD11b⁺). Plots on the right show frequency of Dextran-FITC⁺ cells among the respective population. D-E) Summary of results in deep (D) and superficial (E) CLNs. Data of two independent experiments with n=2 mice per group are shown. Graphs show mean \pm SEM.

Since dextran FITC showed slightly increased frequencies during intrathecal injection and is smaller in size than Alexa Fluor 488, it was further used for the labeling of mammalian MOG. To investigate if myelin antigens translocate from CSF to CLNs, 20 μ g mammalian MOG-FITC or PBS was injected intrathecally in combination with 20 μ g dextran Alexa 647 as positive control (Figure 3). Intrathecal injection of MOG-FITC and dextran Alexa 647 shows MOG-FITC⁺ cells in the CNS (Figure 3 A), but positive cells were neither found in d CLNs nor in s CLNs, whereas dextran Alexa 647 was found in both indicating that injection process was successful (Figure 3 B). As in the previous experiment, dextran 647 was mostly carried by CD11b⁺ cells, however, there was no evidence that MOG-FITC was carried by those cells (data not shown).

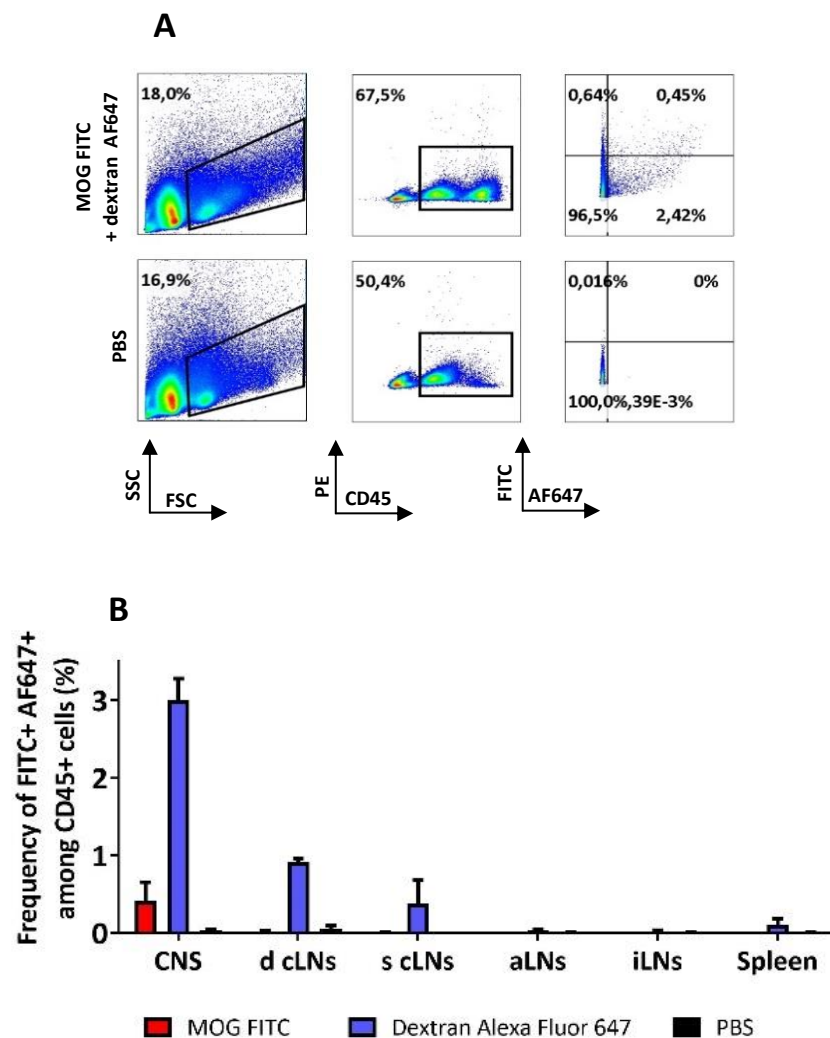


Figure 3: After intrathecal delivery MOG-FITC does not translocate to CLNs.

SJL/ J WT mice were intrathecally injected with 20 μ g of MOG-FITC (red bars), dextran Alexa 647 (blue) or PBS (black bars), organs were harvested after 24 hours and analyzed by flow cytometry. A) Plots show gating strategy and frequency of MOG-FITC⁺ cells and dextran Alexa 647⁺ cells in CNS. B) Summary of frequencies of MOG-FITC⁺ and dextran⁺ cells in different organs. Mean \pm SEM of two independent experiments with n=2 mice per group are shown.

To exclude potential degradation of intrathecally injected conjugated fluorophores, PLP-GFP reporter mice were used to track transport of PLP during active EAE. PLP-GFP is a fusion protein and has higher stability than conjugated fluorophores. Fusion proteins might be more resistant to internal decomposition by macrophages and therefore PLP-GFP may be more suitable to show antigen transport in EAE. Mice were immunized with MOG₃₅₋₅₅ peptide in complete Freund's Adjuvant and injected with Pertussis toxin on day 0 and 2 to induce active EAE. Mice were sacrificed before and at onset of disease (day 8 and 10 after immunization) and different organs were analyzed for the presence of PLP-GFP positive cells by FACS (Figure 4). During onset very few GFP⁺ leukocytes were visible in the spleen of PLP-GFP reporter mice compared to WT BL6 mice but not in other organs. During the peak of disease there were almost no GFP⁺ cells detectable in any organ.

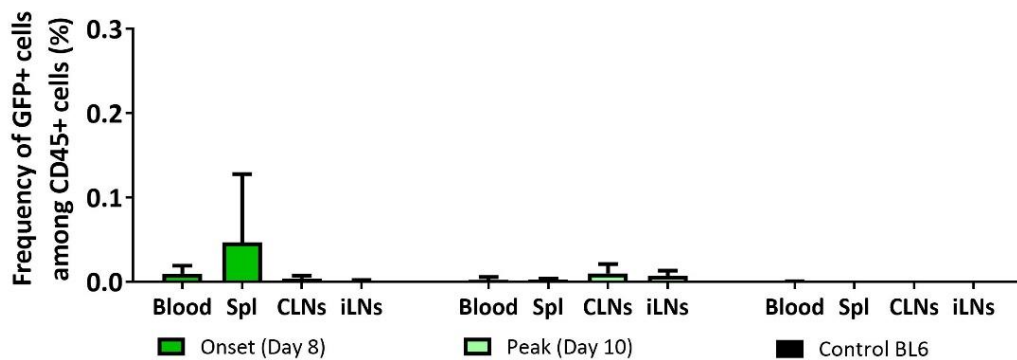


Figure 4: PLP-GFP is not visible in draining lymph nodes of CNS during EAE.

Mice were analyzed on day 8 and 10 after immunization by FACS. Graph shows frequency of GFP⁺ cells among CD45⁺ cells in different organs. Mean \pm SEM of two independent experiments with n=3 for onset (Score 1, 1, 2) and n=3 for peak (Score 2, 2, 3) are shown.

3.1.2 Detection of CNS autoantigens in CLNs with immunohistochemistry

To address the question if auto-antigen is transported from the CNS to regional lymph nodes and whether it is associated with a certain cell type, visualization of myelin antigens within the CLNs via immunohistochemistry was attempted.

Immunohistochemical staining with antibodies against the myelin proteins PLP, MBP and MOG was established (Figure 5 A-D). MBP⁺ (A), PLP⁺ (B) and MOG⁺ (C) cells were localized in medullary cords or subcapsular sinus (structures that contain mostly macrophages) but were not found within T cell (CD4⁺) or B cell (B220⁺) zones of CLNs. MBP⁺, PLP⁺ and MOG⁺ cells were

visible in sick RR mice (score 2.5) as well as in non-transgenic littermates (NTLs). No positive signal was detected in isotype control - treated samples.

Since we observed positive staining for myelin antigens not only in the sick RR mice but also in healthy NTLs (Figure 5 A-C), additional staining with anti-MOG F(ab)₂ antibody was performed to exclude unspecific staining caused by antibody capture through Fc receptors (D). Using anti-MOG F(ab)₂ antibody (Z2-F(ab)₂) no staining could be detected in the CLNs of sick RR mice and NTLs, although the positive control in spinal cord tissue showed MOG staining indicating that the anti-MOG F(ab)₂ antibody faithfully detected MOG.

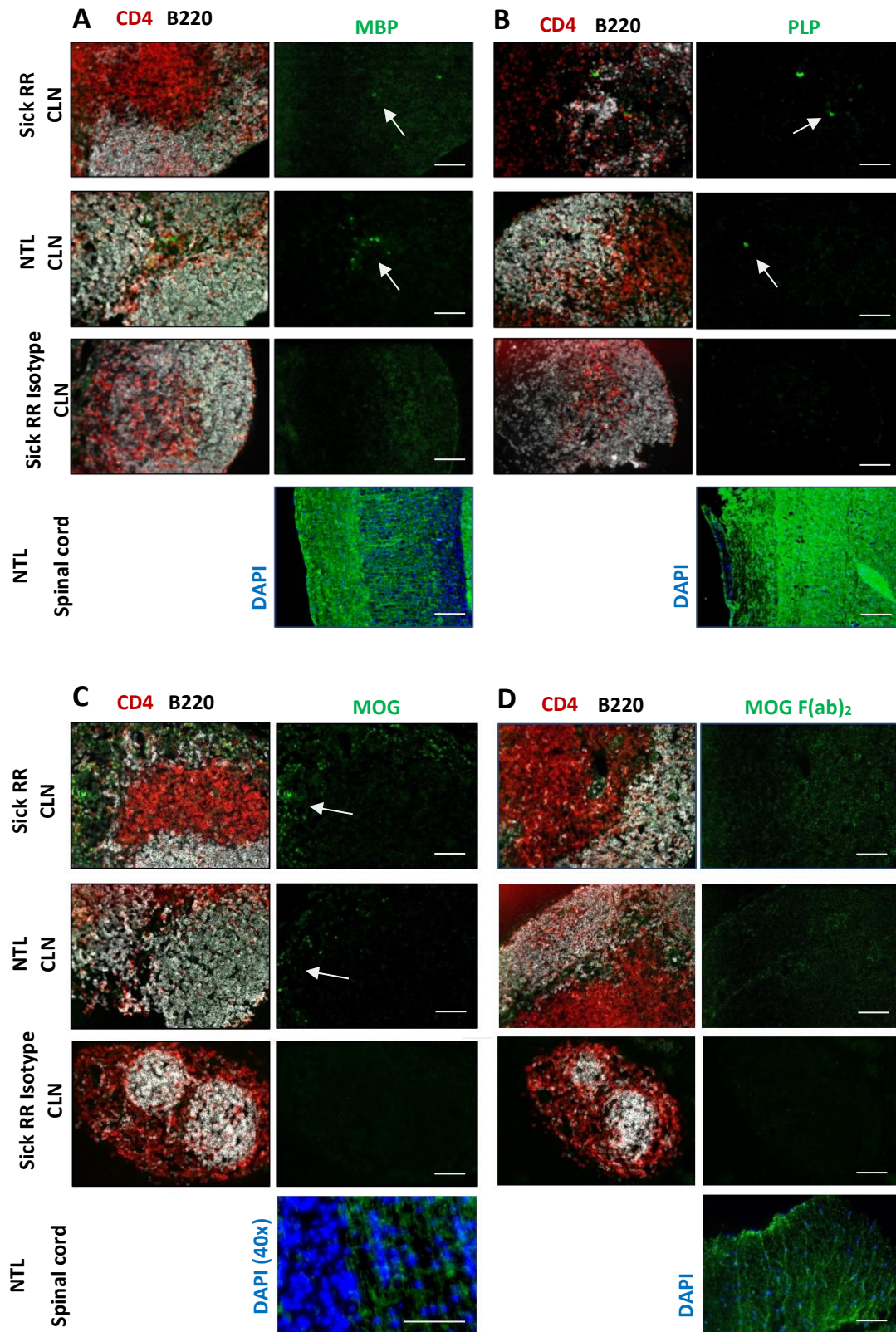


Figure 5: Staining for myelin proteins in cervical lymph nodes of sick RR mice and non-transgenic littermates. Microscopic images of CLN sections from sick RR mice (score 2-3) and NTLs, (A) Myelin basic protein (MBP) is shown in green, (B) proteolipid-protein (PLP) in green, (C) MOG in green (with 8.18c5 antibody), (D) MOG in green (with Z2 F(ab)₂ antibody), anti-CD4 staining for T cells in red, anti-B220 staining for B cells in white and DAPI in blue. As a positive control spinal cord sections were stained with the same antibodies against MBP, PLP, and MOG. Representative data of 3-4 individual mice are shown. Magnification 20 x. Scale bar 100 μ m.

Given that MOG-positive staining was predominantly found in the subcapsular sinus of CLNs co-staining with the macrophage markers CD11b or CD68 was performed on tissue from NTLs and $\text{MOG}^{-/-}$ mice to determine whether macrophages capture the anti-MOG antibody unspecifically. MOG and CD11b/CD68 signals co-localized within the same area in the lymph node in NTLs but also in $\text{MOG}^{-/-}$ mice suggesting an unspecific binding of the anti-MOG antibody (8.18c5) to Fc receptors on macrophages (Figure 6). This indicates that this could also be the case for PLP and MBP signals. However, it cannot be concluded that the myelin proteins are not present in the CLN, only that they cannot be reliably detected. They could be degraded so that antibodies are no longer able to recognize them.

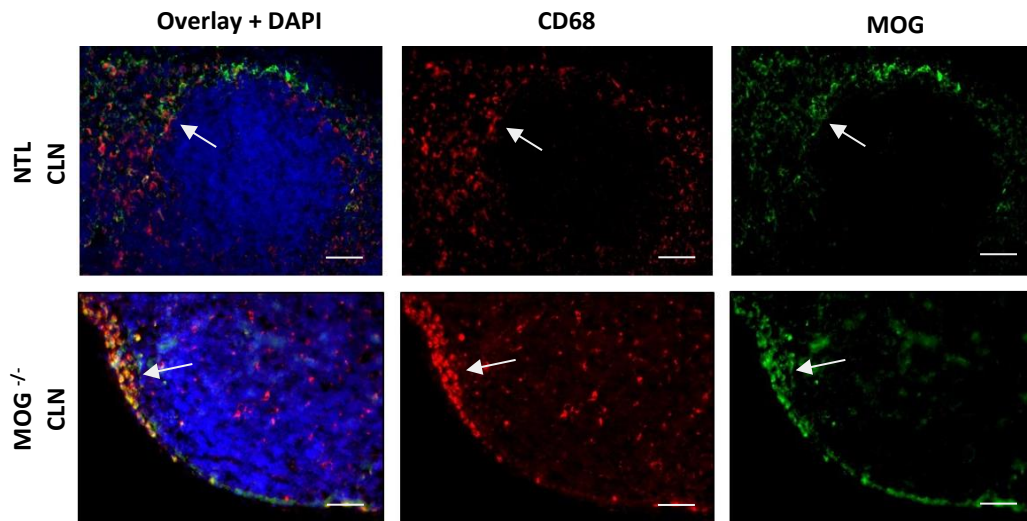


Figure 6: Staining for MOG and CD11b or CD68 on CLN of non-transgenic littermates and $\text{MOG}^{-/-}$ mice
Microscopic images of CLN sections of NTLs (n=3) (upper panel) and $\text{MOG}^{-/-}$ mice (n=2) (lower panel), MOG staining is shown in green, CD68 staining for macrophages in red, and DAPI in blue. Magnification 20 x. Scale bar 100 μm .

3.1.3 Detection of MOG in exosomes from different cell types

Since we could not observe draining of soluble MOG-FITC from the CNS to the CLNs (Fig.3), the possibility that myelin antigens are transported *via* exosomes was explored next. Exosomes from MS patients have been shown to express myelin protein, correlated with disease activity and were highest in relapsing-remitting MS [118]. Therefore, the role of exosomes as a potential delivery system of auto-antigens was investigated. Isolation of exosomes from EL4 cells, EL4-MOG cells and bone marrow-derived dendritic cells (BMDCs) from WT or H2M mice was established. As exosomes can originate from different cell sources, EL4 cells derived from T cell lymphoma and corresponding EL4-MOG cells which express MOG on their surface, as well as BMDCs from WT and MOG expressing H2M mice were used to investigate the potential of exosomes to transport MOG.

In order to establish isolation and characterization of exosomes, EL-4 cells were grown in exosome-free media. Exosomes were isolated from the culture supernatant via several centrifugation steps and characterized by electron microscopy, western blot, nanosight or FACS. In the literature, typical characteristics for exosomes are size and presence of markers for multivesicular body formation [87, 119]. Previous studies documented exosomes to be smaller than 150 nm in size and to express exosome intracellular markers like Alix, a regulator of the endo-lysosomal system, and Tsg101 which has been associated with the biogenesis of multivesicular bodies [120]. Also, extracellular markers like CD63 and CD9, depending on cellular origin of the exosome, have been described as markers for exosomes [121].

Analysis of the microvesicles isolated from EL4 cells and BMDCs by electron microscopy showed round membrane-structures between 50-120 nm (Figure 7), indicating that they fulfill the size criterion described for exosomes.

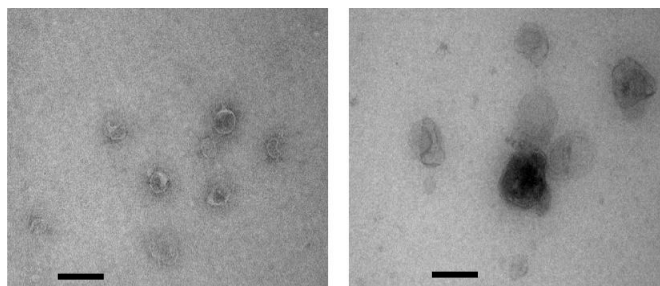
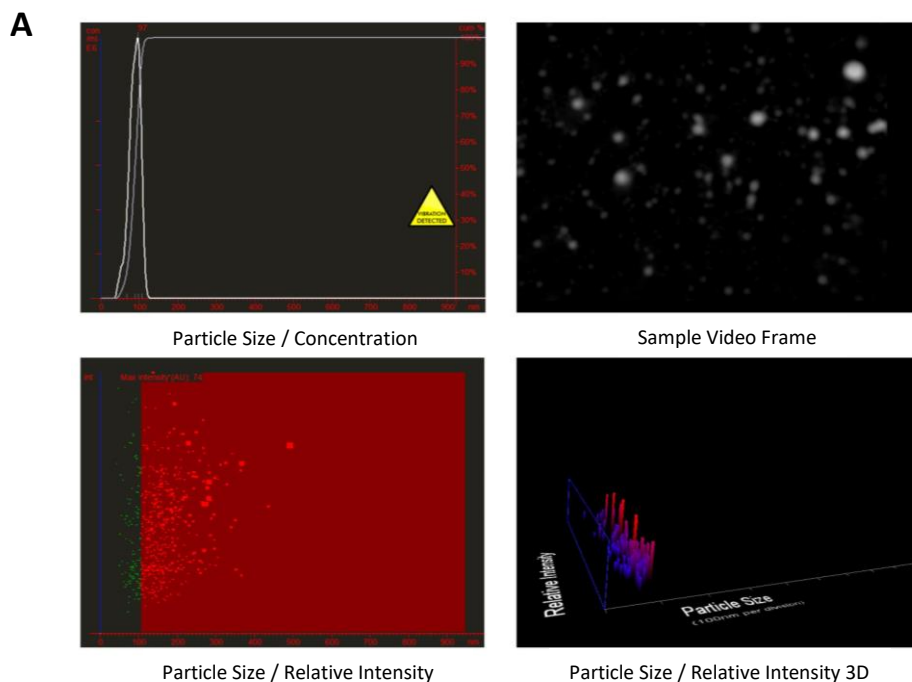


Figure 7: Isolation of exosomes from EL-4 cells and BMDCs.

Electron microscopy images of microvesicles isolated from EL-4 cells (left) and BMDCs (right) reveal rounded membranaceous structures measuring on average less than 150 nm. Scale bars, 100 nm; original magnification 100,000 x. Representative data from 3 individual experiments.

Characterization of EL4 cell-derived microvesicles by nanosight, a technique that utilizes Nanoparticle Tracking Analysis to characterize nanoparticles from 10 - 2000 nm in solution, showed a mean particle size of 130 nm (Figure 8 A) similar to the previously documented size of exosomes. Flow cytometric analysis of EL4-MOG derived exosomes showed the presence of the cell surface markers CD9, CD63 and CD90.2 (Figure 8 B). Moreover, exosomes derived from EL-4 MOG cells showed positive staining for MOG compared to exosomes derived from EL-4 cells. Exosomes isolated from BMDCs of C57BL/6 used as controls and H2M mice, which overexpress MOG on every cell type, showed similar characteristics. Consistent with their cellular origin exosomes from BMDCs also carried CD86, CD80 and MHC class I on their surface. Additionally, H2M exosomes expressed MOG on the surface in contrast to exosomes from C57BL/6 BMDCs (Figure 8 B). Markers of multivesicular body formation including Alix and Tsg101 and MOG were detected in protein lysates from EL-4 MOG cells and exosome lysates by Western blot (Figure 8 C). In contrast to cell lysates, the endoplasmic reticulum marker calnexin was absent in the exosome fraction indicating purity of exosomes. Immunolabeling for Tsg101 was stronger in exosomes than in cell lysate suggesting microvesicles originate from vesicle budding. Moreover, MOG seemed to be enriched in exosomes. In addition, levels of MOG mRNA in EL-4 MOG and EL-4 exosomes were analyzed via qPCR, and showed an enrichment of MOG mRNA in exosomes derived from EL-4 MOG cells (Figure 8 D). As expected, no expression of MOG was detected in exosomes derived from EL4 cells. Thus, these exosomes containing MOG could be used for further studies investigating their potential to activate autoreactive T and B cells.



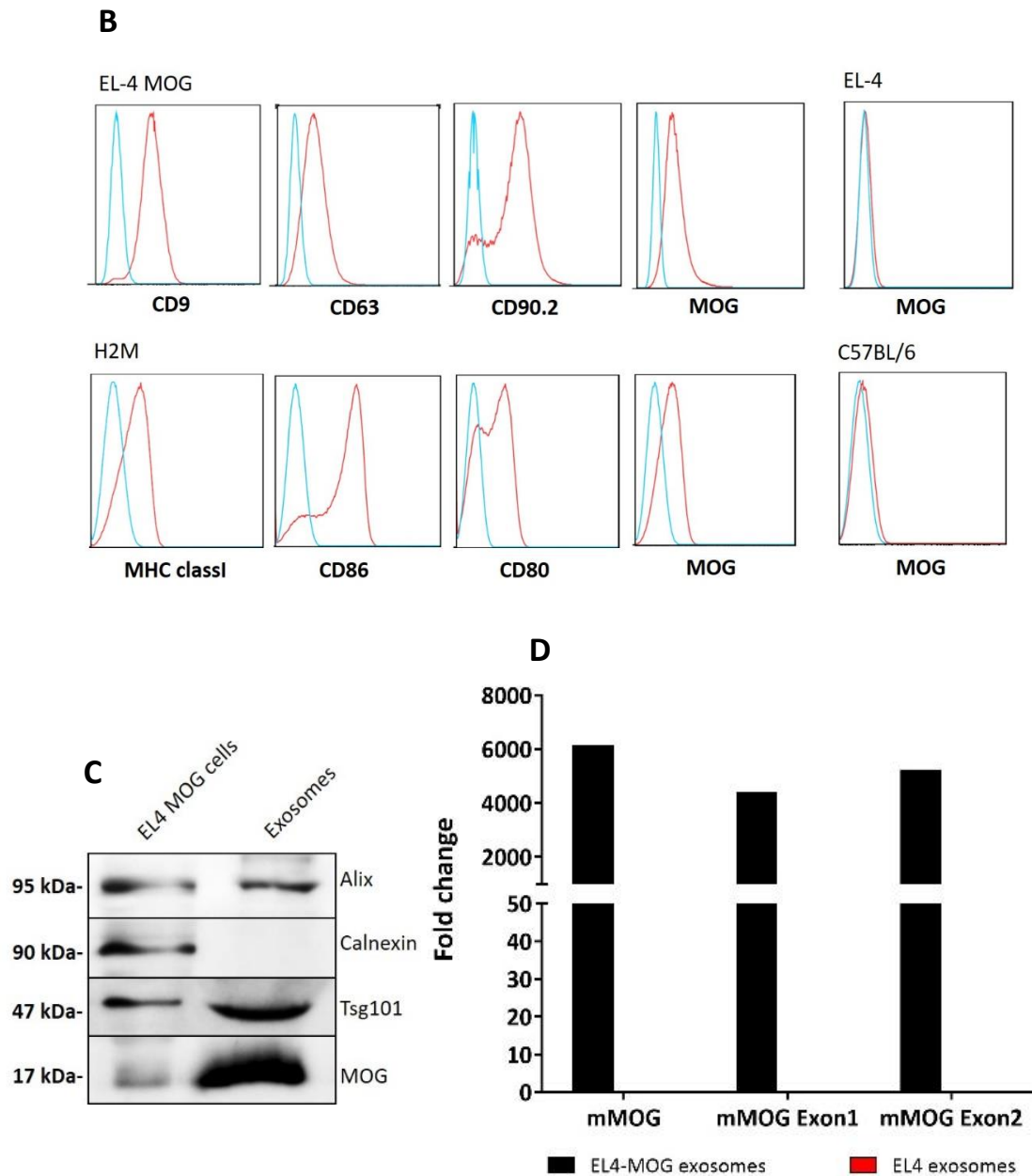
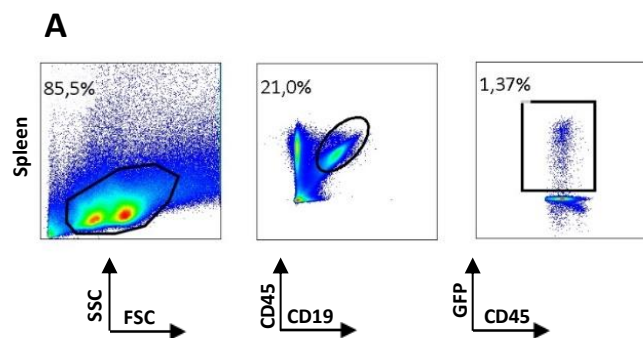


Figure 8: Characterization of EL4, EL4-MOG and BMDC-derived exosomes.

A) Exosomes in solution are measured via Nanosight. Left upper plot shows particle size and concentration of exosomes in solution. Right upper plot shows a snapshot of a video of motion of exosomes in solution. Lower left plot shows selection of particle size for calculation. Lower right plot shows 3D distribution of particle size to relative density. Vesicles are analyzed by the rate of Brownian motion to particle size. Representative data from 2 individual experiments. B) FACS analysis of exosomes isolated from EL4-MOG cells and H2M BMDCs. Red lines show beads coupled with exosomes, incubated with antibodies. Blue lines represent beads only incubated with antibody as negative control. C) Lysate of EL-4 MOG cells and corresponding exosomes were analysed by western blot, testing for the exosomal markers Alix and Tsg101, endoplasmic reticulum marker Calnexin, and MOG, using specific antibodies. Graph is representative of 3 individual experiments. D) Relative expression of MOG mRNA in EL4-MOG derived exosomes (black bars) and in EL4 derived exosomes (red bars).

3.2 B cell activation studies in the intestine

The stimuli leading to activation of autoreactive lymphocytes have been commonly attributed to environmental factors such as composition of the microbiota. In a previous study from our laboratory it was demonstrated that RR mice housed under completely germ-free conditions are protected from spontaneous EAE due to impaired Th17 cell differentiation in the intestine and MOG-specific B cell recruitment [68, 122]. After re-colonization, mice promptly developed disease again. Thus, a two-phase scenario was proposed that starts out in the GALT with expansion and activation of autoreactive T cells, which then recruit autoantibody-producing B cells and migrate to the CLNs and CNS. However, it is unclear whether autoreactive B cells are initially activated together with autoreactive T cells in the gut either by bystander activation or *via* molecular mimicry by microbial antigens and consequently migrate to the CLNs and/or the CNS to promote the development of EAE, or whether autoreactive B cells are exclusively primed in the CLNs. In order to perform B cell activation and migration studies, B cells with fluorescent reporters were adoptively transferred into recipient mice. To be able to track where MOG-specific B cells migrate over time during development of EAE, GFP reporter mice were utilized. To establish the experimental system, first, splenocytes were isolated from actin-GFP mice, in which all cells express GFP, and 25×10^6 total splenocytes were injected intraperitoneally into WT mice. 3, 5 and 7 days after transfer, different organs of the recipients were screened for the presence of GFP⁺ B cells. GFP⁺ B cells were found in low frequencies in Peyer's Patches (PP), spleen (Spl), aLNs and mesenteric (mLNs), as well as in duodenum (Duo), ileum (Il) and colon (Co) (Figure 9 A, B).



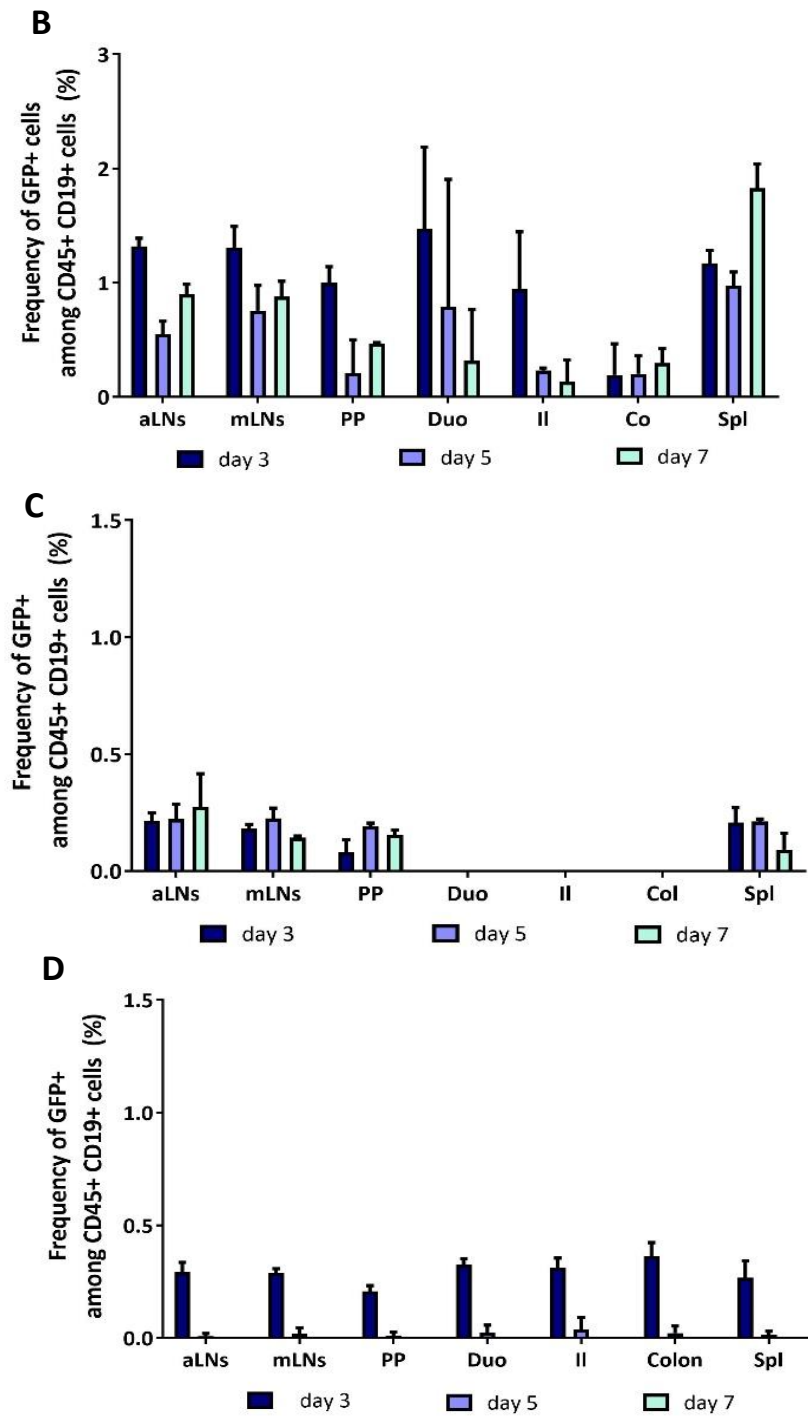


Figure 9: Transfer of actin-GFP cells into WT mice results in low frequencies of GFP⁺ cells in intestinal segments.

A) Plots show gating strategy and frequency of GFP⁺ B cells. B) Frequency of actin-GFP B cells in different organs at indicated time points after transfer of total splenocytes. 25×10^6 total splenocytes from actin-GFP mice were injected into WT mice. Mice were killed on day 3, 5 and 7 after injection and organs were analyzed by FACS. C) Frequency of actin-GFP B cells in different organs at indicated time points after transfer of purified B cells. 10×10^6 purified B cells from actin-GFP mice were injected into WT mice (n=2 per time point). D) Purification of

mononuclear cells from the intestinal segments via density gradient. Mean \pm SEM of two independent experiments with n=2 mice per group are shown.

Lowest frequencies of GFP⁺ B cells were found in duodenum, ileum and colon. In an attempt to increase frequencies of surviving B cells, purified actin-GFP B cells were injected into WT mice. However, while low frequencies of GFP⁺ B cells were visible in spleen, PP, aLNs and mLNs, B cells were not detectable in duodenum, ileum and colon (Figure 9 C). To improve recovery of B cells from the lamina propria, cell isolation was optimized with Percoll density gradient centrifugation. Using this method at least some GFP⁺ B cells could be detected in duodenum, ileum and colon (compare Figure 9 C and D); however, overall frequencies of B cells remained very low.

In addition to low frequencies, analysis of transferred B cells was further complicated by the sensitivity of the GFP signal to fixation and intracellular staining procedures. For later cytokine profile studies by FACS, cells have to be fixed and permeabilized in order to perform intracellular cytokine staining. B cells can produce several different cytokines and can be subdivided into discrete cytokine-producing “regulatory” and “effector” B cell subsets. Regulatory B cells (B_{reg}) are distinguished by their ability to secrete IL-10, IL-35, or TGF β -1, while effector B cell populations produce cytokines such as IL-2, IL-4, GM-CSF, IL-6 or IFN γ , IL-12 and TNF α [67]. Unfortunately, fixation and permeabilization of actin-GFP cells led to loss of GFP signal (Figure 10 A). In order to best preserve the GFP signal during all stainings, different fixation and permeabilization conditions were tested. After fixation for 5-30 min and intracellular staining of cells, GFP staining was completely lost. Washing without permeabilization buffer did not rescue the GFP⁺ signal. Previous reports suggested that pre-fixation with PFA may prevent loss of fluorescent signals. Therefore, stainings with different pre-fixation conditions after surface staining were tested. Pre-fixation of cells reduced the loss of GFP signal, however, the signal was still not comparable to signal obtained with unfixed and unpermeabilized cells. Furthermore, a GFP Booster (Chromotek) which allows stabilization of fusion proteins was tested. However, the GFP Booster also only partially preserved the GFP signal (Figure 10 B).

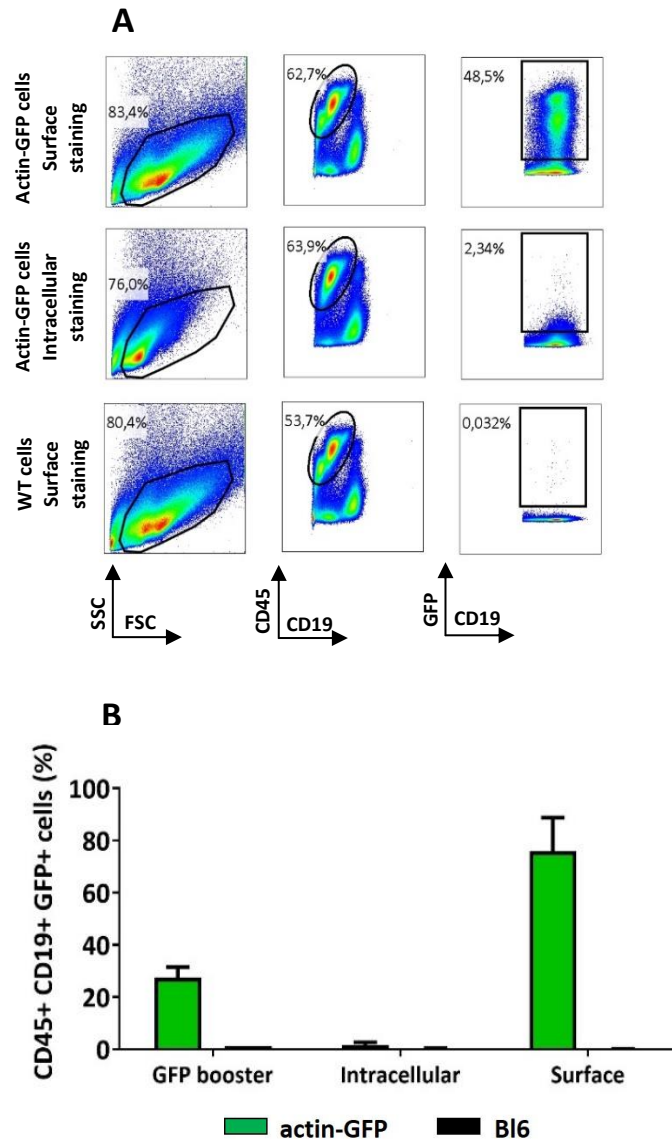


Figure 10: Loss of GFP signal during intracellular staining and washing.

A) Splenocytes isolated from actin-GFP mice were washed in FACS buffer without fixation/permeabilization (upper panel) or fixed and washed with permeabilization buffer for intracellular staining (middle panel). Lower panel shows WT cells as control. B) Intracellular staining of actin-GFP splenocytes with GFP booster. Cells are gated on CD45⁺, CD19⁺ and GFP⁺ cells. Data of 2 individual experiments are shown.

3.3 *In-vitro* induced GC B cells are a new tool for B cells studies in EAE

B cell activation is a crucial step in the initiation of MS and it has been shown that B cells are also essential for the development of spontaneous EAE [34]. However, it is not clear where autoantigen-specific B cells are originally activated and recruited. Upon transfer MOG-specific B cells migrate to germinal centers in CLNs in RR mice indicating that CLNs may be an important site for B cell activation. However, due to the extremely low frequency of endogenous MOG-specific B cells in RR mice ($\leq 1\%$) it is very challenging to study their origin, development, migration pattern and pathogenic properties (such as repertoire, phenotype, cytokine profile etc.). In addition, the frequency of endogenous MOG-specific B cells is too low to be able to manipulate them *ex vivo* and use them for transfer studies. To overcome these limitations, a cell culture system originally developed by Kitamura and colleagues [116] was established which allows us to expand primary B cells over several days and differentiate them into GC B cells and plasmablasts (Figure 11). The activated, *in vitro* induced GC B cells (iGB) and plasmablasts can be used for B cell studies in EAE. In this chapter, establishment of the culture system and transfer of iGB cells were investigated.

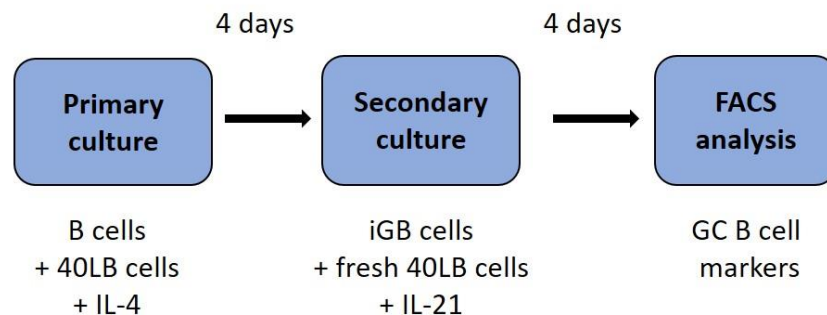


Figure 11: Schematic representation of the iGB culture system.

Primary B cells are cultured on a layer of irradiated or Mitomycin C treated 40LB cells in the presence of IL-4 for 4 days (Primary culture). Then, proliferated iGB cells are transferred onto fresh 40LB cells for 4 days in the presence of IL-21 (Secondary culture). Afterwards, B cells are analyzed for expression of GC and plasmacell markers, as well as isotype switch via FACS.

3.3.1 The iGB cell culture system

In response to T cell-dependent antigens, B cells proliferate extensively to form GC, and then differentiate into memory B cells or long-lived plasma cells. In the T cell dependent response, antigen specific B cells present the antigen to primed cognate T helper cells in the lymphoid follicles and clonally proliferate upon receiving signals via CD40-ligand (CD40L) and IL-4 from

the T helper cells. The CD40 - CD40L interaction is required for T helper cell - mediated B cell activation and thus for GC formation, and for generation of memory B cells [123]. In addition, IL-21 signalling is required for high proliferation rates, IgG1 production, efficient GC formation, affinity maturation and long lived plasma cell formation, but not for memory B cell development in mice [124]. IL-21 induces class switch recombination (CSR) to IgG and Blimp1 expression. Therefore, the culture system is based on signals mediated by CD40-CD40L interaction, BAFF and the cytokines IL-4 and IL-21 to drive B cell proliferation, differentiation and survival. Kitamura and colleagues created a BALB/c 3T3 fibroblast cell line, which constitutively expresses CD40L and BAFF (40LB feeder cells). Together with additional cytokines (IL-4 and IL-21) these cells act as a replacement for T helper cells and provide the required stimuli for B cells to expand and differentiate *in vitro*. 40LB feeder cells have to be irradiated in order to not overgrow B cells and influence culture conditions.

To set up the culture system, B cells were first isolated from spleens of BL6 or SJL/J mice and cultured in the primary culture for 4 days on irradiated or mitomycin treated 40LB feeder cells in the presence of IL-4. For the secondary culture, B cells from the primary culture were collected and were again cultured for 4 days in presence of IL-21 with fresh irradiated 40LB cells (800.000 B cells are seeded per 10 cm dish). After the primary (day 4) and secondary culture (day 8), B cells were counted and analyzed by FACS. B cells cultured without cytokines are not able to perform isotype switch or differentiate into plasmablasts and are used as control group. In Figure 12 A an overview picture of the iGB culture on day 0 and 4 is shown. By day 4 B cells formed proliferation clusters on 40LB cells. Overall, the expansion factor of B cells differed between primary and secondary culture, but not between mouse strains (Figure 12 B-C). In the presence of IL-4, B cells expanded 3-10 fold, whereas presence of IL-21 in the secondary culture induced up to a 500-fold expansion (Figure 12 D).

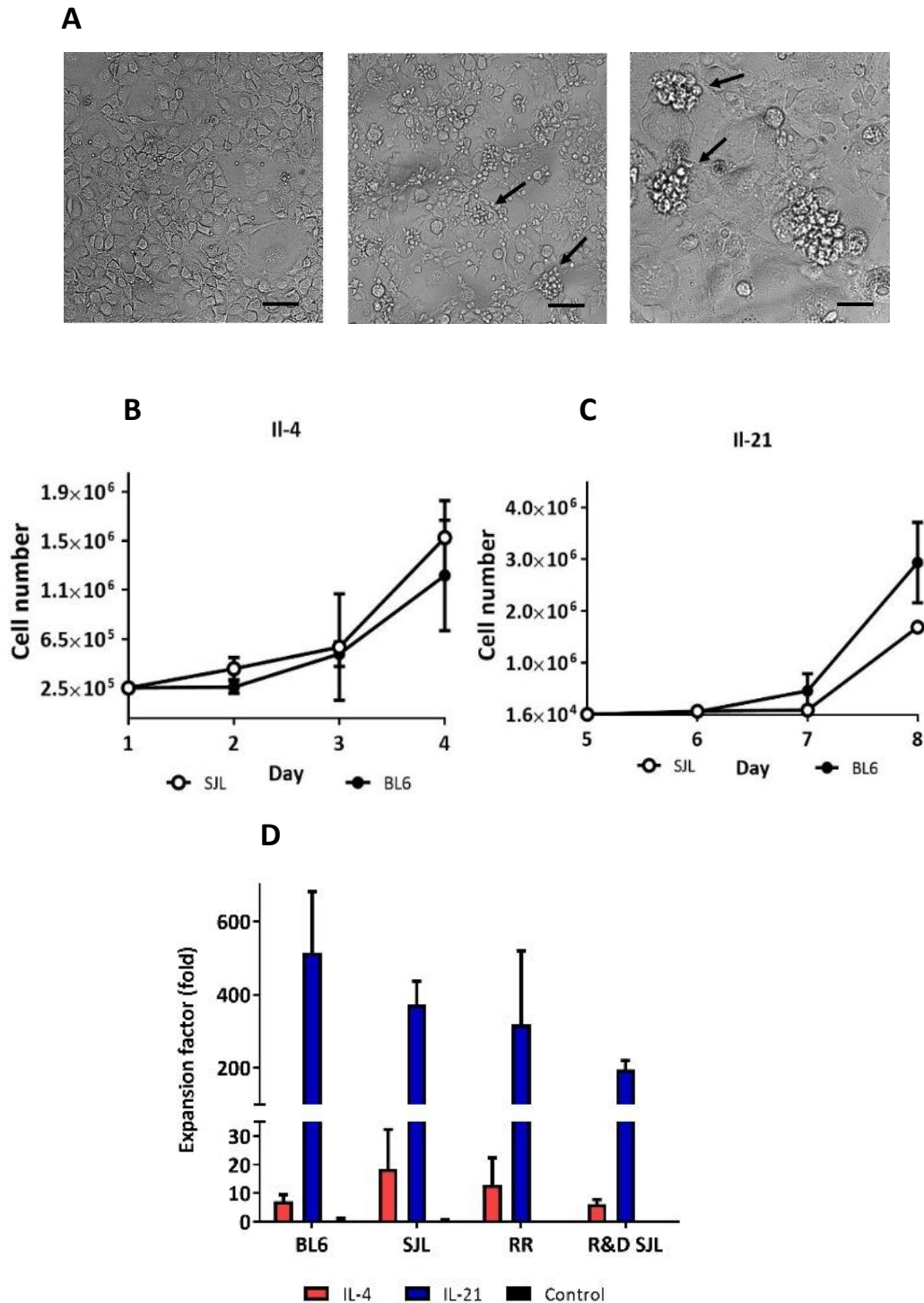


Figure 12: Expansion of B cells derived from different mouse strains in primary and secondary iGB culture.

A) Brightfield microscopy of proliferating B cells cultured on 40LB cells. Microscopic images of iGB cell culture dishes on day 1 (left) and 4 (middle and right). Scale bar 50 μ m. Magnification 20x. Arrows show proliferating clusters of B cells. Magnification 10x (right panel 20x). B) Graph shows expansion of B cells isolated from BL6 and SJL mice during primary culture in the presence of IL-4 (day 1-4). C) Graph shows expansion of B cells isolated from BL6 and SJL mice during secondary culture in the presence of IL-21 (day 4-8). D) Expansion factor of B cells derived from BL6, SJL, RR and R&D SJL mice cultured 4 days with IL-4 (red bars) followed by 4 days with IL-21 (blue bars), or without cytokines (black bars). Graphs show mean \pm SEM from 3 independent experiments with $n \geq 3$ mice per group.

Next, phenotyping of B cells in the iGB culture was performed via flow cytometry. At the end of the primary culture, IL-4 had induced BCR class switching from IgM to IgG1 in about 10-20% of B cells (Figure 13). After the secondary culture in the presence of IL-21, B cells had completed the isotype switch, i.e. they did not express IgM anymore and the majority (60-80%) now expressed IgG1. Compared to Kitamura's studies [116], a much lower frequency of IgE⁺ cells during the entire culture period was obtained. Development of IgA⁺ B cells, as well as IgG2a⁺ and IgG2b⁺ B cells was rare in all mouse strains (Figure 13 and data not shown). As expected, the frequency of CD138⁺ plasmablasts increased over time, especially during the secondary culture. However, overall plasmablast frequency was quite variable between experiments. All B cells except CD138⁺ cells exhibited a germinal center B cell phenotype characterized by expression of GL7⁺, Fas⁺, and PNA⁺ and downregulation of the naïve B cell marker CD38. No differences in B cell phenotype among different mouse strains were detected.

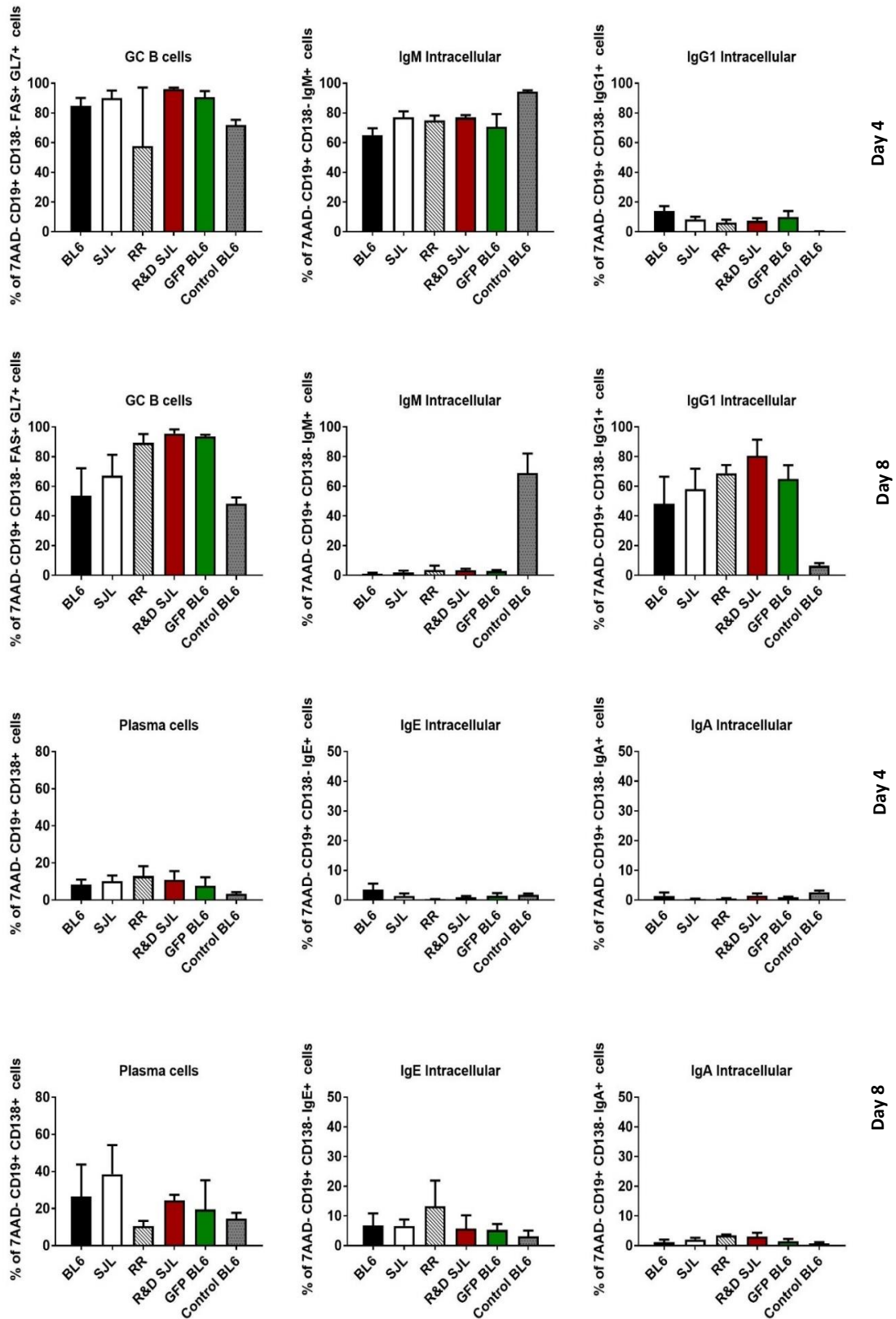


Figure 13: Flow cytometric analysis of indicated markers in iGB cells cultured with IL-4 and IL-21.

Expression of FAS, GL7, PNA and CD38 were analyzed in 7AAD- and CD138- cells after primary (day 4) and secondary culture (day 8). IgM, IgA, IgE and IgG1 expression was analyzed in cells gated on CD138- and H2Kd- cells after primary (day 4) and secondary culture (day 8). Graphs show Mean \pm SEM from 3 independent experiments with $n \geq 3$ mice per group.

3.3.2 Adjustment of the iGB culture system for low B cell numbers

To grow small numbers of B cells isolated from various organs, the effect of dish size on B cell expansion was tested (Figure 14). In the primary culture the expansion rate of iGB cells in different dish sizes was consistent. In contrast, the expansion factor of iGB cells in the secondary culture was higher in 10cm dish, 6 and 12 well plates compared to the smaller formats (24, 48 and 96 well plates). Characterization of phenotype via flow cytometry showed similar GC B cell marker expression as well as BCR class switching in all formats (data not shown).

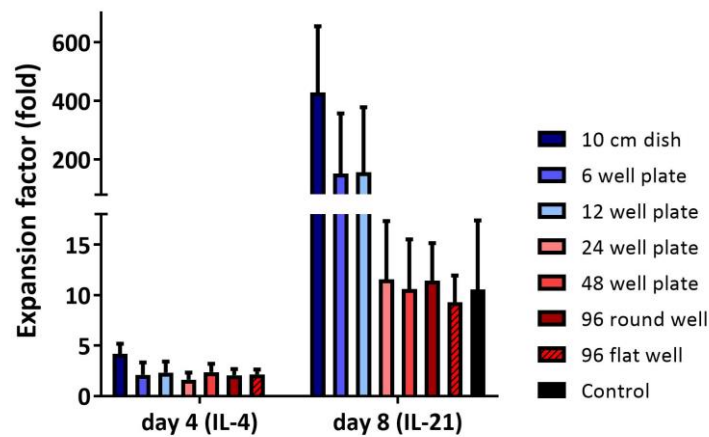


Figure 14: Expansion of iGB cells in different cell culture plates.

B cells were plated on 40LB cells for 8 days. Mean \pm SEM from 5 independent experiments with $n = 2$ is shown.

To test the effect of purity on B cell expansion, B cells were either purified to $\geq 95\%$ with a B cell isolation kit or whole splenocytes were cultured on 40LB cells (Figure 15). Under both conditions, B cells were expanding equally well and showed similar expression of GC B cell markers and isotype switch (Figure 15 B-D). Other cell types including T cells, macrophages and DCs largely died during the iGB culture after 4 days. Although there are still some macrophages and T cells detectable, they do not expand and seem to have no influence on B cell expansion and differentiation (Figure 15 A). Furthermore, culture of B cells derived from the CNS of a sick rMOG immunized SJL/J mouse without prior purification was successful. CNS-derived B cells also showed GC marker expression (Figure 15 E). Importantly, CNS-derived B cells produced higher titers of total anti-MOG IgG than B cells derived from spleen (Figure 15 F). These data suggest that purification of B cells before iGB culture is not required. Since only B cells receive survival and proliferation signals in the iGB culture system, the risk of losing rare B cells such as autoantigen-specific B cells from the CNS during purification processes can be reduced by plating all cells.

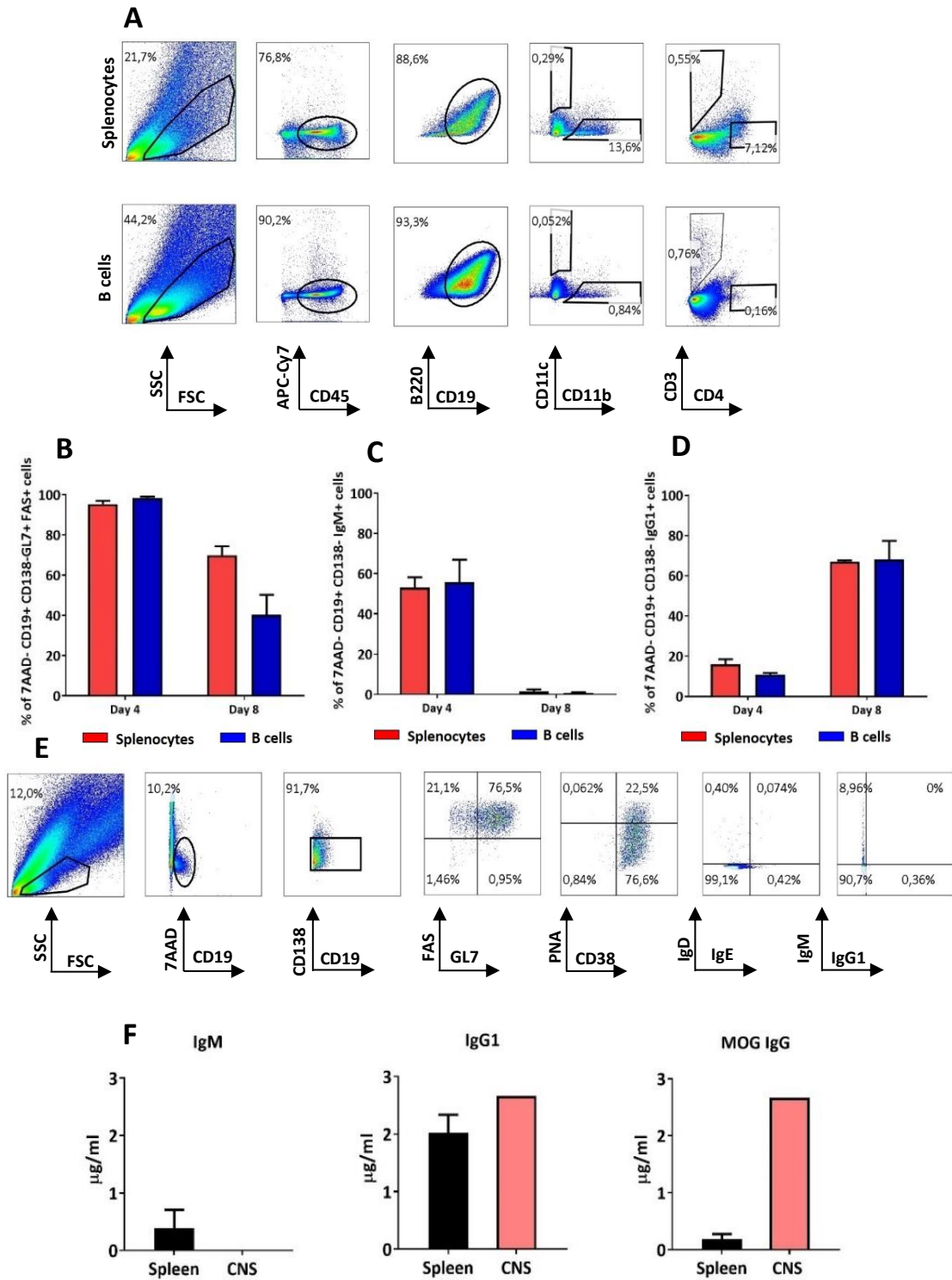


Figure 15: Comparison of total splenocytes, purified, and CNS-derived B cells in the iGB culture.

A) Representative FACS analysis of the iGB culture on day 4 using either whole splenocytes or purified B cells as starting material. CD45⁺ cells in the culture were analyzed for presence of different cell types including B cells (CD19, B220), macrophages (CD11b), dendritic cells (CD11c) and T cells (CD4, CD3). B-D) Phenotypic comparison of primary (d4) and secondary (d8) iGB cultures using either total splenocytes (red bars) or purified B cells (blue bars) as starting material. Cells were analyzed for expression of GC markers (B), as well as isotype switch from IgM (C) to IgG1 (D). Mean ± SEM from 1 experiment with n = 3 is shown. E) Expansion of CNS-derived B cells from a sick rMOG immunized mouse on day 4 of culture. Cells are gated on 7AAD⁻, CD138⁻ and CD19⁺ cells and analyzed for GC markers (FAS, GL7, PNA and CD38) and isotype switch (IgM, IgG1, IgE and IgD). F) Amount of total IgM, IgG1, and MOG IgG levels in spleen and CNS.

total IgG1 and MOG-specific IgG antibodies in the supernatant of iGB cultures from CNS vs. spleen derived B cells from a MOG-immunized mouse was determined by ELISA.

3.3.3 Tracking tools for iGB cells *in vitro* and *in vivo*

To examine if B cells expressing fluorescent reporter proteins can be expanded *in vitro* for tracking B cell migration/fate upon transfer, GFP⁺ B cells from actin-GFP mice and RFP⁺ B cells from R&D mice were tested in the iGB culture (Figure 16 A). Unfortunately, RFP signal decreased drastically during culture and was not detectable any longer after 4 days of culture. Even though GFP signal was stable until day 4 it also decreased during secondary culture. Fluorescent signal decreases probably due to high proliferation rates of iGB cells, but may come back upon adoptive transfer. However, these fluorescent reporters may not be the perfect tool to detect all transferred B cells especially if they are expanding rapidly.

Due to detection problems with fluorescent reporter proteins tracking of donor B cells via allotype was investigated. TH mice were backcrossed onto both C57BL/6 (BL6) and SJL/J (SJL) genetic backgrounds. Endogenous and knock-in Ig H chains can be readily identified serologically by their allotypes. C57BL/6 and SJL/J mice produce Ig of allotype b (Igh^b), whereas the targeted Ig H gene locus in TH mice is derived from the strain 129/Sv, with allotype a (Igh^a) [31]. B cells from SJL or BL6 WT mice were mixed 1:1 with B cells from SJL or B6 TH mice (Figure 16 B). As expected, IgM^a and IgM^b expression on day 1 is similar in all groups. On day 8 IgM^a and IgM^b levels are dramatically decreased due to isotype switch. Detection of IgG1^a and IgG1^b was investigated but no signal was found after 8 days of culture suggesting that the available reagents are not suitable for flow cytometry (data not shown). Thus, detection of allotype for tracking B cell fate upon transfer seems only useful before isotype switch to IgG1 because IgM is downregulated after activation. Since B cell fate after transfer is unclear, a detection tool is needed that reliably labels B cells regardless of their differentiation and proliferation status. Therefore, the use of allelic markers for donor B cell detection after transfer was evaluated. B cells from heterozygous CD45.1/2 mice were cultured on 40LB cells (Figure 16 C). Expression of allelic markers remained stable over the entire culture period suggesting that allelic markers are suitable for long term tracking of highly proliferating iGB cells.

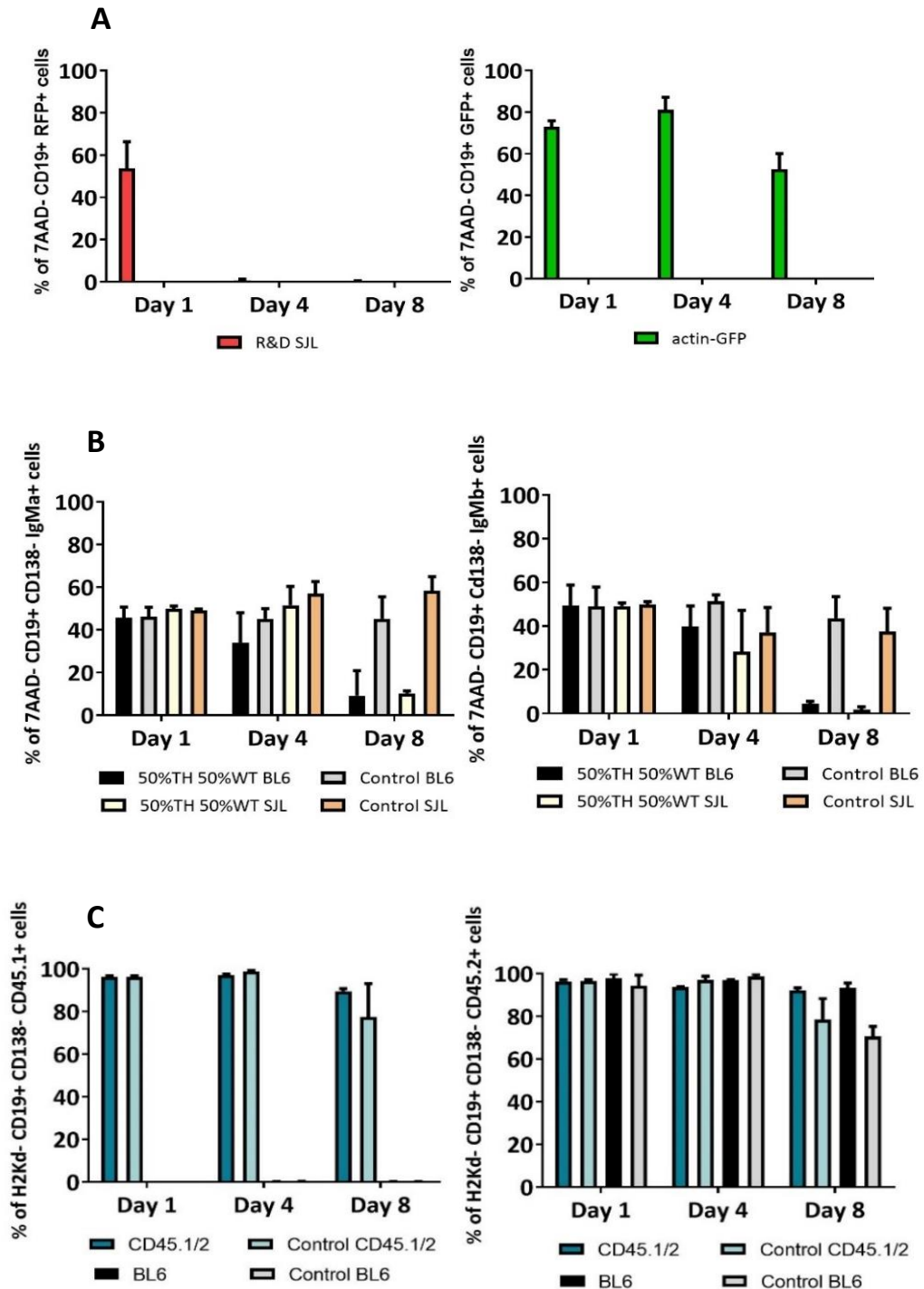


Figure 16: Testing of different reporter cells for tracking B cell fate after transfer.

A) iGB culture of RFP and GFP B cells. RFP B cells derived from R&D mice (red bars) and GFP B cells derived from actin-GFP mice (green bars) were cultured for 8 days on 40LB cells in presence of IL-4 and IL-21. Expression of fluorescent proteins was measured at the indicated time points in live B cells via flow cytometry. B) Detection of different allotypes due to genetic backgrounds. WT B cells from BL6 or SJL mice were mixed 1:1 with TH B cells and cultured for 8 days on 40LB cells. BL6 WT/TH (black bars), their control (grey bars), SJL WT/TH (yellow bars) and their respective controls (orange bars) were analyzed for presence of IgM^{a+} and IgM^{b+} B cells (gated on 7AAD- CD19+ CD138- cells) with flow cytometry. C) Detection of CD45.1 and 2 during iGB culture. B cells from CD45.1/2 heterozygous mice were cultured for 8 days on 40LB cells and analyzed by flow cytometry. CD45.1+ and CD45.2+ cells were pre-gated on H2Kd- CD19+ CD138- cells. Representative data of 2 independent experiments with n=2 mice is shown. Mean \pm SEM.

3.3.4 Expansion of MOG-specific B cells in the iGB culture

To study behavior of MOG-specific B cells from RR mice or immunized mice in the iGB culture, B cells from CLNs and spleen of sick RR and MOG/Alum immunized mice were cultured on 40LB cells (Figure 17 A). In line with prior results from our laboratory, *ex vivo* not more than 1% of B cells in RR mice and MOG-immunized mice were MOG-specific as they were able to bind a tetramerized mammalian MOG protein (MOG_{tet}). Since MOG-specific B cells likely have been activated *in vivo*, we speculated that they expand even more in the iGB culture than naïve B cells. However, no enrichment or selective expansion of these MOG-specific B cells was detectable with MOG_{tet}-staining after 8 days of iGB culture (Figure 17 A), indicating that either MOG-specific B cells have a similar expansion factor as naïve B cells, or that they cannot be detected anymore via MOG_{tet} staining after iGB culture.

To test whether MOG-specific B cells in the iGB culture are reliably detected via MOG_{tet} staining, B cells from TH mice were mixed with B cells from WT BL6 mice (1:1) and cultured on 40LB cells (Figure 17 B). While on day 1 most of the MOG-specific B cells are detectable with MOG tetramer staining (about 40% of the 1:1 mixture), after 4 days MOG_{tet} staining is slightly decreased compared to the control culture. Similar to the loss of signal observed for the fluorescent reporter proteins (see 4.1.3) MOG-specific B cells could not be detected via MOG_{tet} staining anymore after 8 days of iGB culture. This phenomenon might be due to MOG_{tet} binding better to IgM⁺ cells, where multiple immunoglobulins are linked together by strong covalent bonds than to IgG1⁺ cells with only two antigen binding sites.

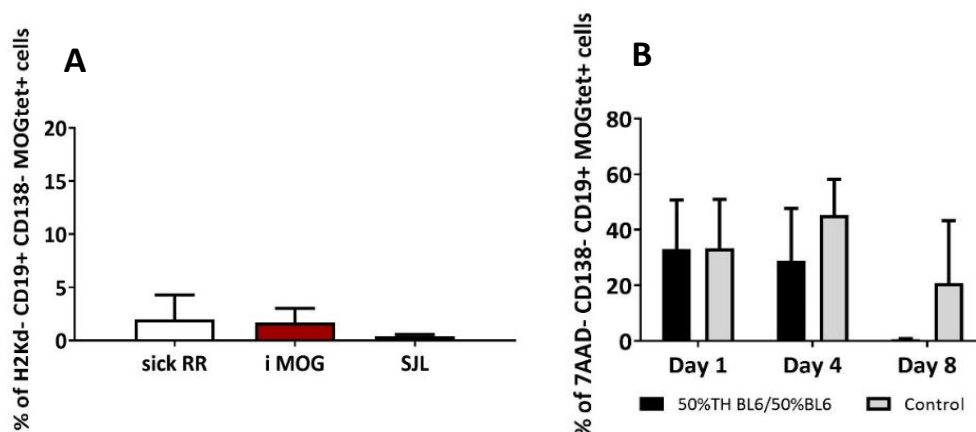


Figure 17: Expansion of MOG-specific B cells in iGB cell culture.

A) Expansion of B cells from sick RR or MOG immunized mice in iGB culture. B cells from sick RR mice, MOG/Alum immunized mice (iMOG) or SJL WT control mice were cultured for 8 days on 40LB cell in presence of IL-4 and IL-21. B cells (H2Kd⁻ CD19⁺ CD138⁻ cells) were analyzed with flow cytometry for presence of MOGtet⁺ B cells. B) Detection of MOG specific TH B cells with MOGtet staining. B cells from BL6 WT and TH mice were mixed 1:1 and

cultured for 8 days on 40LB cells in presence of IL-4 and IL-21 (black bars) or without cytokines (grey bars). Mean \pm SEM from 2 independent experiments with $n = 2$ is shown.

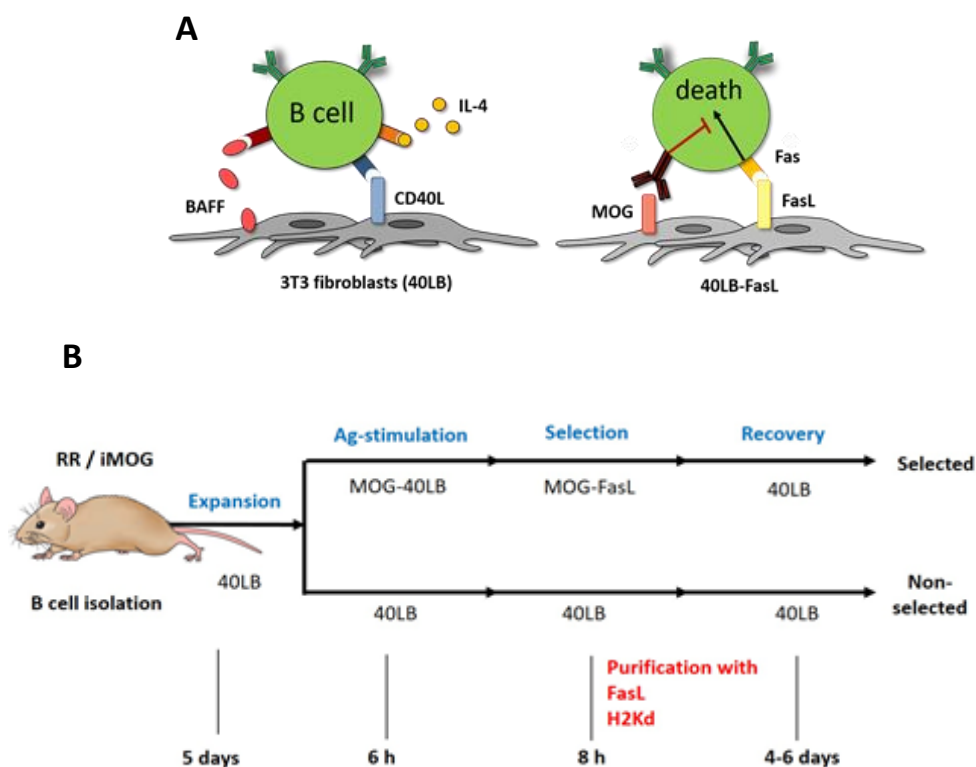
3.3.5 Selective expansion of MOG-specific B cells with the FAIS system

As previously reported, not more than 1% of B cells in CLNs of RR mice are MOG-specific. Moreover, expansion of B cells from sick RR and MOG immunized mice did not result in enrichment of MOG-specific B cells during normal iGB culture. Therefore, a protocol to selectively expand MOG-specific B cells in the iGB culture was tested. In analogy to the selective expansion of HEL-specific B cells in iGB culture shown by Kitamura and colleagues [117], we created MOG-40LB cells and MOG-FasL cells for selective expansion of MOG-specific B cells taking advantage of the fact that iGB cells are sensitive to Fas-induced cell death unless their antigen receptors receive a survival signal by their specific antigen (FAIS system) (Figure 18 A). MOG-40LB cells and MOG-FasL were created in our lab via viral transduction. Both cell lines express MOG, CD40L and BAFF (Figure 18 B). Antigen specific selection of MOG-specific B cells was performed as described previously for HEL [117]: First, B cells were expanded for 5 days on normal 40LB cells. Second, B cells were stimulated for 6h on MOG-40LB cells. Third, B cells were plated on MOG-FasL cells for 8h for antigen-specific selection. In this step, only MOG-specific cells should be protected from Fas-FasL- induced cell death. Afterwards, B cells were purified and cultured for 4-6 days on 40LB cells for recovery. For these experiments B cells were either isolated from SJL/J mice immunized with rMOG, or B cells from TH mice were mixed at a ratio of 1:99 with cells from SJL WT mice and cultured under antigen-specific selection conditions (Figure 18 C-D). In the first 6 days B cells expanded up to 10 fold. As expected, during the selection procedure the majority of the B cells died. However, after 4-5 days recovery there was no evidence that MOG-specific B cells survived the selection process better than WT cells, since preferential expansion of MOG-specific B cells at the end of the culture was not observed. In order to optimize the protocol for selective expansion of MOG-specific B cells, different culture conditions were tested (data not shown). After 4 or 6 days on 40LB cells, expanded iGB cells were either stimulated for 6h or overnight on MOG-40LB cells. Selection procedure was either performed on FasL or MOG-FasL cells. To reduce stressful procedures for fragile iGB cells, purification steps before and after antigen stimulation were eliminated, and only purification after selection was performed to remove toxic FasL cells from the recovery culture. B cell stimulation on MOG-40LB cells overnight showed slightly lower B cell expansion than stimulation for 6h. B cell selection on FasL versus MOG-FasL cells resulted in equally low numbers of surviving B cells. Removal of purification steps before and after antigen stimulation increased the overall

number of remaining B cells. However, none of these modifications selectively increased the survival/expansion of MOG-specific B cells. Furthermore, the difficulties to detect MOG-specific B cells by MOG_{tet} staining further complicated the interpretation of the results.

It is possible, that the FAIS protocol is not applicable to all sorts of antigens characterized by very different BCR affinities and binding properties. Thus, being an autoantigen MOG probably has lower affinity than the foreign antigen HEL, which was used in the original FAIS protocol. To test this hypothesis, selective expansion of HEL-specific B cells as published before by Kitamura was tested. Splenic B cells from swHEL mice which are 90–95% HEL-specific and can switch to all Ig isotypes [107] were mixed in a frequency of 15% or 50% with WT BL6 splenic B cells and selectively expanded with the FAIS system. Pure WT BL6 and pure HEL-specific B cells were used as negative and positive control as WT cells should not survive the selection process.

Unfortunately, the selective expansion of HEL-specific B cells (Figure 18 E-F) was not reproducible in our hands. Additionally, HEL-specific B cell selection from HEL immunized mice was investigated (data not shown). WT BL6 mice were immunized with HEL protein, and after 3 weeks HEL-specific IgG titers were measured. Mice with high titers of HEL-specific antibodies were sacrificed and B cells from spleen and draining LNs were expanded in the iGB culture. However, again there was no enrichment of HEL-specific B cells after FAIS selection.



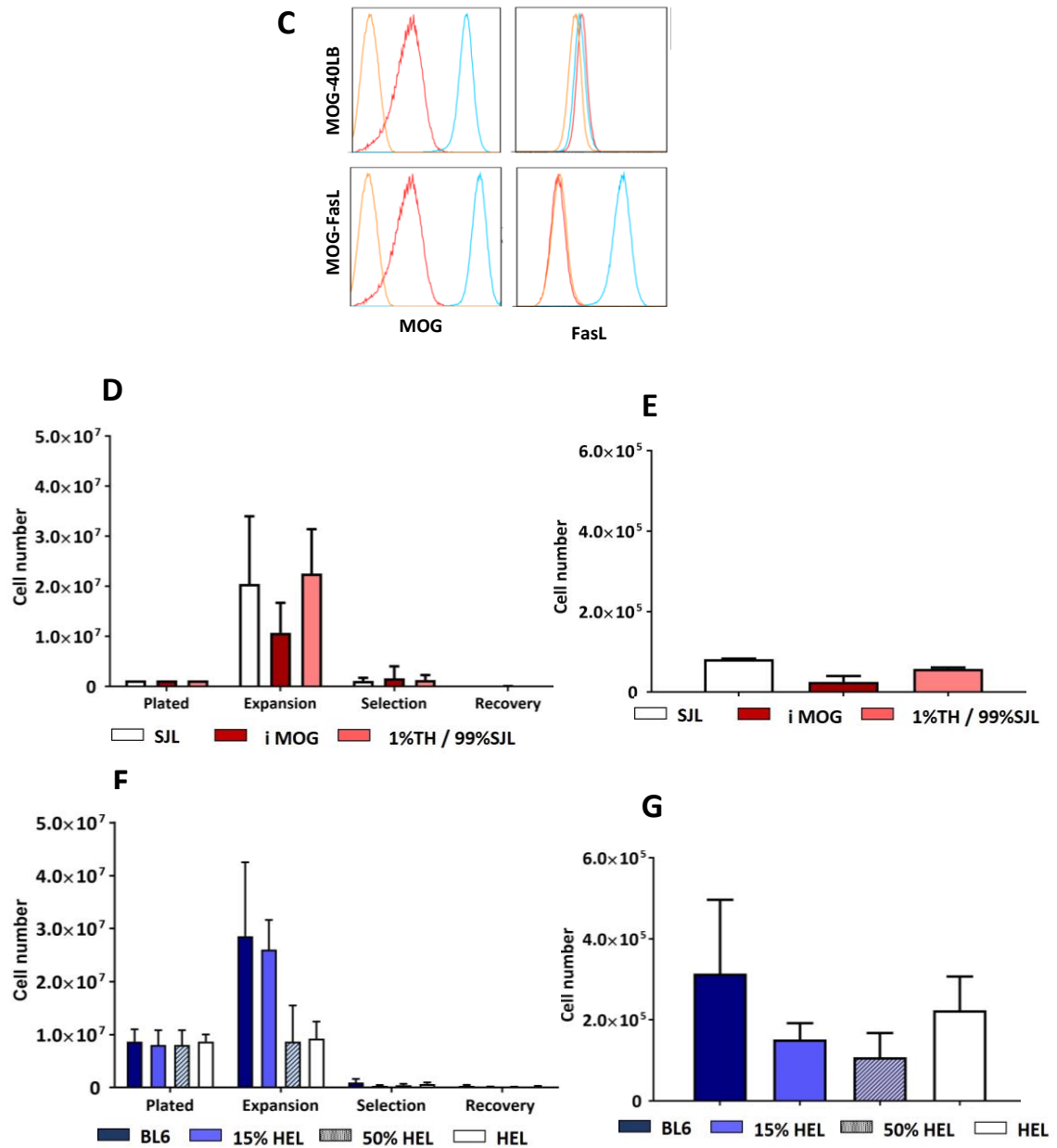
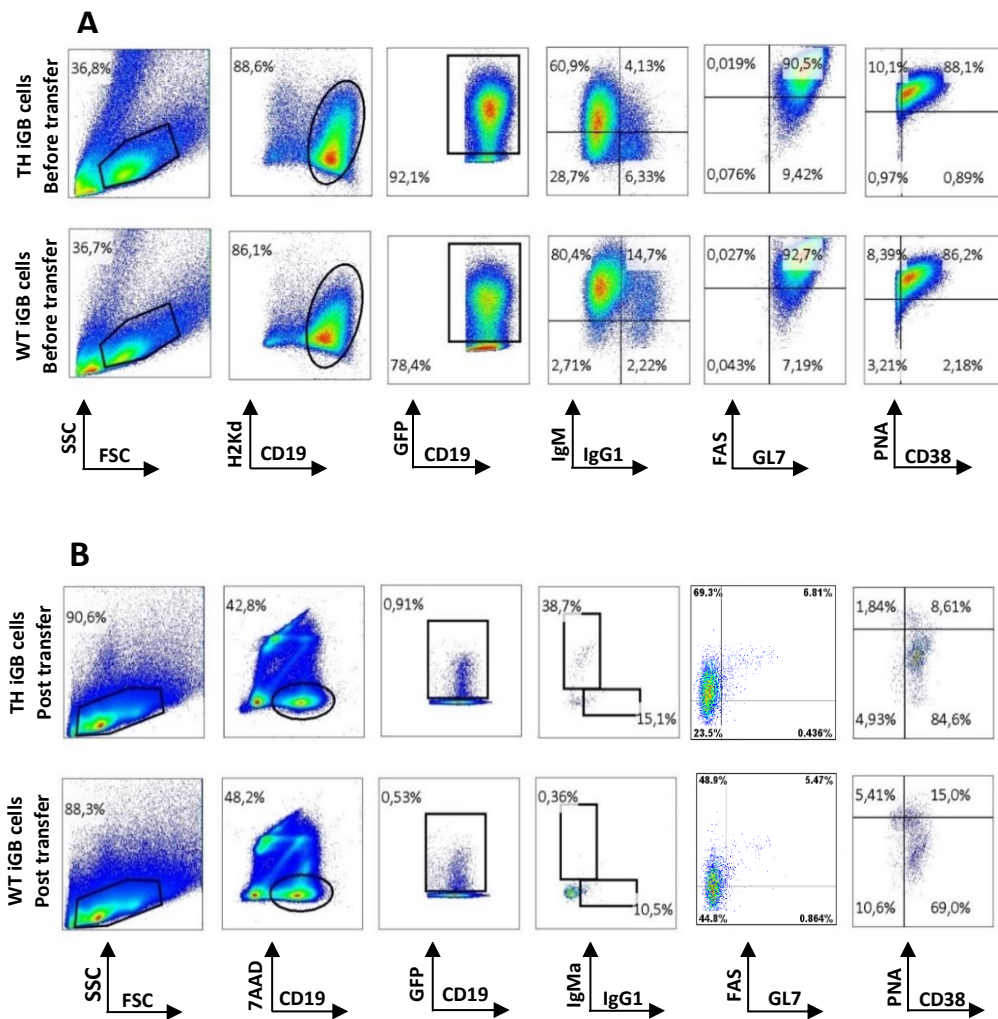


Figure 18: Selective expansion of antigen-specific cells in the FAIS system.

A) BALB/c 3T3 fibroblasts were transfected with mouse CD40L and BAFF cDNA (40LB cells). Primary B cells are cultured with 40LB cells as feeder layer in the presence of IL-4 or IL-21. For antigen-specific B cell selection 40LB cells were first transduced with pSIREN-RetroQ-shFas vector and then Fas negative cells were further transduced with pMX-FasLIREs-hCD8 vector. Draft modified from [59] B) Schematic representation of antigen-specific selection protocol (FAIS). Purified B cells or whole splenocytes were cultured for 4 days on 40LB cells with IL-4 and 2 days with IL-21. For antigen stimulation, B cells were cultured on MOG-40LB cells for 6h. Afterwards B cells were selected with MOG-FasL or FasL cells for 8h. B cells were purified by removal of FasL⁺ and H2Kd⁺ feeder cells and were allowed to recover on 40LB cells for 4-6 days. C) Flow cytometry analysis of MOG-40LB (upper panel) and MOG-FasL (lower panel) cells. MOG-40LB and MOG-FasL cells (blue lines) were tested for expression of MOG (left panel) and FasL (right panel) in comparison to regular 40LB cells (red lines) and unstained control cells (yellow lines). D) Selection of MOG-specific B cells from rMOG immunized SJL/J mice, as well as B cells from TH SJL mice mixed 1:99 with WT cells. Graph shows B cell numbers in the different phases of the FAIS protocol. E) Number of surviving B cells after 5 days recovery. F) Selection of HEL-specific B cells from swHEL mice mixed with WT BL6 cells. G) Number of surviving B cells after 5 days recovery. Mean \pm SEM from 3 independent experiments with $n \geq 2$ mice is shown.

3.3.6 Adoptive transfer of TH or WT iGB cells as a tool for B cell studies

To study function, properties and pathogenic potential of MOG-specific iGB cells adoptive transfer of WT and TH iGB cells was performed. 2D2 mice [30], which carry a transgenic MOG-specific TCR and in which the incidence of spontaneous EAE is very low (<5%), were used as recipients to test whether transfer of MOG-specific iGB cells can trigger development of disease. To be able to track B cells after transfer, splenocytes were either isolated from actin-GFP or CD45.1/2 mice crossed with TH mice. Whole splenocytes were cultured for 4 days in iGB culture with IL-4, stimulated with or without rMOG for 1-2 h, and then injected. Mice were observed at least 16-18 days post transfer or, in case of disease development, analyzed 2 days after first showing clinical signs of EAE. At the time of transfer WT and TH x GFP iGB cells showed a GC phenotype after 4 days of culture, and the majority of B cells were still IgM⁺ (Figure 19 A).



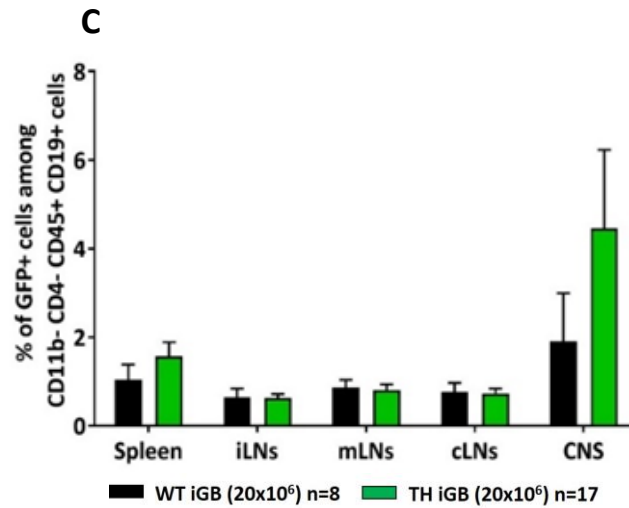


Figure 19: Phenotype of TH and WT iGB cells before and after transfer into 2D2 mice.

Actin-GFP and GFPxTH splenocytes were cultured for 4 days on 40LB feeder cells with IL-4. After iGB culture, cells were washed and around 20x10⁶ iGB cells were injected into 2D2 mice. Mice were monitored for development of EAE and sacrificed at the latest 18 days post transfer. A) Gating strategy and phenotype of TH and WT iGB cells in culture at the time of transfer. GFP⁺ B cells (H2Kd⁻ CD19⁺ GFP⁺) were analyzed for expression of IgM, IgG1, FAS, GL7, PNA and CD38. B) Gating strategy and phenotype of transferred GFP⁺ cells in recipient mice 18 days post transfer. GFP⁺ B cells (7AAD⁻ CD19⁺ GFP⁺) were analyzed for expression of IgMa, IgG1, FAS, GL7, PNA and CD38. C) Frequency of transferred GFP⁺ iGB cells in spleen, inguinal, mesenteric and cervical lymph nodes and CNS. CD11b⁻ CD4⁻ CD19⁺ cells were analyzed for expression of GFP⁺. Mean \pm SEM from >3 independent experiments with WT iGB n=8, TH iGB n=17 are shown.

After transfer, IgM^a expression was significantly higher in mice that received MOG-stimulated TH iGB cells compared to TH iGB cells without pre-stimulation, and not detectable in recipients of WT iGB cells, as expected (Figure 20). IgG1 expression was low in all mice, however, significantly increased in spleen and iLNs of recipients of MOG-stimulated TH iGB cells compared to recipients of WT iGB and non-stimulated TH iGB cells. Additionally, IgG1 expression in transferred cells in the CNS was slightly higher than in other organs especially in TH iGB recipients, while IgM expression in the CNS was markedly reduced compared to the periphery. As described by Kitamura, after transfer WT iGB cells still expressed moderate levels of Fas but had downregulated GL7 (Figure 19B and 20). However, recipients of TH iGB cells showed significantly higher FAS expression compared to WT iGB cells. All transferred cells still expressed CD38 but were negative for PNA. Thus, after transfer into recipient mice B cells displayed an activated/memory phenotype rather than a germinal center B cell phenotype. After 16-18 days GFP⁺ cells were equally distributed between inguinal, mesenteric and cervical lymph nodes with a slight but not significant enrichment in spleen (Figure 19 C). No preferential accumulation of GFP⁺ B cells was visible in any of the peripheral organs. Among CNS infiltrating B cells, the frequency of GFP⁺ B cells was increased compared to peripheral organs, however, the overall frequency of CNS-infiltrating B cells compared to infiltrating T cells was very low, indicating that transferred B cells may not play a major role in the inflammatory processes in the CNS in this model. Phenotyping of transferred cells

indicated that TH iGB cells are more activated showing increased FAS expression in all organs (Figure 20).

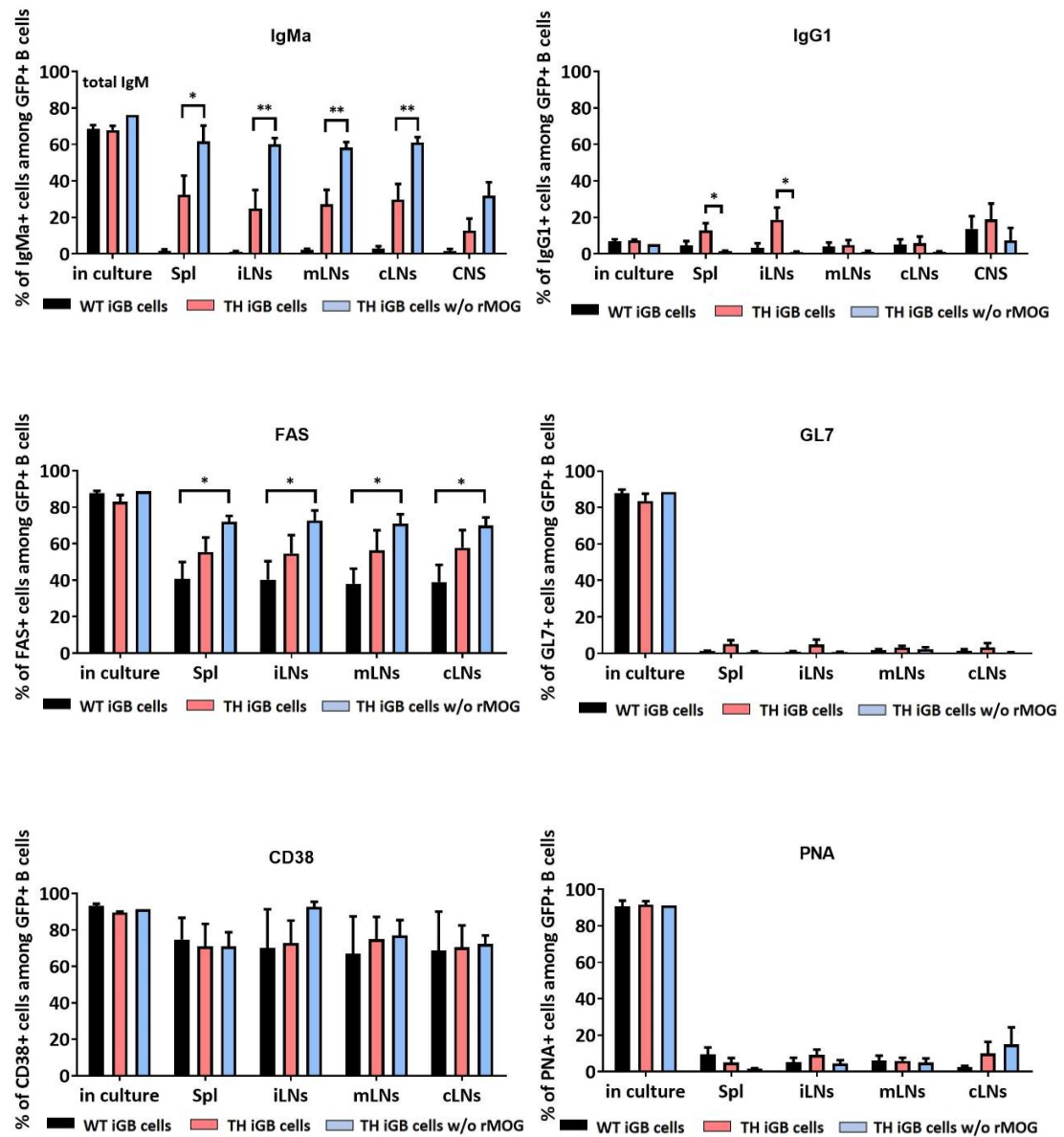


Figure 20: Phenotyping of transferred iGB cells in different organs.

Characterization of WT, TH and TH iGB cells without MOG before transfer (in culture) and re-isolated from spleen, inguinal, mesenteric and cervical lymph nodes as well as CNS of recipient mice 16-18 days after transfer. Cells were gated on size, 7AAD⁻ or CD4⁺, CD11b⁻ or CD138⁻, CD19⁺, GFP⁺ cells. Mean \pm SEM from >3 independent experiments with WT iGB n=9, TH iGB n=12 and TH iGB cells without rMOG n=7 are shown. *P<0.05, ***P<0.01, ****P<0.001, t-test for IgM^a or 1-way ANOVA, Kruskal Wallis test – Dunn's multiple comparison test.

3.3.7 TH iGB cells trigger development of EAE in 2D2 recipient mice

Importantly, transfer of TH iGB cells into 2D2 mice resulted in development of EAE with high severity in about 50-60% of recipients between 7-11 days post transfer, whereas recipients of WT iGB cells remained healthy (Figure 21 A and B). Interestingly, recipients of MOG-pulsed TH iGB cells developed EAE with similar incidence and mean maximum scores as recipients of unpulsed TH iGB cells, indicating that provision of exogenous MOG antigen is not required for the pathogenicity of TH iGB cells. Overall, the incidence of EAE in 2D2 mice after transfer of TH iGB cells was increased dramatically above the rate of spontaneous EAE in 2D2 mice which typically lies below 5% [30]. Serum ELISA analysis from 2D2 recipient mice showed high titers of MOG-specific IgMa and IgG1a in recipients of TH iGB cells (Figure 21 C). Taken together, TH iGB cells are able to induce EAE in 2D2 mice, even without stimulation by autoantigen and can be used as a new tool to study the role of B cells in initiation of EAE.

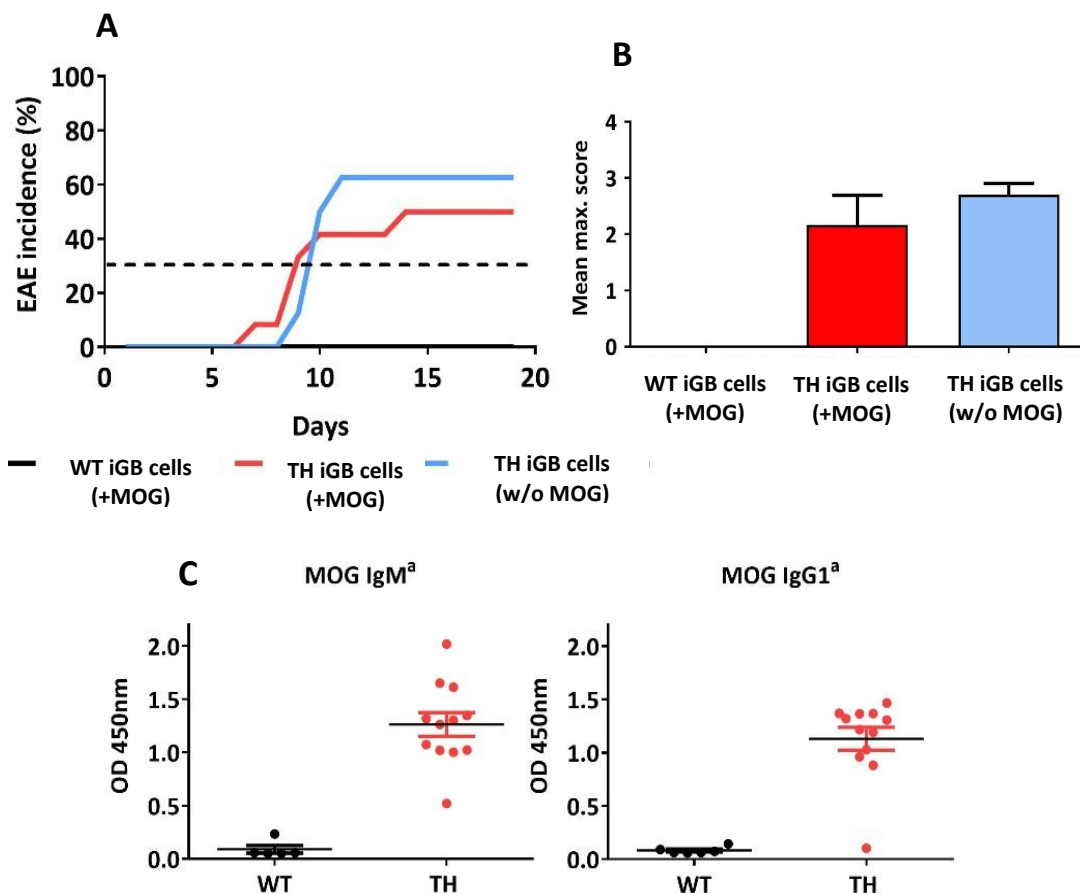


Figure 21: Adoptive transfer of TH iGB cells triggers development of EAE in 2D2 mice

A) EAE incidence in 2D2 mice after transfer of either WT iGB cells, or TH iGB cells stimulated with or without MOG. B) Mean maximum EAE score in 2D2 recipient mice. Only sick mice were included in the graph. C) Presence of MOG-specific IgMa and IgG1a in the serum of 2D2 recipient mice was determined by ELISA. Mean \pm SEM from >3 independent experiments with WT iGB recipients n=8, TH iGB recipients n=12 and TH iGB cells without rMOG recipients n=8 are shown.

4 DISCUSSION

4.1 Antigen transport

According to the literature and latest findings [68, 78, 81], recruitment of B cells through auto-antigen transport may play an important role in the development of EAE. Therefore, drainage pathways of auto-antigens *via* cells or exosomes from the CNS to CLNs were investigated.

After intrathecal injection of dextran-FITC, dextran-Alexa Fluor 488 and 647, dextran positive leukocytes were detected in CLNs indicating a direct drainage pathway from the CNS to the regional lymph system (Figure 2). However, further studies with intrathecal injection of MOG-FITC could not confirm translocation of auto-antigen to regional lymph nodes (Figure 3). Dextran-FITC (70 kDa) is smaller in size than MOG-FITC (110 kDa), which might alter migration properties of the soluble molecules. Thus, mammalian MOG may be too big to pass from CNS to regional lymph nodes without degradation. In an alternative approach, tracking of CNS antigen during the development of EAE using PLP-GFP reporter mice (Figure 4) was tested, but almost no GFP⁺ lymphocytes or myeloid cells were found in CLNs or other organs. Positive staining for PLP, MBP and MOG in the CLNs of sick RR mice would support the hypothesis that auto-antigens are transported from CNS to CLNs. However, positive staining was not only detected in the CLNs of sick RR mice, but also in the CLNs of healthy NTLs (Figure 5 A-C) and - for MOG - in MOG-deficient mice (Figure 6). To exclude unspecific Fc receptor binding, staining with anti-MOG F(ab)₂ antibody was performed (Figure 5 D). Although the anti-MOG F(ab)₂ antibody detected MOG in the CNS, positive staining was no longer detectable in the CLNs of sick RR mice and NTLs. These data suggest that the regular MOG-specific antibody binds unspecifically to Fc receptors on macrophages. Concordantly, MOG staining did not colocalize with B220 and CD4 but with the macrophage markers CD11b/CD68 (Figure 6). Given that no PLP-GFP signal was detectable in the CLNs using reporter mice, it is likely that the observed positive signals for PLP and MBP are also false positive signals caused by unspecific capture of the staining antibodies via Fc receptors on macrophages.

Immunohistological analysis of CLNs of RR mice and FACS analysis of CLNs of PLP-GFP mice with EAE suggest that myelin antigens are either not transported to CLNs of sick mice or are no longer detectable due to degradation of the epitopes recognized by the antibodies: thus, it is possible, that by the time the auto-antigens reach the CLNs their epitopes are already destroyed by antigen-processing in APCs and can therefore no longer be detected by

antibodies. Additionally, unspecific staining of PLP and MBP may not only be due to Fc receptor binding but also due to the recognition of other isoforms expressed in the periphery [125-127]. Thus, the shorter isoform of PLP, DM20, has been detected in the periphery in thymic cortical epithelium [127], and Golli-MBP isoforms were shown to be expressed in fetal thymus and spleen [125]. Therefore, it is possible that these isoforms also exist in CLNs where they may be detected by the antibodies used here. In contrast to MBP and PLP, expression of MOG isoforms outside the CNS has not been observed [126], and in line with this, the anti-MOG F(ab)₂ antibody did not stain cells in CLNs. These data suggest that the positive signal for myelin antigens in CLNs of RR mice is due to unspecific binding of antibodies to Fc receptors on macrophages, and that myelin antigens are not transported as whole proteins from the CNS to CLNs during EAE. However, presence of processed myelin antigens (fragments/peptides) in CLNs cannot be excluded, and thus it is still possible that processed myelin antigens are transported to CLNs and presented to autoreactive lymphocytes. Future studies should concentrate on using proteomics as a tool for myelin antigen detection as it is much more sensitive for small amounts of protein fragments.

Several studies have analyzed tissues from MS patients as well as EAE tissues (CSF, spinal cord and brain), however the only myelin protein found to be significantly increased in CSF of MS patients and aEAE in all proteomic studies was MBP, probably because it is the most prominent protein of the myelin sheath [128]. There are no proteomic studies analyzing CLNs in EAE, but technically, it is possible to perform tissue-based proteomics. Nevertheless, there is still a detection limit for proteins/peptides which might be too low to detect small amounts of myelin proteins/peptides in early disease stage of sEAE. In addition, since myelin proteins may only be transiently present in CLNs of RR mice, identifying the right time point for a proteomic analysis would be crucial and challenging in RR mice given the late onset of spontaneous disease after 3-4 months of age. In that regard, 2D2xTH mice might be the better option for proteomic analysis of CLNs due to the earlier onset of disease around 6 weeks of age.

Exosomes can modulate immune functions, affect communication between cells and are able to transport various proteins [82, 84, 85, 87]. Since neuronal antigens have been found in CLNs of marmoset monkeys with active EAE and in patients with MS [80, 81], one hypothesis is that exosomes function as a transport system for autoantigens between CNS and CLNs. To be able to test this hypothesis, first a method for the isolation and characterization of microvesicles from different cell sources was established (Figure 7-8). Isolated nanoparticles showed the typical size and shape of exosomes and expressed exosome markers like Alix,

Tsg101, CD63, and CD9, as well as corresponding cell type markers. Furthermore, exosomes isolated from EL4-MOG and H2M BMDCs were able to carry MOG on their surface and even showed an enrichment of MOG compared to their cellular origin (Figure 10 B, D). As shown by previous reports, exosomes can perform cell-independent microRNA (miRNA) biogenesis and are an enriched source of mRNAs [129, 130]. Thus, enrichment of MOG mRNA in exosomes compared to their cellular origin is possible. These data indicate that exosomes from EL4 cells and BMDCs can be successfully isolated, and that exosomes derived from EL4-MOG cells or H2M BMDCs have the potential to transport MOG and present it on the surface. As exosomes can stimulate T cells by direct or indirect antigen presentation [131, 132], *in vitro* T cell activation assays with MOG enriched exosomes could be performed. To determine whether T cells are activated directly through antigen presentation on exosomes or indirectly by transfer of exosomal antigen to APCs, different experiments have to be performed: MOG-containing exosomes could be directly co-cultured with MOG-specific T cells from RR mice or OSE mice. Alternatively, B cell/DCs could be co-cultured with exosomes and then T cells could be added later to test whether exosomal MOG is transferred to APCs, which in turn present it to T cells. Qazi et al. showed that B cells are required for exosomal T cell activation, as B cell signaling-deficient mice show decreased splenocyte proliferation in response to ovalbumin loaded exosomes [133]. Considering these data, it is possible that exosomes activate T cells by antigen–MHC complex transfer to B cells leading to indirect antigen presentation. Thus, exosomes shed from EL-4 MOG cells injected directly into RR mice may accelerate and exacerbate EAE induction. This would be the first clue that exosomes are a potential factor in myelin antigen transport and activation of autoreactive T cells in spontaneous EAE.

However, exosome studies in mice have several limitations: firstly, isolation of exosomes is only feasible from fluids like cell culture supernatant, urine, blood and CSF. There are no reports confirming successful exosome isolation from tissue. Secondly, determining the relevance of exosomes as a transportation system for myelin antigens *in vivo* would require isolation of exosomes from the CSF of sick RR mice. However, the amount of CSF that can be obtained from sick mice (2-5 μ l) is not sufficient for reliable characterization or meaningful functional analysis or transfer of exosomes. Thirdly, intravenous injection of exosomes to mice is lethal due to aggregation of vesicles and blocking of capillaries (personal communication with Dr. Mikael Simons). Taken together, it is currently not feasible to show the physiological role of exosomes as a transportation system for myelin antigens and related B cell or T cell activation in RR mice.

4.2 B cell activation studies in the intestine

According to recent findings, recruitment of MOG-specific B cells may be an important factor in development of EAE. RR mice are fully protected from spontaneous EAE, when housed under germ-free conditions. Furthermore, MOG-specific B cells get recruited to CLN of these mice suggesting that the microbiota and the autoantigen cooperate somehow for the generation of a pathogenic autoimmune response in this model [68]. As we were not able to demonstrate autoantigen transport of MOG from CNS to CLNs, an alternative possibility is that autoreactive B cells are activated by a microbial foreign protein mimicking MOG in the intestine first and migrate to CLNs afterwards. To study whether B cells are activated in the gut by molecular mimicry, transfer studies with MOG-specific B cells into RR recipient mice were planned to determine the B cell activation status in different intestinal segments, as well as in other organs. To establish the experimental system, transfer experiments with actin-GFP reporter cells were performed but revealed several limitations.

First of all, even transfer of 25×10^6 splenocytes or 10×10^6 purified B cells from actin-GFP mice resulted in very low frequencies of GFP⁺ cells in intestinal segments (Figure 9). To draw reliable conclusions regarding activation of transferred B cells in different segments of the intestine, transferring a high number of B cells per mouse is necessary. However, since the actin-GFP transgene is lethal in homozygotic embryos, heterozygous mice have to be used in which not all cells are actin-GFP⁺. Therefore, many mice are required to provide enough B cells to perform transfer experiments. Furthermore, GFP signal is lost during the intracellular staining procedure (Figure 10) which is necessary to measure intracellular markers such as cytokines and transcription factors and thereby characterize the transferred B cells. Even with optimized staining conditions approximately 60 % of the signal was lost during fixation, permeabilization and staining. To overcome staining procedure limitations, GFP⁺ B cells could be isolated and sorted from the intestinal segments and expression of intracellular markers like cytokines and transcription factors could be determined on the RNA level.

One reason for the low overall frequencies and persistence of transferred B cells could be their activation status. When B cells do not bind their antigen or receive some other activation/survival signal for example via CD40, IL-4 or IL-21 they die easily. B cells need T cell help for their survival, proliferation and differentiation [134]. In future studies, B cells could be either pre-activated with antigen or cytokines before transfer, or they could be transferred in combination with T cells of the same antigen specificity. This would of course mask natural B cell activation *in vivo*, which we would like to determine, but at least migration

patterns could still be investigated. Furthermore, B cells have no reason to migrate from the intestine to CLNs or CNS when they do not encounter antigen. Another option to study activation of autoreactive B cells in the intestine would be to provide a strong controlled stimulus by gavaging of MOG protein to host mice, especially if B cell activation stimuli provided by bacterial proteins or metabolites in the gut are too low to see an effect. This approach could be used to study migration of activated MOG-reactive B cells from the gut to other locations.

Low B cell frequencies were probably a result of poor B cell survival in an immunocompetent host that does not provide much antigen or cytokine stimuli for their survival, proliferation and differentiation [134]. An option to overcome this is to use R&D mice carrying RFP and the human DTR on their B cells, which allows for depletion of B cells *via* administration of diphtheria toxin. Therefore, a niche for transferred B cells could be created allowing survival of these cells. Another nice feature of these mice is that host B cells are easy to distinguish from transferred GFP⁺ B cells by RFP expression. However, in this experimental set-up it might be difficult to differentiate between B cell proliferation/activation caused by lymphopenia versus recognition of auto-antigen.

4.3 New tool for B cell studies in EAE

Several limitations and difficulties have hindered meaningful studies to investigate the recruitment, activation and properties of antigen-specific B cells in EAE. To overcome the limitations posed by low frequencies of autoantigen-specific B cells and to be able to characterize and manipulate different B cell populations a new culture system for B cell expansion and selection was established.

The iGB cell culture system from Kitamura et al. [116] was successfully adapted for our purposes and needs. B cells were expanded and characterized from BL6, SJL/J, R&D SJL/J, actin-GFP BL6 and RR mice (Figure 12). B cells from all strains expanded 8-10 fold in the primary culture and about 300 fold in the secondary culture. Expansion rates were similar in BL6 and SJL/J mice. B cells were also characterized with flow cytometry. They showed a clear GC phenotype and isotype switch from IgM to IgG1 in presence of IL-21 (Figure 13). Culture conditions were miniaturized to optimize expansion of low B cell numbers from different organs (Figure 14). Moreover, culture of fluorescently labeled B cells from R&D SJL/J and actin-GFP mice for later transfer experiments was tested. Unfortunately, RFP signal from R&D SJL mice decreased dramatically during iGB culture; however, actin-GFP remained reasonably

bright during iGB culture and proved suitable for transfer experiments (Figure 16 and Figure 19). Additionally, the congenic markers CD45.1 and CD45.2 can be used for tracking B cells during iGB culture and in future transfer experiments. In order to track MOG-specific B cells, MOG tetramer staining both on B cells from MOG-immunized mice as well as on B cells from TH mice during iGB culture was performed. Unfortunately, MOG tetramer staining also decreased over the culture period (Figure 16). This could be due to MOGtet binding better to IgM⁺ than to IgG1⁺ cells. To find a solution for detection of B cells after transfer, allotype specific markers for TH B cell detection, which reliably differentiated TH B cells from WT B cells were tested. However, allotype specific marker detection was only established for IgM^α and thus only useful for transfer experiments of primary culture iGB cells before isotype switch.

Cell culture conditions were modified to avoid loss of B cells during isolation procedure. Thus, whole splenocytes can be plated on 40LB cells without prior B cell isolation. Other cell types including T cells, macrophages and dendritic cells largely died during iGB culture and did not influence B cell expansion or differentiation (Figure 15). Culture of CNS-derived B cells from a sick mouse was successfully performed and showed expansion and differentiation to iGB cells. Collectively, the iGB cell culture system is a useful tool to expand and differentiate low numbers of B cells from different organs and actin-GFP or congenic markers are the most promising candidates to track B cells in adoptive transfer experiments.

Additionally, we tried to establish a FAIS cell culture system for selective expansion of MOG-specific B cells in order to study the rare MOG-specific B cells emerging from the endogenous repertoire in RR mice. For this purpose MOG-40LB and MOG-FasL feeder cells were created (Figure 19). In contrast to published data selective expansion of Ag-specific B cells was not successful. Different culture conditions were tested in order to optimize Ag-specific B cell expansion, but the modifications did not significantly improve survival/expansion of selected B cells. MOG-specific B cells are either not selected and do not recover after the B cell selection step or are not any longer detectable by MOG tetramer due to downregulation of the BCR or reduced binding affinity of the isotype-switched BCR to MOG tetramer. As a prove of principle selective expansion of HEL-specific B cells was investigated which was already published by Kitamura [117] (Figure 18). However, published results were not reproducible in our hands and HEL-specific B cells seemed to not survive or recover better than WT cells. One reason why selective expansion of MOG-specific B cells failed could be that selection only works for certain antigens depending on protein size, epitope and binding affinity. However, also expansion of HEL-specific B cells failed and therefore the reason could be that

cells are extremely sensitive to culture conditions such as supplemented growth factors, type of medium and cytokines. Therefore, it should be considered to standardize culture conditions from the published protocol. Taken together, adaptation of the FAIS system for different antigens is not trivial and seems to be very sensitive to external factors. Thus, we could not utilize this system to expand and characterize MOG-specific B cells.

Another approach to expand and characterize MOG-specific B cells is to do transcriptomics. As culture of CNS derived B cells from a sick mouse was successful, clones of these B cells could be expanded with the new iGB culture tool. B cells could be isolated from the CNS of sick RR mice, single sorted into 96 well plates with feeder cells and after clonal expansion analyzed for their antigen titers. Clones with high titers of MOG-specific antibodies could be then further analyzed with transcriptomics for their target epitopes. This method could provide insights into heterogeneity of B cell auto-antigens. Dornmair et al. were able to combine biochemical analysis, proteomics, and transcriptomics to molecularly characterize distinct OCB antibodies of MS patients [61]. They characterized three auto-antigens, however, all of them were ubiquitous intracellular proteins, not specific to brain tissue. The combination of the expansion of single clones in iGB cell culture as well as the tools from Dornmair et al. could help to overcome the limitation of the FAIS culture system.

Next, the iGB cell culture system was used as a tool to expand/manipulate TH B cells *in vitro* and transfer them to recipient mice. Firstly, we wanted to test if B cell activation in iGB culture leads to a better survival upon transfer compared to naïve B cells used in our B cell activation studies in the intestine. Secondly, we wanted to analyze and characterize role, function and properties of MOG-specific B cells in the initiation of EAE instead of focusing on expansion of MOG-specific B cells *in vitro*. To do so, adoptive transfer of actin-GFP WT and TH iGB cells into 2D2 recipient mice was performed (Figure 21). The adoptive transfer of TH B cells into 2D2 mice was chosen because in contrast to RR mice the incidence of spontaneous EAE in single transgenic 2D2 mice is close to 0%, and previous studies suggest a prominent role for B cells as APCs in this model [32, 33, 135]. Therefore, day 4 iGB cells were transferred assuming they retain good APC function. TH iGB cells were able to induce EAE in about 60% of 2D2 recipient mice even without pre-stimulation with rMOG. These data suggest that exogenous MOG is not required for induction of spontaneous EAE, since adoptive transfer of TH iGB cells stimulated with or without MOG induced EAE with similar incidence and severity. In recipients of MOG-stimulated TH iGB cells the frequency of IgM^a-positive cells among transferred cells was reduced, while the frequency of IgG1-positive cells in spleen and iLNs was increased compared to recipients of unstimulated TH iGB cells (Figure 20). These data

could indicate that stimulation with MOG before transfer leads to a higher fraction of surviving isotype-switched TH B cells in the host. FAS expression in transferred cells in recipients of unstimulated TH iGB cells was significantly higher than in recipients of WT iGB cells and trending higher than in recipients of MOG-stimulated TH iGB cells suggesting that transferred TH iGB cells maintain a higher activation status upon *in vivo* transfer, which may result from interaction with MOG-specific T cells in 2D2 recipients. Moreover, TH and WT iGB cells were equally distributed in spleen, iLNs, mLNs, CLNs and CNS. No enrichment of iGB cells in mLNs was detected suggesting that B cells do not preferentially migrate to the intestine. Therefore, there is no indication for B cell activation in the intestine at least in the 2D2 mouse; however, manipulation of B cells *in vitro* before transfer might also conceal this phenomenon.

These data suggest that exogenous MOG is not required for induction of EAE. Recipients of TH iGB cells showed increased FAS expression on transferred cells compared to recipients of WT iGB cells indicating higher activation status. The reason for this may be active cooperation between 2D2 T and TH iGB cells, as observed in the OSE model: the presence of MOG-specific T cells led to massive production of MOG-specific IgG1 antibody, and MOG-specific B cells also enhanced MOG-specific T cell proliferation and activation [32, 34]. One argument why pre-stimulation of MOG is not necessary could be that TH iGB cells are able to find and present endogenous MOG and that APC function of transferred TH iGB cells is of major importance in this setting. 2D2 mice are prone to develop optic neuritis and may also have subclinical inflammation in the CNS [30] This could be the reason why the BBB in 2D2 is more leaky compared to WT mice and so, transferred B cells may have access to endogenous MOG by entering the CNS or by antigen leaking from optic nerve/CNS to the periphery. This would be in line with several reports showing that B cell antigen presentation is sufficient to drive neuroinflammation in EAE: thus, a recent study demonstrated that increasing the precursor frequency of MOG-specific B cells but not the addition of soluble MOG-specific antibody is sufficient to drive EAE in mice expressing MHC class II only in B cells [136]. Additionally, another group showed that MHC class II-dependent B cell APC function is required for induction of CNS autoimmunity independent of myelin-specific antibodies [137]. They demonstrate that in models that require participation of B cells their cellular function is necessary and sufficient for induction of CNS autoimmunity. Moreover, it was shown that B cells promote induction of EAE by facilitating reactivation of T cells in the CNS, and that B cells are the predominant MHC class II-expressing subset in the naïve CNS, and they constitutively express proinflammatory cytokines [138]. On the other hand, MOG-specific IgM^a and IgG1^a were also detected in the serum of our TH iGB cell recipients (Figure 21), and

thus at present we cannot exclude that antibodies also contribute to pathogenesis in our model. Supporting this idea, it was recently shown that myelin-reactive antibodies are capable of initiating an encephalitogenic immune response by targeting endogenous CNS antigen to otherwise inert myeloid APC [139]. Kinzel et al. demonstrated that constitutive production of Ab against MOG was sufficient to promote EAE even in the absence of B cells, when mice carried MOG-specific T cells. In line with that, Flach et al. found that myelin-specific antibodies produced by autoreactive B cells after activation in the periphery diffused into the CNS together with the first invading pathogenic T cells [135].

Thus, in our model it remains to be determined whether transferred B cells function primarily as APCs and cytokine producers, or whether their function as antibody producers is crucial in the initiation of EAE. The successful establishment of iGB cell differentiation and expansion provides opportunities to test this, for example one can compare adoptive transfer of TH memory iGB cells vs. TH plasmablasts, to determine whether APC function or antibody production is more important for induction of EAE. If 2D2 recipients of TH plasmablasts develop no or attenuated EAE, MOG autoantibodies might not be essential in the initiation of EAE development but may play a role only in later stages of the disease. This would be in line with recent studies of B cell depletion in relapsing-remitting MS, where treatment with rituximab reduced inflammatory brain lesions and clinical relapses even though plasmablasts are not depleted by this treatment [70]. If the APC-function of the transferred TH iGB cells proves to be essential for initiation of disease, further experiments could be performed to identify the molecular players contributing to B cell pathogenicity during antigen presentation. Here, cytokines are important candidates since they may directly influence polarization of the interacting T cells during antigen presentation. Thus, for example IFN- γ produced by B cells could enhance Th1 polarization, while IL-6 could enhance Th17 differentiation. In addition, B cells can also produce pro-inflammatory cytokines acting on non-T cells including GM-CSF and LT, as well as anti-inflammatory cytokines like IL-10. Importantly, due to the high proliferation rates in the iGB culture system TH B cells could be manipulated *via* retroviral transduction to express different pro- or anti-inflammatory cytokines like LT- α , GM-CSF, IFN- γ or IL-10. Such an approach could provide valuable insight into effector B cell functions required for initiation of EAE development (Figure 23).

B cell aggregates reminiscent of tertiary lymphoid organs (TLOs) were discovered in the meninges of MS patients, leading to the hypothesis that differentiation and maturation of auto-pathogenic B and T cells may also occur inside the CNS [51]. It has been shown that Th17 and LT- derived signals initiate formation of TLOs within the brain meninges [140, 141].

B cells can support the normal development and maintenance of lymphoid structures and ectopic follicles [142]. In addition, B cells can form ectopic lymphoid follicle-like structures during chronic inflammatory conditions [143-145]. Increased expression of LT was detected in the SJL-immunization model at onset and upon relapses, and neutralization of LT decreased expression of the B cell attracting chemokine CXCL13 in the CNS [146], however, the cellular source of LT was not identified here. Considering that LT $\alpha_1\beta_2$ expression on B cells is required for FDC activation during GC responses [147], it is possible that expression of LT- α by B cells also plays an important role in shaping the proinflammatory milieu during TLO formation and thereby contribute to B cell pathogenicity during EAE.

Lately, a proinflammatory GM-CSF expressing human memory B cell subset was described, which is increased in frequency and more readily induced in MS patients compared to healthy controls [62]. GM-CSF expressing B cells efficiently activated myeloid cells *in vitro*, and B cell depletion therapy resulted in decreased proinflammatory myeloid responses of MS patients *in vivo*. A signal transducer and activator of transcription 5 (STAT5) - and STAT6-dependent mechanism was required for B cell GM-CSF production and reciprocally regulated the generation of regulatory IL-10 expressing B cells. Thus, balance between effector and regulatory B cells seems to be important for development of MS and could also be relevant in different stages of spontaneous EAE.

In 2014, Bao et al. identified IFN- γ producing innate B cells [148]. Another group showed one year later that B cells expressing IFN- γ suppress Treg-cell differentiation and promote autoimmune experimental arthritis [149]. Furthermore, Lees et al. showed that regional CNS responses to IFN- γ determine lesion localization patterns during EAE pathogenesis [150]. Moreover, IFN- β has been used successfully to treat MS [151, 152] reducing exacerbations in relapsing-remitting MS, whereas IFN- γ provokes acute relapses [153]. Sosa et al. showed that IFN- γ ameliorates EAE by limiting myelin lipid peroxidation [154]. Using mice deficient for IFN- γ or IFN- γ R or treating mice with neutralizing IFN- γ mAb, they found that the number of APCs containing myelin Ag in the CNS of mice with EAE was decreased, despite significantly more severe clinical disease, suggesting a previously unrecognized role for IFN- γ in controlling the disease process via modulating myelin Ag scavenging in the CNS. Unfortunately, they have not investigated the role of B cells in this process. Thus, it would be interesting to test the role of IFN- γ expressing B cells during spontaneous EAE.

As mentioned before, dysregulation between effector and regulatory B cells might be important in the initiation of EAE. CD20 antibody-mediated B cell depletion before EAE induction resulted in exacerbated disease symptoms and increased encephalitogenic T cell

influx into the CNS [66]. Additionally, some patients treated with rituximab developed psoriasis, and a patient suffering from ulcerative colitis developed a severe exacerbation of the disease upon rituximab treatment, which coincided with elimination of regulatory IL-10-producing B cells in the intestinal mucosa [155, 156]. Without IL-10, mice are not able to recover from EAE [157]. Thus, the therapeutic effect of B cell depletion for the treatment of autoimmunity may depend on the relative contributions and the timing of these opposing B cell activities during the course of disease initiation and pathogenesis. Therefore, the impact of regulatory IL-10 overexpressing B cells in EAE should be investigated.

Overall, different B cell functions may be important during different stages of EAE. Thus, it should be considered at what time point which manipulated B cells and cytokines could play a role. It would be also interesting to investigate if IL-10 producing B cells could suppress pathogenic effects of B cells during initiation phase by transferring them in parallel with LT, GM-CSF or IFN- γ producing B cells. Furthermore, adoptive transfer of regulatory B cells could be performed in RR mice to determine if IL-10 producing B cells could delay onset or completely protect mice from spontaneous disease.

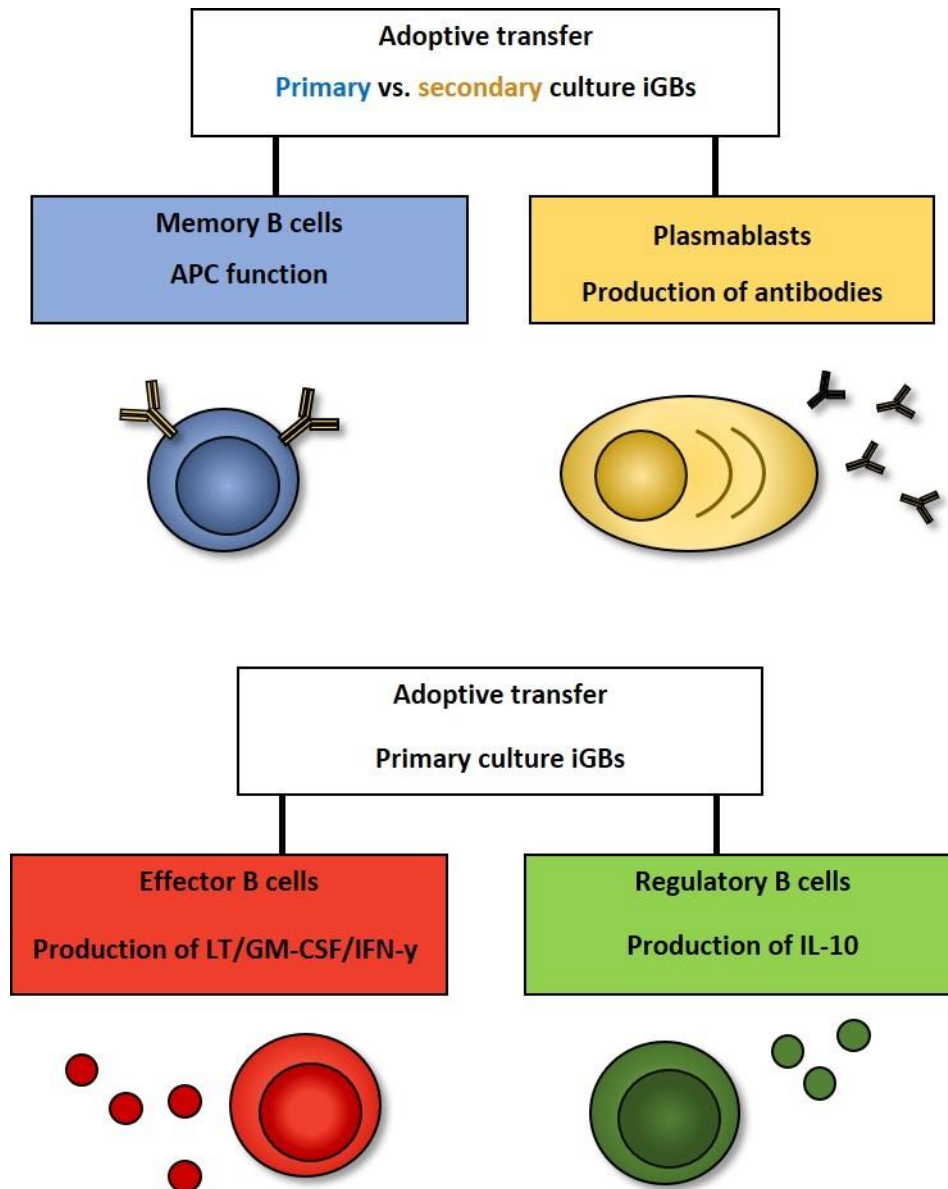


Figure 22: Schematic representation of future experiments

Comparison of adoptive transfer of TH memory iGB cells and TH plasmablasts to study importance of APC-function versus production of auto-antibodies in initiation of disease (top.) Manipulation of TH iGB cells with retroviral transduction to express either pro-inflammatory cytokines such as GM-CSF, or anti-inflammatory cytokines such as IL-10 to study their role as effector or regulatory cells in EAE (created by Bettina Martin).

5 CONCLUSION

The aim of this study was to investigate the activation and pathogenic potential of MOG-specific B cells during development of spontaneous EAE. First, antigen transport and priming of autoreactive B cells was investigated by studying CNS drainage pathways, detection of auto-antigens transported from the CNS to CLNs and by studying exosomes as a potential transport system. Second, B cell activation in the intestine and recruitment to CLNs were studied *via* B cell transfer experiments. Due to several methodological limitations, presence of myelin auto-antigens in CNS regional LNs could not be unequivocally demonstrated neither by translocation of fluorescently labeled myelin proteins from CNS to CLNs in RR mice, nor by fluorescent PLP fusion protein in actively induced EAE, nor by direct immunohistochemical staining of myelin proteins in CLNs. Furthermore, investigating the role of exosomes as a transportation and B cell activation vehicle were difficult due to missing methods to show physiological relevance of myelin containing exosomes in development of EAE. Therefore, we next investigated potential B cell activation by myelin mimicking proteins on microbes in the intestine *via* transfer of GFP B cells. However, since transfer of GFP B cells did not show enrichment of B cells in intestine or mLNs, and since meaningful analysis was hindered by very low B cell frequencies presumably due to poor survival of transferred B cells, a new B cell culture system allowing expansion and differentiation of primary B cells was established [116]. In this third part of the thesis we could show that the iGB cell culture system is a useful tool to expand and differentiate low numbers of B cells from different organs and actin-GFP or congenic markers are suitable for tracking B cells in adoptive transfer experiments. Furthermore, we could demonstrate for the first time, that MOG-specific TH iGB cells can be successfully transferred into 2D2 mice and are able to induce EAE in about 60% of 2D2 recipient mice even without pre-stimulation with rMOG. These data suggest that exogenous MOG is not required for induction of EAE. Recipients of TH iGB cells showed increased FAS expression on transferred cells compared to recipients of WT iGB cells indicating higher activation status. The reason for this may be active cooperation between 2D2 T and TH iGB cells, as observed in the OSE model, where the presence of MOG-specific T cells led to massive production of MOG-specific IgG1 antibody, and MOG-specific B cells also enhanced MOG-specific T cell proliferation and activation [32, 33]. While the final trigger of disease development is difficult to determine in the OSE mouse due to the simultaneous presence and development of MOG-specific B and T cells, our transfer of MOG-specific iGB cells into 2D2 recipients clearly shows that B cells have the capacity to deliver the necessary signals that trigger development of disease. The exact nature of these signals can now be

investigated and thus we have laid the groundwork here for important future studies. Thus, B cells could next be manipulated during iGB culture *via* retroviral transduction to express pro- and anti-inflammatory cytokines to study activation and pathogenic potential in EAE. Moreover, limitation of low B cell survival can be overcome to study activation in intestinal segments.

Overall, it is very important to better understand the different roles B cells can play during EAE and MS pathogenesis in order to further improve treatment options in MS, since B cell depletion therapies are not always successful for all patients and can be accompanied by serious side effects.

6 REFERENCES

1. Organization, W.H., *Atlas multiple sclerosis resources in the world 2008*, WHO, Editor. 2008.
2. Compston, A. and A. Coles, *Multiple sclerosis*. *Lancet*, 2008. **372**(9648): p. 1502-17.
3. Frischer, J.M., et al., *The relation between inflammation and neurodegeneration in multiple sclerosis brains*. *Brain*, 2009. **132**(Pt 5): p. 1175-89.
4. Dendrou, C.A., L. Fugger, and M.A. Friese, *Immunopathology of multiple sclerosis*. *Nat Rev Immunol*, 2015. **15**(9): p. 545-58.
5. McKay, K.A., et al., *Risk factors associated with the onset of relapsing-remitting and primary progressive multiple sclerosis: a systematic review*. *Biomed Res Int*, 2015. **2015**: p. 817238.
6. Tremlett, H., Z. Yinshan, and V. Devonshire, *Natural history of secondary-progressive multiple sclerosis*. *Mult Scler*, 2008. **14**(3): p. 314-24.
7. Alonso, A. and M.A. Hernan, *Temporal trends in the incidence of multiple sclerosis: a systematic review*. *Neurology*, 2008. **71**(2): p. 129-35.
8. Miller, D.H. and S.M. Leary, *Primary-progressive multiple sclerosis*. *Lancet Neurol*, 2007. **6**(10): p. 903-12.
9. Cooper, G.S., M.L. Bynum, and E.C. Somers, *Recent insights in the epidemiology of autoimmune diseases: improved prevalence estimates and understanding of clustering of diseases*. *J Autoimmun*, 2009. **33**(3-4): p. 197-207.
10. Wingerchuk, D.M., et al., *Revised diagnostic criteria for neuromyelitis optica*. *Neurology*, 2006. **66**(10): p. 1485-9.
11. Takahashi, T., et al., *Anti-aquaporin-4 antibody is involved in the pathogenesis of NMO: a study on antibody titre*. *Brain*, 2007. **130**(Pt 5): p. 1235-43.
12. Sato, D.K., et al., *Distinction between MOG antibody-positive and AQP4 antibody-positive NMO spectrum disorders*. *Neurology*, 2014. **82**(6): p. 474-81.
13. Brodin, P., et al., *Variation in the human immune system is largely driven by non-heritable influences*. *Cell*, 2015. **160**(1-2): p. 37-47.
14. International Multiple Sclerosis Genetics, C., et al., *Analysis of immune-related loci identifies 48 new susceptibility variants for multiple sclerosis*. *Nat Genet*, 2013. **45**(11): p. 1353-60.
15. Alcina, A., et al., *Multiple sclerosis risk variant HLA-DRB1*1501 associates with high expression of DRB1 gene in different human populations*. *PLoS One*, 2012. **7**(1): p. e29819.
16. Gregory, A.P., et al., *TNF receptor 1 genetic risk mirrors outcome of anti-TNF therapy in multiple sclerosis*. *Nature*, 2012. **488**(7412): p. 508-11.

17. Tasan, M., et al., *Selecting causal genes from genome-wide association studies via functionally coherent subnetworks*. Nat Methods, 2015. **12**(2): p. 154-9.
18. Hedstrom, A.K., et al., *Shift work at young age is associated with increased risk for multiple sclerosis*. Ann Neurol, 2011. **70**(5): p. 733-41.
19. Belbasis, L., et al., *Environmental risk factors and multiple sclerosis: an umbrella review of systematic reviews and meta-analyses*. Lancet Neurol, 2015. **14**(3): p. 263-73.
20. Ji, Q., A. Perchellet, and J.M. Goverman, *Viral infection triggers central nervous system autoimmunity via activation of CD8+ T cells expressing dual TCRs*. Nat Immunol, 2010. **11**(7): p. 628-34.
21. Olson, J.K., et al., *A virus-induced molecular mimicry model of multiple sclerosis*. J Clin Invest, 2001. **108**(2): p. 311-8.
22. Harkiolaki, M., et al., *T cell-mediated autoimmune disease due to low-affinity crossreactivity to common microbial peptides*. Immunity, 2009. **30**(3): p. 348-57.
23. Steinbach, K., et al., *Neutrophils amplify autoimmune central nervous system infiltrates by maturing local APCs*. J Immunol, 2013. **191**(9): p. 4531-9.
24. Carlson, T., et al., *The Th17-ELR+ CXC chemokine pathway is essential for the development of central nervous system autoimmune disease*. J Exp Med, 2008. **205**(4): p. 811-23.
25. Christy, A.L., et al., *Mast cell activation and neutrophil recruitment promotes early and robust inflammation in the meninges in EAE*. J Autoimmun, 2013. **42**: p. 50-61.
26. Handel, A.E., M.R. Lincoln, and S.V. Ramagopalan, *Of mice and men: experimental autoimmune encephalitis and multiple sclerosis*. Eur J Clin Invest, 2011. **41**(11): p. 1254-8.
27. Olitsky, P.K. and R.H. Yager, *Experimental disseminated encephalomyelitis in white mice*. J Exp Med, 1949. **90**(3): p. 213-24.
28. Lyons, J.A., et al., *B cells are critical to induction of experimental allergic encephalomyelitis by protein but not by a short encephalitogenic peptide*. Eur J Immunol, 1999. **29**(11): p. 3432-9.
29. Hjelmstrom, P., et al., *B-cell-deficient mice develop experimental allergic encephalomyelitis with demyelination after myelin oligodendrocyte glycoprotein sensitization*. J Immunol, 1998. **161**(9): p. 4480-3.
30. Bettelli, E., et al., *Myelin oligodendrocyte glycoprotein-specific T cell receptor transgenic mice develop spontaneous autoimmune optic neuritis*. J Exp Med, 2003. **197**(9): p. 1073-81.
31. Litzemberger, T., et al., *B lymphocytes producing demyelinating autoantibodies: development and function in gene-targeted transgenic mice*. J Exp Med, 1998. **188**(1): p. 169-80.

32. Bettelli, E., et al., *Myelin oligodendrocyte glycoprotein-specific T and B cells cooperate to induce a Devic-like disease in mice*. J Clin Invest, 2006. **116**(9): p. 2393-402.
33. Krishnamoorthy, G., et al., *Spontaneous optico-spinal encephalomyelitis in a double-transgenic mouse model of autoimmune T cell/B cell cooperation*. J Clin Invest, 2006. **116**(9): p. 2385-92.
34. Pollinger, B., et al., *Spontaneous relapsing-remitting EAE in the SJL/J mouse: MOG-reactive transgenic T cells recruit endogenous MOG-specific B cells*. J Exp Med, 2009. **206**(6): p. 1303-16.
35. Hellings, N., et al., *T-cell reactivity to multiple myelin antigens in multiple sclerosis patients and healthy controls*. J Neurosci Res, 2001. **63**(3): p. 290-302.
36. McMahon, E.J., et al., *Epitope spreading initiates in the CNS in two mouse models of multiple sclerosis*. Nat Med, 2005. **11**(3): p. 335-9.
37. Pesic, M., et al., *2-photon imaging of phagocyte-mediated T cell activation in the CNS*. J Clin Invest, 2013. **123**(3): p. 1192-201.
38. Bartholomaeus, I., et al., *Effector T cell interactions with meningeal vascular structures in nascent autoimmune CNS lesions*. Nature, 2009. **462**(7269): p. 94-8.
39. Jager, A., et al., *Th1, Th17, and Th9 effector cells induce experimental autoimmune encephalomyelitis with different pathological phenotypes*. J Immunol, 2009. **183**(11): p. 7169-77.
40. Frisullo, G., et al., *IL17 and IFNgamma production by peripheral blood mononuclear cells from clinically isolated syndrome to secondary progressive multiple sclerosis*. Cytokine, 2008. **44**(1): p. 22-5.
41. Tzartos, J.S., et al., *Interleukin-17 production in central nervous system-infiltrating T cells and glial cells is associated with active disease in multiple sclerosis*. Am J Pathol, 2008. **172**(1): p. 146-55.
42. Cao, Y., et al., *Functional inflammatory profiles distinguish myelin-reactive T cells from patients with multiple sclerosis*. Sci Transl Med, 2015. **7**(287): p. 287ra74.
43. Kebir, H., et al., *Preferential recruitment of interferon-gamma-expressing TH17 cells in multiple sclerosis*. Ann Neurol, 2009. **66**(3): p. 390-402.
44. Segal, B.M., et al., *Repeated subcutaneous injections of IL12/23 p40 neutralising antibody, ustekinumab, in patients with relapsing-remitting multiple sclerosis: a phase II, double-blind, placebo-controlled, randomised, dose-ranging study*. Lancet Neurol, 2008. **7**(9): p. 796-804.
45. Thakker, P., et al., *IL-23 is critical in the induction but not in the effector phase of experimental autoimmune encephalomyelitis*. J Immunol, 2007. **178**(4): p. 2589-98.
46. Hohlfeld, R., et al., *The search for the target antigens of multiple sclerosis, part 1: autoreactive CD4+ T lymphocytes as pathogenic effectors and therapeutic targets*. Lancet Neurol, 2015.

47. Hohlfeld, R., et al., *The search for the target antigens of multiple sclerosis, part 2: CD8+ T cells, B cells, and antibodies in the focus of reverse-translational research*. *Lancet Neurol*, 2016. **15**(3): p. 317-31.
48. Magliozzi, R., et al., *Meningeal B-cell follicles in secondary progressive multiple sclerosis associate with early onset of disease and severe cortical pathology*. *Brain*, 2007. **130**(Pt 4): p. 1089-104.
49. Annunziata, P., et al., *Absence of cerebrospinal fluid oligoclonal bands is associated with delayed disability progression in relapsing-remitting MS patients treated with interferon-beta*. *J Neurol Sci*, 2006. **244**(1-2): p. 97-102.
50. Wekerle, H., *B cells in multiple sclerosis*. *Autoimmunity*, 2017. **50**(1): p. 57-60.
51. Mitsdoerffer, M. and A. Peters, *Tertiary Lymphoid Organs in Central Nervous System Autoimmunity*. *Front Immunol*, 2016. **7**: p. 451.
52. Choi, S.R., et al., *Meningeal inflammation plays a role in the pathology of primary progressive multiple sclerosis*. *Brain*, 2012. **135**(Pt 10): p. 2925-37.
53. Dalakas, M.C., *B cells as therapeutic targets in autoimmune neurological disorders*. *Nat Clin Pract Neurol*, 2008. **4**(10): p. 557-67.
54. Meinl, E., M. Krumbholz, and R. Hohlfeld, *B lineage cells in the inflammatory central nervous system environment: migration, maintenance, local antibody production, and therapeutic modulation*. *Ann Neurol*, 2006. **59**(6): p. 880-92.
55. Brickshawana, A., et al., *Investigation of the KIR4.1 potassium channel as a putative antigen in patients with multiple sclerosis: a comparative study*. *Lancet Neurol*, 2014. **13**(8): p. 795-806.
56. O'Connor, K.C., et al., *Self-antigen tetramers discriminate between myelin autoantibodies to native or denatured protein*. *Nat Med*, 2007. **13**(2): p. 211-7.
57. Derfuss, T., et al., *Contactin-2/TAG-1-directed autoimmunity is identified in multiple sclerosis patients and mediates gray matter pathology in animals*. *Proc Natl Acad Sci U S A*, 2009. **106**(20): p. 8302-7.
58. Mathey, E.K., et al., *Neurofascin as a novel target for autoantibody-mediated axonal injury*. *J Exp Med*, 2007. **204**(10): p. 2363-72.
59. Owens, G.P., et al., *Antibodies produced by clonally expanded plasma cells in multiple sclerosis cerebrospinal fluid*. *Ann Neurol*, 2009. **65**(6): p. 639-49.
60. von Budingen, H.C., et al., *Clonally expanded plasma cells in the cerebrospinal fluid of MS patients produce myelin-specific antibodies*. *Eur J Immunol*, 2008. **38**(7): p. 2014-23.
61. Brandle, S.M., et al., *Distinct oligoclonal band antibodies in multiple sclerosis recognize ubiquitous self-proteins*. *Proc Natl Acad Sci U S A*, 2016. **113**(28): p. 7864-9.
62. Li, R., et al., *Proinflammatory GM-CSF-producing B cells in multiple sclerosis and B cell depletion therapy*. *Sci Transl Med*, 2015. **7**(310): p. 310ra166.

63. Barr, T.A., et al., *B cell depletion therapy ameliorates autoimmune disease through ablation of IL-6-producing B cells*. J Exp Med, 2012. **209**(5): p. 1001-10.
64. Bar-Or, A., et al., *Abnormal B-cell cytokine responses a trigger of T-cell-mediated disease in MS?* Ann Neurol, 2010. **67**(4): p. 452-61.
65. Iwata, Y., et al., *Characterization of a rare IL-10-competent B-cell subset in humans that parallels mouse regulatory B10 cells*. Blood, 2011. **117**(2): p. 530-41.
66. Matsushita, T., et al., *Regulatory B cells inhibit EAE initiation in mice while other B cells promote disease progression*. J Clin Invest, 2008. **118**(10): p. 3420-30.
67. Lund, F.E., *Cytokine-producing B lymphocytes-key regulators of immunity*. Curr Opin Immunol, 2008. **20**(3): p. 332-8.
68. Berer, K., et al., *Commensal microbiota and myelin autoantigen cooperate to trigger autoimmune demyelination*. Nature, 2011. **479**(7374): p. 538-41.
69. Berer, K., H. Wekerle, and G. Krishnamoorthy, *B cells in spontaneous autoimmune diseases of the central nervous system*. Mol Immunol, 2011. **48**(11): p. 1332-7.
70. Hauser, S.L., et al., *B-cell depletion with rituximab in relapsing-remitting multiple sclerosis*. N Engl J Med, 2008. **358**(7): p. 676-88.
71. Kappos, L., et al., *Ocrelizumab in relapsing-remitting multiple sclerosis: a phase 2, randomised, placebo-controlled, multicentre trial*. Lancet, 2011. **378**(9805): p. 1779-87.
72. Laman, J.D. and R.O. Weller, *Drainage of Cells and Soluble Antigen from the CNS to Regional Lymph Nodes*. J Neuroimmune Pharmacol, 2013.
73. Kaminski, M., et al., *Migration of monocytes after intracerebral injection*. Cell Adh Migr, 2012. **6**(3): p. 164-7.
74. Szentistvanyi, I., et al., *Drainage of interstitial fluid from different regions of rat brain*. Am J Physiol, 1984. **246**(6 Pt 2): p. F835-44.
75. Hatterer, E., et al., *How to drain without lymphatics? Dendritic cells migrate from the cerebrospinal fluid to the B-cell follicles of cervical lymph nodes*. Blood, 2006. **107**(2): p. 806-12.
76. Louveau, A., et al., *Structural and functional features of central nervous system lymphatic vessels*. Nature, 2015. **523**(7560): p. 337-41.
77. Phillips, M.J., M. Needham, and R.O. Weller, *Role of cervical lymph nodes in autoimmune encephalomyelitis in the Lewis rat*. J Pathol, 1997. **182**(4): p. 457-64.
78. van Zwam, M., et al., *Surgical excision of CNS-draining lymph nodes reduces relapse severity in chronic-relapsing experimental autoimmune encephalomyelitis*. J Pathol, 2009. **217**(4): p. 543-51.
79. Planas, A.M., et al., *Brain-derived antigens in lymphoid tissue of patients with acute stroke*. J Immunol, 2012. **188**(5): p. 2156-63.

80. van Zwam, M., et al., *Brain antigens in functionally distinct antigen-presenting cell populations in cervical lymph nodes in MS and EAE*. J Mol Med (Berl), 2009. **87**(3): p. 273-86.
81. de Vos, A.F., et al., *Transfer of central nervous system autoantigens and presentation in secondary lymphoid organs*. J Immunol, 2002. **169**(10): p. 5415-23.
82. Thery, C., M. Ostrowski, and E. Segura, *Membrane vesicles as conveyors of immune responses*. Nat Rev Immunol, 2009. **9**(8): p. 581-93.
83. Cocucci, E., G. Racchetti, and J. Meldolesi, *Shedding microvesicles: artefacts no more*. Trends Cell Biol, 2009. **19**(2): p. 43-51.
84. Valadi, H., et al., *Exosome-mediated transfer of mRNAs and microRNAs is a novel mechanism of genetic exchange between cells*. Nat Cell Biol, 2007. **9**(6): p. 654-9.
85. Skog, J., et al., *Glioblastoma microvesicles transport RNA and proteins that promote tumour growth and provide diagnostic biomarkers*. Nat Cell Biol, 2008. **10**(12): p. 1470-6.
86. Sheng, H., et al., *Insulinoma-released exosomes or microparticles are immunostimulatory and can activate autoreactive T cells spontaneously developed in nonobese diabetic mice*. J Immunol, 2011. **187**(4): p. 1591-600.
87. Fruhbeis, C., D. Frohlich, and E.M. Kramer-Albers, *Emerging roles of exosomes in neuron-glia communication*. Front Physiol, 2012. **3**: p. 119.
88. Zhang, H., et al., *CD4(+) T cell-released exosomes inhibit CD8(+) cytotoxic T-lymphocyte responses and antitumor immunity*. Cell Mol Immunol, 2011. **8**(1): p. 23-30.
89. Raposo, G., et al., *B lymphocytes secrete antigen-presenting vesicles*. J Exp Med, 1996. **183**(3): p. 1161-72.
90. Kohm, A.P., K.G. Fuller, and S.D. Miller, *Mimicking the way to autoimmunity: an evolving theory of sequence and structural homology*. Trends Microbiol, 2003. **11**(3): p. 101-5.
91. Lehmann, P.V., et al., *Spreading of T-cell autoimmunity to cryptic determinants of an autoantigen*. Nature, 1992. **358**(6382): p. 155-7.
92. Sender, R., S. Fuchs, and R. Milo, *Revised Estimates for the Number of Human and Bacteria Cells in the Body*. PLoS Biol, 2016. **14**(8): p. e1002533.
93. Hooper, L.V., D.R. Littman, and A.J. Macpherson, *Interactions between the microbiota and the immune system*. Science, 2012. **336**(6086): p. 1268-73.
94. Renz, H., P. Brandtzaeg, and M. Hornef, *The impact of perinatal immune development on mucosal homeostasis and chronic inflammation*. Nat Rev Immunol, 2012. **12**(1): p. 9-23.
95. Stecher, B. and W.D. Hardt, *Mechanisms controlling pathogen colonization of the gut*. Curr Opin Microbiol, 2011. **14**(1): p. 82-91.

96. Moreau, M.C. and G. Corthier, *Effect of the gastrointestinal microflora on induction and maintenance of oral tolerance to ovalbumin in C3H/HeJ mice*. Infect Immun, 1988. **56**(10): p. 2766-8.
97. Sommer, F. and F. Backhed, *The gut microbiota--masters of host development and physiology*. Nat Rev Microbiol, 2013. **11**(4): p. 227-38.
98. Honda, K. and D.R. Littman, *The microbiome in infectious disease and inflammation*. Annu Rev Immunol, 2012. **30**: p. 759-95.
99. Scher, J.U., et al., *Expansion of intestinal Prevotella copri correlates with enhanced susceptibility to arthritis*. Elife, 2013. **2**: p. e01202.
100. Alam, C., et al., *Effects of a germ-free environment on gut immune regulation and diabetes progression in non-obese diabetic (NOD) mice*. Diabetologia, 2011. **54**(6): p. 1398-406.
101. Kamada, N., et al., *Role of the gut microbiota in immunity and inflammatory disease*. Nat Rev Immunol, 2013. **13**(5): p. 321-35.
102. Ochoa-Reparaz, J., et al., *Role of gut commensal microflora in the development of experimental autoimmune encephalomyelitis*. J Immunol, 2009. **183**(10): p. 6041-50.
103. Ochoa-Reparaz, J., et al., *Induction of a regulatory B cell population in experimental allergic encephalomyelitis by alteration of the gut commensal microflora*. Gut Microbes, 2010. **1**(2): p. 103-108.
104. Berer, K., et al., *Gut microbiota from multiple sclerosis patients enables spontaneous autoimmune encephalomyelitis in mice*. Proc Natl Acad Sci U S A, 2017.
105. Kawamoto, S., et al., *A novel reporter mouse strain that expresses enhanced green fluorescent protein upon Cre-mediated recombination*. FEBS Lett, 2000. **470**(3): p. 263-8.
106. Pircher, H., et al., *Viral escape by selection of cytotoxic T cell-resistant virus variants in vivo*. Nature, 1990. **346**(6285): p. 629-33.
107. Phan, T.G., et al., *B cell receptor-independent stimuli trigger immunoglobulin (Ig) class switch recombination and production of IgG autoantibodies by anergic self-reactive B cells*. J Exp Med, 2003. **197**(7): p. 845-60.
108. Mallon, B.S., et al., *Proteolipid promoter activity distinguishes two populations of NG2-positive cells throughout neonatal cortical development*. J Neurosci, 2002. **22**(3): p. 876-85.
109. Mues, M., *Imaging migration and activation of lymphocytes: transgenic expression of fluorescent indicators*. Dissertation, LMU München: Fakultät für Biologie, in Fakultät für Biologie. 2012, Ludwig-Maximilians-Universität <https://edoc.ub.uni-muenchen.de/16019/>. p. 100.
110. Kerlero de Rosbo, N., et al., *Demyelination induced in aggregating brain cell cultures by a monoclonal antibody against myelin/oligodendrocyte glycoprotein*. J Neurochem, 1990. **55**(2): p. 583-7.

111. Linnington, C., et al., *Augmentation of demyelination in rat acute allergic encephalomyelitis by circulating mouse monoclonal antibodies directed against a myelin/oligodendrocyte glycoprotein*. Am J Pathol, 1988. **130**(3): p. 443-54.
112. Linnington, C., et al., *T cells specific for the myelin oligodendrocyte glycoprotein mediate an unusual autoimmune inflammatory response in the central nervous system*. Eur J Immunol, 1993. **23**(6): p. 1364-72.
113. Linnington, C., M. Webb, and P.L. Woodhams, *A novel myelin-associated glycoprotein defined by a mouse monoclonal antibody*. J Neuroimmunol, 1984. **6**(6): p. 387-96.
114. Al-Rasbi, Z.N.S.H., *B cell recruitment in spontaneous relapsing remitting (RR) experimental autoimmune encephalomyelitis (EAE)*, in Medizinische Fakultät. 2014, Ludwig-Maximilians-Universität: <http://hdl.handle.net/11858/00-001M-0000-002A-DF64-6>. p. 80.
115. Piddlesden, S.J., et al., *The demyelinating potential of antibodies to myelin oligodendrocyte glycoprotein is related to their ability to fix complement*. Am J Pathol, 1993. **143**(2): p. 555-64.
116. Nojima, T., et al., *In-vitro derived germinal centre B cells differentially generate memory B or plasma cells in vivo*. Nat Commun, 2011. **2**: p. 465.
117. Moutai, T., et al., *A novel and effective cancer immunotherapy mouse model using antigen-specific B cells selected in vitro*. PLoS One, 2014. **9**(3): p. e92732.
118. Galazka, G., et al., *Multiple sclerosis: Serum-derived exosomes express myelin proteins*. Mult Scler, 2017: p. 1352458517696597.
119. Fruhbeis, C., et al., *Neurotransmitter-triggered transfer of exosomes mediates oligodendrocyte-neuron communication*. PLoS Biol, 2013. **11**(7): p. e1001604.
120. Baietti, M.F., et al., *Syndecan-syntenin-ALIX regulates the biogenesis of exosomes*. Nat Cell Biol, 2012. **14**(7): p. 677-85.
121. Yu, L., et al., *Exosomes with membrane-associated TGF-beta1 from gene-modified dendritic cells inhibit murine EAE independently of MHC restriction*. Eur J Immunol, 2013.
122. Wesemann, D.R., et al., *Microbial colonization influences early B-lineage development in the gut lamina propria*. Nature, 2013. **501**(7465): p. 112-5.
123. Foy, T.M., et al., *gp39-CD40 interactions are essential for germinal center formation and the development of B cell memory*. J Exp Med, 1994. **180**(1): p. 157-63.
124. Ettinger, R., et al., *IL-21 induces differentiation of human naive and memory B cells into antibody-secreting plasma cells*. J Immunol, 2005. **175**(12): p. 7867-79.
125. Pribyl, T.M., et al., *The human myelin basic protein gene is included within a 179-kilobase transcription unit: expression in the immune and central nervous systems*. Proc Natl Acad Sci U S A, 1993. **90**(22): p. 10695-9.

126. Bruno, R., et al., *Multiple sclerosis candidate autoantigens except myelin oligodendrocyte glycoprotein are transcribed in human thymus*. Eur J Immunol, 2002. **32**(10): p. 2737-47.
127. Feng, J.M., et al., *Expression of soma-restricted proteolipid/DM20 proteins in lymphoid cells*. J Neuroimmunol, 2003. **144**(1-2): p. 9-15.
128. Farias, A.S., et al., *Ten years of proteomics in multiple sclerosis*. Proteomics, 2014. **14**(4-5): p. 467-80.
129. Melo, S.A., et al., *Cancer Exosomes Perform Cell-Independent MicroRNA Biogenesis and Promote Tumorigenesis*. Cancer Cell, 2014. **26**(5): p. 707-21.
130. Cheng, L., et al., *Exosomes provide a protective and enriched source of miRNA for biomarker profiling compared to intracellular and cell-free blood*. J Extracell Vesicles, 2014. **3**.
131. Utsugi-Kobukai, S., et al., *MHC class I-mediated exogenous antigen presentation by exosomes secreted from immature and mature bone marrow derived dendritic cells*. Immunol Lett, 2003. **89**(2-3): p. 125-31.
132. They, C., et al., *Indirect activation of naive CD4+ T cells by dendritic cell-derived exosomes*. Nat Immunol, 2002. **3**(12): p. 1156-62.
133. Qazi, K.R., et al., *Antigen-loaded exosomes alone induce Th1-type memory through a B-cell-dependent mechanism*. Blood, 2009. **113**(12): p. 2673-83.
134. Rush, J.S. and P.D. Hodgkin, *B cells activated via CD40 and IL-4 undergo a division burst but require continued stimulation to maintain division, survival and differentiation*. Eur J Immunol, 2001. **31**(4): p. 1150-9.
135. Flach, A.C., et al., *Autoantibody-boosted T-cell reactivation in the target organ triggers manifestation of autoimmune CNS disease*. Proc Natl Acad Sci U S A, 2016. **113**(12): p. 3323-8.
136. Parker Harp, C.R., et al., *B cell antigen presentation is sufficient to drive neuroinflammation in an animal model of multiple sclerosis*. J Immunol, 2015. **194**(11): p. 5077-84.
137. Molnarfi, N., et al., *MHC class II-dependent B cell APC function is required for induction of CNS autoimmunity independent of myelin-specific antibodies*. J Exp Med, 2013. **210**(13): p. 2921-37.
138. Pierson, E.R., I.M. Stromnes, and J.M. Goverman, *B cells promote induction of experimental autoimmune encephalomyelitis by facilitating reactivation of T cells in the central nervous system*. J Immunol, 2014. **192**(3): p. 929-39.
139. Kinzel, S., et al., *Myelin-reactive antibodies initiate T cell-mediated CNS autoimmune disease by opsonization of endogenous antigen*. Acta Neuropathol, 2016. **132**(1): p. 43-58.
140. Pikor, N.B., et al., *Integration of Th17- and Lymphotoxin-Derived Signals Initiates Meningeal-Resident Stromal Cell Remodeling to Propagate Neuroinflammation*. Immunity, 2015. **43**(6): p. 1160-73.
141. Peters, A., et al., *Th17 cells induce ectopic lymphoid follicles in central nervous system tissue inflammation*. Immunity, 2011. **35**(6): p. 986-96.

142. Fu, Y.X. and D.D. Chaplin, *Development and maturation of secondary lymphoid tissues*. Annu Rev Immunol, 1999. **17**: p. 399-433.
143. Armengol, M.P., et al., *Thyroid autoimmune disease: demonstration of thyroid antigen-specific B cells and recombination-activating gene expression in chemokine-containing active intrathyroidal germinal centers*. Am J Pathol, 2001. **159**(3): p. 861-73.
144. Serafini, B., et al., *Detection of ectopic B-cell follicles with germinal centers in the meninges of patients with secondary progressive multiple sclerosis*. Brain Pathol, 2004. **14**(2): p. 164-74.
145. Takemura, S., et al., *Lymphoid neogenesis in rheumatoid synovitis*. J Immunol, 2001. **167**(2): p. 1072-80.
146. Columba-Cabezas, S., et al., *Suppression of established experimental autoimmune encephalomyelitis and formation of meningeal lymphoid follicles by lymphotoxin beta receptor-Ig fusion protein*. J Neuroimmunol, 2006. **179**(1-2): p. 76-86.
147. Myers, R.C., et al., *Lymphotoxin alpha1beta2 expression on B cells is required for follicular dendritic cell activation during the germinal center response*. Eur J Immunol, 2013. **43**(2): p. 348-59.
148. Bao, Y., et al., *Identification of IFN-gamma-producing innate B cells*. Cell Res, 2014. **24**(2): p. 161-76.
149. Olalekan, S.A., et al., *B cells expressing IFN-gamma suppress Treg-cell differentiation and promote autoimmune experimental arthritis*. Eur J Immunol, 2015. **45**(4): p. 988-98.
150. Lees, J.R., et al., *Regional CNS responses to IFN-gamma determine lesion localization patterns during EAE pathogenesis*. J Exp Med, 2008. **205**(11): p. 2633-42.
151. Murdoch, D. and K.A. Lyseng-Williamson, *Spotlight on subcutaneous recombinant interferon-beta-1a (Rebif) in relapsing-remitting multiple sclerosis*. BioDrugs, 2005. **19**(5): p. 323-5.
152. Giovannoni, G., F.E. Munschauer, 3rd, and F. Deisenhammer, *Neutralising antibodies to interferon beta during the treatment of multiple sclerosis*. J Neurol Neurosurg Psychiatry, 2002. **73**(5): p. 465-9.
153. Satoh, J. and Y. Kuroda, *Differing effects of IFN beta vs IFN gamma in MS: gene expression in cultured astrocytes*. Neurology, 2001. **57**(4): p. 681-5.
154. Sosa, R.A., et al., *IFN-gamma ameliorates autoimmune encephalomyelitis by limiting myelin lipid peroxidation*. Proc Natl Acad Sci U S A, 2015. **112**(36): p. E5038-47.
155. Dass, S., E.M. Vital, and P. Emery, *Development of psoriasis after B cell depletion with rituximab*. Arthritis Rheum, 2007. **56**(8): p. 2715-8.
156. Goetz, M., et al., *Exacerbation of ulcerative colitis after rituximab salvage therapy*. Inflamm Bowel Dis, 2007. **13**(11): p. 1365-8.

-
157. Fillatreau, S., et al., *B cells regulate autoimmunity by provision of IL-10*. Nat Immunol, 2002. **3**(10): p. 944-50.

7 RESOURCES AND CONTRIBUTIONS

Active EAE experiments in PLP-eGFP mice were performed by Dr. Elisa Romanelli.

PLP-eGFP mice were provided by Prof. Dr. Martin Kerschensteiner.

Exosome analysis on NanoSight was performed in Dr. Anja Schneider's lab.

Electron microscope pictures were performed by Marianne Braun.

40LB, FasL-40LB and HEL-40LB cell lines were provided by Daisuke Kitamura.

SW_{HEL} mice were generated in Robert Brink's group and provided by David Voehringer.

8 CURRICULUM VITAE

PERSONAL DETAILS

Date of birth 12.01.1987 in Tuttlingen, Germany
Nationality German

WORK EXPERIENCE

- 02/2017 – present
Tuttlingen
- Project Manager at Aesculap AG, BBraun**
Department Medical Scientific Affairs
Tasks: Writing Clinical Evaluation Reports, Life Cycle Management, Post Market Clinical Follow-Up, Risk Management, clinical content input for marketing, preclinical study design
- 02/2013 - 01/2017
Munich
- PhD at Max-Planck-Institute for Neurobiology**
Institute for Neuroimmunology, Prof. Hartmut Wekerle
Tasks: Project management, cooperation and negotiation with international collaborators, development of problem-solving strategies, presentations, scientific writing
- 05/2012 - 08/2012
Brisbane, Australia
- Research assistant at the University of Queensland**
Institute of Molecular Bioscience, Dr. Dagmar Wilhelm
Tasks: Experimental research, project work, optimizing & analyzing methods, international working environment
- 08/2011 - 01/2012
Tuttlingen
- Employee in logistics at Henke-Sass, Wolf GmbH**
Medical devices, surgical und endoscopic instruments
Tasks: Quality control, coordination of incoming goods & logistics, supply of production orders
- 04/2001 - 06/2006
Tuttlingen
- Employee for family business Werner Forscher GmbH and Regine Strobel**, CNC lathe and milled parts for eroding
Tasks: Production of serial parts for turning & grinding machines, processing, quality control, warehouse & logistics

EDUCATION

- 02/2013 - present
Munich **PhD in Neuroimmunology at Ludwig-Maximilian University**
Thesis: "Activation and pathogenic potential of MOG-specific B cells in spontaneous experimental autoimmune encephalomyelitis"
- 10/2006 - 07/2011
Karlsruhe **Studies of Molecular Biology at Institute of Technology**
Specialization: Molecular Biology, Zoology, Microbiology
Mark: 1,7
- 09/1997 - 07/2006
Tuttlingen **Allgemeine Hochschulreife at Otto-Hahn-Gymnasium**
Subjects: Biology, German, English, Maths, Art,
Mark: 2,8

QUALIFICATIONS

- Languages **German:** Native speaker
English: Fluent oral and written (C2)
French and Spanish: Basic communication (A2)
- Computer **MS Word, Excel, Powerpoint and Outlook:**
Very good knowledge
Adobe Photoshop and Illustrator: Good knowledge
SAP: Basics

INTERNSHIPS

- 05/2010 – 08/2010
Karlsruhe **Scientific assistant at Institute of Technology in Karlsruhe**
Department of Genetics, PD Dr. Christoph Basse
- 03/2010
Heidelberg **Internship at German Cancer Research Center**
Department of Cancer Growth Control, Prof. Peter Angel
- 08/2009
Freiburg **Practical training at Max-Planck-Institute for Immunology**
Department of Molecular Embryology, Dr. Marc Stemmler

9 ACKNOWLEDGEMENTS

At first, I would like to thank Prof. Dr. Hartmut Wekerle for giving me the opportunity to work in his group and carry out my PhD at the Max-Planck-Institute for Neurobiology. His door was always open, also in struggling times he guided and supported me with courteous conduct.

Moreover, I am thankful to my supervisor Dr. Anneli Peters for her constant scientific, technical and personal support through the most significant time of my PhD. She consistently allowed the project to be my own work but steered me in the right direction whenever she thought I needed it. I could not have imagined having a better advisor and mentor for my PhD study.

I also want to express my gratitude to PD Dr. Oliver Griesbeck from the Max-Planck-Institute of Neurobiology, my principle supervisor and Prof. Dr. Laura Busse at the Ludwigs-Maximilians University as first and second reader of this thesis, and I am gratefully indebted to them for their very valuable comments.

I wish to acknowledge my thesis advisor committee: PD Dr. Josef Mautner, PD Dr. Naoto Kawakami, and PD Dr. Dieter Jenne for their critical input into my project. My sincere thanks to the members of my thesis examination board from the Ludwig Maximilians University: Prof. Dr. Wolfgang Enard, PD Dr. Josef Mautner, PD Dr. Heermann and Prof. Dr. Christian Leibold.

The assistance and support of my lab members made my thesis possible and made it an unforgettable time. Thanks to Veronica Solis, Katarina Pinjusic, Monika Schaubeck, Clemens Gödel, Helene Zephir and Michail Koutrolos for the stimulating discussions, and for all the fun we have had in the last four years.

A very special mention has to go to my friends. With tender and loving care they followed me through good and bad times. Especially all my climbers made my time in Munich unbelievable pleasant. They gave me the energy and self-confidence to finish my PhD.

Last, I want to deeply thank my parents for supporting me spiritually throughout writing my thesis and my life in general. Mama und Papa, ich liebe euch.

